



**Novel Factors from *Phytophthora palmivora* Promote Its Infection
and a Potential Elicitor from *Acanthophora spicifera*
Enhances *Hevea brasiliensis* Resistance**

Sittiporn Pettongkhao

**A Thesis Submitted in Partial Fulfillment of the Requirements for
the Degree of Doctor of Philosophy in Biochemistry**

Prince of Songkla University

2019

Copyright of Prince of Songkla University



**Novel Factors from *Phytophthora palmivora* Promote Its Infection
and a Potential Elicitor from *Acanthophora spicifera*
Enhances *Hevea brasiliensis* Resistance**

Sittiporn Pettongkhao

**A Thesis Submitted in Partial Fulfillment of the Requirements for
the Degree of Doctor of Philosophy in Biochemistry**

Prince of Songkla University

2019

Copyright of Prince of Songkla University

Thesis Title Novel Factors from *Phytophthora palmivora* Promote Its Infection and a Potential Elicitor from *Acanthophora spicifera* Enhances *Hevea brasiliensis* Resistance

Author Mr. Sittiporn Pettongkhao

Major Program Biochemistry

Major Advisor

.....
 (Assoc. Prof. Dr. Nunta Churngchow)

Examining Committee:

.....Chairperson
 (Assoc. Prof. Dr. Prapaporn Utarabhand)

.....Committee
 (Assoc. Prof. Dr. Nunta Churngchow)

.....Committee
 (Asst. Prof. Dr. Ladda Leelawatwattana)

.....Committee
 (Dr. Nion Chirapongsatonkul)

The Graduate School, Prince of Songkla University, has approved this thesis as partial fulfillment of the requirements for the Doctor of Philosophy Degree in Biochemistry.

.....
 (Prof. Dr. Damrongsak Faroongsarng)
 Dean of Graduate School

This is to certify that the work here submitted is the result of the candidate's own investigations. Due acknowledgement has been made of any assistance received.

.....Signature
(Assoc. Prof. Dr. Nunta Churngchow)
Major Advisor

.....Signature
(Mr. Sittiporn Pettongkhao)
Candidate

I hereby certify that this work has not been accepted in substance for any degree, and is not being currently submitted in candidature for any degree.

.....Signature

(Mr. Sittiporn Pettongkhao)

Candidate

ชื่อวิทยานิพนธ์	แฟกเตอร์จากเชื้อ <i>Phytophthora palmivora</i> ที่สามารถส่งเสริมตัวเองในการก่อโรค และอิลิซิเตอร์จากสาหร่ายหนามมงกุฏ (<i>Acanthophora spicifera</i>) ที่มีศักยภาพในการเพิ่มความต้านทานโรคให้กับยางพารา
ผู้เขียน	นายสิทธิพร เพชรทองขาว
สาขาวิชา	ชีวเคมี
ปีการศึกษา	2561

บทคัดย่อ

Phytophthora palmivora เป็นโอโอไมซีส (Oomycete) ที่สามารถทำลายพืชได้หลายชนิด จนถึงขณะนี้ความรู้ที่เกี่ยวข้องกับปัจจัยในการพัฒนาโครงสร้างของเชื้อ เพื่อทำให้เกิดโรคมียังมีน้อยมาก ในการศึกษาครั้งนี้ ผู้วิจัยได้แยกไกลโคโปรตีน 15 kDa จากน้ำเลี้ยงเชื้อ *P. palmivora* และระบุชนิดของโปรตีนด้วยวิธี Liquid Chromatography-Tandem Mass Spectrometry (LC-MS/MS) หลังจากนั้นได้ทำการแยกยีนที่สร้างไกลโคโปรตีน 15 kDa พบมี 2 variants คือ *Ppal15kDaA* และ *Ppal15kDaB* แล้วพบว่าต้นยาสูบที่ได้ฝากถ่ายยีนดังกล่าวด้วย *Agrobacterium* มีการติดเชื้อ *P. palmivora* เพิ่มขึ้น ผู้วิจัยใช้เทคนิค CRISPR/Cas9 เพื่อทำให้เกิดการกลายพันธุ์ของยีน *Ppal15kDa* โดยสามารถสร้าง มิวแทนต์ได้ 6 ไลน์ (line) ที่มีความสามารถในการเกิดโรคลดลงทั้งในใบยาสูบและผลมะละกอ โดยพบว่ามีมิวแทนต์ 2 ไลน์ที่ยีน 15 kDa กลายพันธุ์ทุก copy ได้สูญเสียความสามารถในการก่อโรคเกือบสิ้นเชิง ส่วนมิวแทนต์อีก 4 ไลน์ ที่ยังมียีน wild-type 15 kDa อยู่ มีความสามารถในการก่อโรคที่ลดลงแตกต่างกันไป มิวแทนต์ของยีน 15 kDa ก่อให้เกิดความบกพร่องในการพัฒนาการของเชื้อ ได้แก่ สร้าง sporangium ที่มีขนาดเล็กลง สร้าง germ tube ที่สั้นลง รวมถึงมีความสามารถในการสร้าง appressorium ที่ลดลง ผู้วิจัยยังพบอีกว่ายีน *Ppal15kDa* มีการแสดงออกที่สูงในขณะที่เชื้อกำลังสร้าง appressorium ซึ่งสอดคล้องกับการทดลองข้างต้น ยีนนี้พบได้ใน *Phytophthora* spp. หลายชนิด แต่ยังไม่ทราบการทำงานของยีนดังกล่าว งานวิจัยชิ้นนี้ได้แสดงให้เห็นว่า ยีน *Ppal15kDa* มีบทบาทสำคัญต่อพัฒนาการของเชื้อซึ่งส่งผลต่อการก่อโรคในพืช

อิลิซิเตอร์มีบทบาทสำคัญในปฏิสัมพันธ์ระหว่างพืชกับเชื้อโรค การค้นพบอิลิซิเตอร์ชนิดใหม่ รวมถึงการศึกษาผลกระทบต่อระบบภูมิคุ้มกันของพืชมีความสำคัญมาก ผู้วิจัยได้ศึกษาอิลิซิเตอร์อื่นๆ จากเชื้อ *P. palmivora* หลังจากนั้นนำน้ำเลี้ยงเชื้อไปทำให้ตกตะกอนด้วยเอทานอล พบว่าอิลิซิเตอร์สกัดหยาบที่ได้สามารถกระตุ้นให้เกิดการตายของเซลล์ในใบยาสูบ และทำให้เกิดการสะสมของไฮโดรเจนเปอร์ออกไซด์ อิลิซิเตอร์ดังกล่าวกระตุ้นให้เกิดการสะสมของกรดชา

ลิโซติก (SA) สคอพอเลติน (Scp) และ กรดแอบไซซิก (ABA) ในใบยาสูบและในใบยางพารา และ ยังส่งเสริมให้ใบยางพาราติดเชื้อเพิ่มขึ้น จากการใช้เทคนิค Fourier Transform Infrared Spectrometer (FTIR) บ่งบอกว่าอิลิซิเตอร์สกัดหยาบดังกล่าวประกอบด้วยส่วนที่เป็นคาร์โบไฮเดรต และส่วนที่เป็นโปรตีน พบว่าเอนไซม์ Proteinase K สามารถทำลายความสามารถในการกระตุ้นการ ตายของเซลล์ ผู้วิจัยสามารถแยกอิลิซิเตอร์จากสารสกัดหยาบ ได้ 4 ส่วน คือ เบต้ากลูแคน (F1) ไกล โคโปรตีนขนาดใหญ่ (F2) ไกลโคโปรตีนที่มีหลายขนาด (F3) และ โปรตีน 42 kDa (F4) ส่วนที่ สามารถทำให้เกิดการตายของเซลล์ คือ F2, F3 และ F4 เป็นที่น่าสนใจว่าส่วนที่ทำให้เกิดการตาย ของเซลล์สามารถกระตุ้นให้เกิดการสะสมของกรดซาลิไซลิกที่สูง และสามารถเหนี่ยวนำให้เกิดการ ติดเชื้อ *P. palmivora* ได้มากยิ่งขึ้น *P. palmivora* เป็น hemibiotroph คือสิ่งมีชีวิตในช่วงแรกๆ อาศัย ในเซลล์ที่มีชีวิตและภายหลังสามารถเจริญเติบโตในเซลล์ที่ตายได้ งานวิจัยชิ้นนี้แสดงให้เห็นว่า เชื้อ *P. palmivora* ใช้ประโยชน์จากอิลิซิเตอร์ที่ก่อให้เกิดการตายของเซลล์ส่งเสริมตัวเองในการก่อ โรค

สุดท้ายผู้วิจัยได้ศึกษาอิลิซิเตอร์ที่แยกได้จากสาหร่ายทะเลหนามมงกุฏ (*Acanthophora spicifera*) ซึ่งปัจจุบันสาหร่ายทะเลกลายเป็นแหล่งทางเลือกของอิลิซิเตอร์ที่ใช้เพื่อ กระตุ้นความต้านทานโรคในพืช งานวิจัยชิ้นนี้ได้นำสารสกัดหยาบโพลีแซคคาไรด์จากสาหร่าย หนามมงกุฏมาใช้เพื่อกระตุ้นระบบภูมิคุ้มกันในยางพารา วิเคราะห์การสะสมของกรดซาลิไซลิก และ สคอพอเลติน ด้วยเทคนิค High Performance Liquid Chromatography (HPLC) และศึกษาการ แสดงออกของยีนในระบบ กรดซาลิไซลิกและกรดจัสโมนิค ด้วยวิธี semi-qRT-PCR พบว่า ยางพาราที่ผ่านการฉีดพ่นด้วยโพลีแซคคาไรด์สกัดหยาบสามารถลดการติดเชื้อ *P. palmivora* ได้ สารดังกล่าวเหนี่ยวนำให้เกิดการสะสมของ กรดซาลิไซลิก และ สคอพอเลติน ทั้งยังกระตุ้นการ แสดงออกของยีนในระบบกรดซาลิไซลิก ตรงกันข้าม สารสกัดที่ได้ยับยั้งการแสดงออกของยีนใน ระบบ กรดจัสโมนิค หลังจากทำบริสุทธิ์สารสกัดหยาบโพลีแซคคาไรด์ พบว่าประกอบด้วย โพลี แซคคาไรด์ที่ไม่มีหมู่ซัลเฟต (F1) และมีหมู่ซัลเฟต (F2 และ F3) โดยชนิดที่ไม่มีหมู่ซัลเฟต ไม่ สามารถกระตุ้นให้ยางพาราสร้างสคอพอเลติน สำหรับชนิดที่มีหมู่ซัลเฟตนั้น พบว่าเป็นการจำแนก ชนิดแลมด้า และพบว่า แลมด้าการาจีแนนที่มีประจุลบมากกว่าสามารถกระตุ้นการสร้างสคอพอ เลตินได้ดีกว่า นอกจากนี้แลมด้าการาจีแนนยังยับยั้งกิจกรรมของเอนไซม์ คาตาเลส แต่กระตุ้น กิจกรรมของเอนไซม์เปอร์ออกซิเดส สุดท้ายผู้วิจัยพบว่าแลมด้าการาจีแนน เป็นมิตรต่อพืช คือไม่ ก่อให้เกิดการตายของเซลล์พืช ดังนั้นสารสกัดดังกล่าวสามารถใช้เป็นอิลิซิเตอร์ทางเลือกในการ กระตุ้นระบบภูมิคุ้มกันในยางพาราได้

Thesis Title Novel Factors from *Phytophthora palmivora* Promote Its Infection and a Potential Elicitor from *Acanthophora spicifera* Enhances *Hevea brasiliensis* Resistance

Author Mr. Sittiporn Pettongkhao

Major Program Biochemistry

Academic Year 2018

ABSTRACT

Phytophthora palmivora is a destructive oomycete plant pathogen with a wide host range. So far, little is known about the factors governing its infection structure development and pathogenicity. From the culture filtrate of *P. palmivora*, I identified a secreted glycoprotein of 15 kDa, designated as Ppal15kDa, using liquid chromatography tandem mass spectrometry (LC-MS/MS). Two variants, *Ppal15kDaA* and *Ppal15kDaB* were amplified from a *P. palmivora* papaya isolate. Transient expression of both variants in *Nicotiana benthamiana* by agroinfiltration enhanced *P. palmivora* infection. Six *Ppal15kDa* mutants with diverse mutations were generated via CRISPR/Cas9-mediated gene editing. All mutants were compromised in infectivity on *N. benthamiana* and papaya. Two of the mutants which all *Ppal15kDa* copies were mutated lost almost complete pathogenicity. The pathogenicity of the other four containing at least one wild-type copy of *Ppal15kDa* was compromised at varying levels. The mutants were also affected in development as they produced smaller sporangia, shorter germ tubes, and less appressoria. Interestingly, the affected levels in development corresponded to the levels of reduction in pathogenicity, suggesting that Ppal15kDa plays an important role in normal development of *P. palmivora* infection structures, which contributes to successful infection. Consistent with its role in infection structure development and pathogenicity, *Ppal15kDa* was found to be highly induced during appressorium formation. In addition, Ppal15kDa homologs are broadly present in *Phytophthora* spp, but none were characterized. Altogether, this study identified a novel component involved in development and pathogenicity of *P. palmivora* and possibly many other *Phytophthora* spp.

Elicitors play an important role in plant and pathogen interactions. The discovery of new elicitors and their effects on plant defense responses is significant and challenging. In this study, I investigated novel elicitors from *P. palmivora* and their effects on plant defenses. A crude elicitor isolated by ethanol precipitation from culture filtrates of *P. palmivora* induced cell death in tobacco leaves. When tobacco leaves were infiltrated with this cell death-inducing elicitor, the accumulations of H₂O₂, salicylic acid (SA), scopoletin (Scp) and abscisic acid (ABA) were detected. Accumulations of SA, Scp and ABA were also induced in rubber tree leaves. *P. palmivora* infection significantly increased in rubber tree leaves pretreated with the elicitor and co-treated with the elicitor and zoospores of *P. palmivora*. This elicitor can be described as compound elicitor because Fourier-transform infrared (FTIR) spectroscopy revealed that it consisted of both polysaccharides and proteins. I also found that the cell death effect caused by this compound elicitor was completely neutralized by Proteinase K. The compound elicitor was composed of four fractions which were beta-glucan (F1), high-molecular-weight glycoprotein (F2), broad-molecular-weight glycoprotein (F3) and 42 kDa protein (F4). Interestingly, the broad-molecular-weight glycoprotein (F3) caused the highest level of cell death in tobacco leaves, while the beta-glucan (F1) had no effect. The high-molecular-weight glycoprotein (F2), broad-molecular-weight glycoprotein (F3) and 42 kDa protein (F4) fractions not only caused cell death in tobacco leaves but also induced high levels of SA accumulation. Furthermore, these three fractions clearly promoted *P. palmivora* infection of rubber tree leaves. *P. palmivora* is a hemibiotrophic pathogen. It can survive in dead tissue. This study revealed that *P. palmivora* could use cell death-inducing elicitors to promote its infection.

Elicitors from seaweeds are considered as alternative stimulants of plant defenses against pathogenic infection. Finding new sources of elicitors and exploring their effects on plant defenses is a significant undertaking. In this study, I extracted crude polysaccharide (CPS) from *Acanthophora spicifera* (a red alga) and tested the effects of the compound on rubber tree (*Hevea brasiliensis*) defense responses. Accumulations of SA and Scp were measured by HPLC. The expressions of SA- and Jasmonic acid (JA)-responsive genes were analyzed by semi-qRT-PCR.

Strong anion exchange chromatography and FTIR spectroscopy were used for purification and functional characterization of CPS, respectively. The extracted CPS enhanced rubber tree defenses against *P. palmivora* infection. It induced SA and Scp accumulations and SA-responsive gene expression, but suppressed JA-responsive gene expression. I successfully separated the non-sulphated polysaccharide (F1) from the sulphated polysaccharides (SPS). Both peaks of SPS (F2 and F3) were identified as lambda (λ)-carrageenan. The F3 fraction showed greater elicitor activity on tobacco leaves. It induced SA and Scp accumulations and peroxidase activity but suppressed catalase activity. Furthermore, the purified λ -carrageenan did not cause cell death in tobacco or rubber tree leaves. Therefore, the elicitor from *A. spicifera* could be an alternative plant stimulant.

ACKNOWLEDGEMENT

This study could not be conducted without the kindness of my major advisor, Associate Professor Dr. Nunta Churngchow who gave me the great opportunity to study in the Department of Biochemistry. Furthermore, this thesis could not be successful without the kindness advice of my major advisor and the other advisor in Department of Plant and Environmental Protection Sciences, University of Hawaii at Manoa, Dr. Miaoying Tian. I would like to honestly express my gratitude to them. Moreover, I would like to appreciate Dr. Nion Chirapongsatonkul who provided information and taught me of advanced techniques. I would like to thank my Biochemistry friend (Pee Mung, Pee Joy, Pee Kit, Pee June and Nong Mean) for helping me in everything. I am thankful for financial support including the Excellent Scholarships in Biochemistry, Department of Biochemistry, Faculty of Science, Prince of Songkla University, Thailand; the Graduate School of Prince of Songkla University, Thailand and The Royal Golden Jubilee Graduated Program (RGJ-PHD) through the Thailand Research Fund (TRF) to Mr. Sittiporn Pettongkhao (PHD/0067/2556).

I would like to thank the Phetchaburi Coastal Fisheries Research and Development Center, Phetchaburi, Thailand for providing me *A. spicifera* samples. I thank Anna Chatthong and Tommy Coyne for a generous revision of the manuscripts and valuable comments. I also thank to Dr. Sebastian Schornack, Sainsbury Laboratory Cambridge University (SLCU) who provided valuable comments about the 15 kDa project.

Finally, my graduation would not be achieved without best wish from my family who understand me and help me for everything.

Sittiporn Pettongkhao

CONTENES

	Page
ABSTRACT (Thai)	v
ABSTRACT (English)	vii
ACKNOWLEDGEMENT	x
CONTENTS	xi
LIST OF TABLES	xiii
LIST OF FIGURES	xiv
LIST OF ABBREVIATIONS	xviii
CHAPTER 1 INTRODUCTION AND LITERATURE REVIEW	1
Introduction	1
Review of literature	5
CHAPTER 2 A SECRETED PROTIEN OF 15 kDa PLAYS AN IMPORTANT ROLE IN <i>PHYTOPHTHORA PALMIVORA</i> DEVELOPMENT AND PATHOGENICITY	26
Introduction	26
Objectives	29
Materials and Methods	29
Results	37
Discussion	55
Conclusion	58
CHAPTER 3 NOVEL CELL DEATH-INDUCING ELICITORS FROM <i>PHYTOPHTHORA PALMIVORA</i> PROMOTE INFECTION ON <i>HEVEA</i> <i>BARSILIENSIS</i>	59
Introduction	59
Objectives	61
Materials and Methods	62
Results	67
Discussion	79
Conclusion	84

CONTENES

(Continued)

	Page
CHAPTER 4 SULPHATED POLYSACCHARIDE FROM <i>ACANTHOPHORA SPICIFERA</i> INDUCED <i>HEVEA BRASILIENSIS</i> DEFENSE RESPONSES AGAINST <i>PHYTOPHTHORA PALMIVORA</i> INFECTION	85
Introduction	85
Objectives	88
Materials and Methods	88
Results	93
Discussion	103
Conclusion	107
REFERENCES	108
VITAE	133

LIST OF TABLES

Table	Page
1.1 Absorbance of carrageenans determined with an infrared spectrophotometer	11
1.2 The marker genes of SA, JA, ethylene, and ABA signaling pathways	23
4.1 Specific primers used for semi-qRT-PCR.	91

LIST OF FIGURES

Figure		Page
1.1	Rubber tree plantations	6
1.2	Leaf and seed of rubber tree	6
1.3	Black stripe, leaf-fal, and fruit rot of rubber tree caused by <i>P. palmivora</i>	7
1.4	Infection strategies and lifestyles of oomycetes, typical asexual <i>Phytophthora</i> dispersal structures, leaf colonization, and root colonization	9
1.5	Structure of carrageenans	12
1.6	A zigzag model illustrates the quantitative output of the plant immune system	15
1.7	Schematic representation of ROS-dependent cell death pathways	17
1.8	Schematic representation the level of SA affected NPR3 and NPR4	18
1.9	Proposed pathways for the biosynthesis of SA in plants	20
1.10	Schematic overview of the salicylic acid (SA) signaling pathway	21
1.11	Schematic overview of the jasmonic acid (JA) signaling pathway	22
1.12	Crosstalk between SA and JA/ET pathway through EDS1 and MPK4	25
2.1	Detection of the 15 kDa glycoprotein from culture filtrate of <i>P. palmivora</i>	37
2.2	The nucleotide and amino acid sequences of <i>Ppal15kDaA</i> and <i>Ppal15kDaB</i> with the sgRNA target sequence used for CRISPR/Cas9-mediated gene editing	38
2.3	Multiple single nucleotide polymorphisms (SNPs) at 5' untranslated region (UTR) of <i>Ppal15kDaA</i> and <i>Ppal15kDaB</i>	39
2.4	Amino acid sequence alignment of <i>Ppal15kDa</i> and its homologs in <i>Phytophthora</i> spp.	40
2.5	Phylogenetic analyses of <i>Ppal15kDa</i> and its homologs in <i>Phytophthora</i> spp.	41

LIST OF FIGURES

(Continued)

Figure		Page
2.6	Agrobacterium-mediated transient expression of <i>Ppal15kDa</i> in <i>N. benthamiana</i>	42
2.7	Expression of <i>Ppal15kDa</i> in <i>N. benthamiana</i> leaves enhanced <i>P. palmivora</i> infection	43
2.8	Chromatograms of the partial sequences of <i>Ppal15kDa</i> gene in mutants generated using CRISPR/Cas9 gene editing	44
2.9	The <i>Ppal15kDa</i> nucleotide mutations and the resulted amino acid changes in <i>P. palmivora</i> mutants generated via CRISPR/Cas9 gene editing	45
2.10	Infection assays of <i>N. benthamiana</i> leaves with <i>P. palmivora</i> wild-type (WT) strain and <i>Ppal15kDa</i> mutants	47
2.11	Infection assays of papaya fruits with <i>P. palmivora</i> wild-type (WT) strain and <i>Ppal15kDa</i> mutants	48
2.12	Mycelium growth of WT and mutants. WT and mutants were cultured on 10% unclarified V8 agar	49
2.13	Zoospore germination assay of <i>P. palmivora</i> wild-type (WT) strain and <i>Ppal15kDa</i> mutants	50
2.14	Measurements of the sporangium sizes of <i>P. palmivora</i> WT strain and <i>Ppal15kDa</i> mutants	51
2.15	Micrographs of germ tubes of <i>P. palmivora</i> WT strain and <i>Ppal15kDa</i> mutants	52
2.16	Assays of appressorium formation of <i>P. palmivora</i> WT and <i>Ppal15kDa</i> mutants	53
2.17	Expression of <i>Ppal15kDa</i> in various development stages of <i>P. palmivora</i> by RT-qPCR	55

LIST OF FIGURES

(Continued)

Figure		Page
3.1	Cell death induced by the crude elicitor on tobacco leaves at 24 hours post infiltration, chlorotic cell death on wounded rubber tree leaves and Trypan blue and DAB staining of infiltrated areas on tobacco leaves	68
3.2	High-performance liquid chromatography analysis of time-related concentrations of SA, Scp, and ABA in tobacco leaves after infiltration with the cell death-inducing elicitor and sterile distilled water	70
3.3	High-performance liquid chromatography analysis of SA, Scp, and ABA in rubber tree leaves after treatment with the cell death-inducing elicitor by spraying method, the representatives of disease symptom by a droplet method and disease severity of <i>P. palmivora</i> infection on rubber tree leaves	72
3.4	Fourier transform infrared spectra of cell death-inducing elicitor before separation and F1 fraction	74
3.5	The effect on cell death induction of beta-1,3-glucanase, at 24 hours post infiltration, and Proteinase K at 72 hours post infiltration with a cell death-inducing elicitor	75
3.6	Silver staining after SDS-PAGE and periodic acid-Schiff staining of each fraction	76
3.7	Cell death induction on tobacco leaves by four fractions separated by anion chromatography column at 1X and 5X concentrations and accumulation of SA and Scp in tobacco leaves after infiltration by each fraction	77
3.8	The representative rubber tree leaves and lesion diameter (mm) of rubber tree leaves after co-treatment with each fraction and zoospores of <i>P. palmivora</i>	78
3.9	Purification of the F4 fraction by size exclusion chromatography (Sephadex G-75)	79

LIST OF FIGURES

(Continued)

Figure		Page
4.1	CPS reduced infected leaves (%) and disease severity (%) in rubber tree leaves after infection by <i>P. palmivora</i>	94
4.2	CPS enhanced SA and Scp accumulations in rubber tree leaves	95
4.3	Time course inductions of <i>HbPR-1</i> , <i>HbGLU</i> and <i>HbASI</i> expressions by semi-qRT-PCR	96
4.4	Chromatographic elution profile of F1, F2 and F3 eluted with 0.4, 0.8 and 1.6 M NaCl, respectively, using a strong anion column, Q sepharose	97
4.5	The FTIR spectra of F1, F2 and F3 fractions eluted with 0.4, 0.8 and 1.6 M NaCl, respectively, through a Q sepharose column	98
4.6	Scp contents in tobacco leaves treated with purified F1, F2 and F3 from CPS of <i>A. spicifera</i> and sterile distilled water (DW) and The GPC elution curve of fraction F3	100
4.7	The λ -carrageenan enhanced SA and Scp accumulations in rubber tree leaves	101
4.8	Activity staining of catalase and peroxidase activity in rubber tree leaves were treated with 0.5 mg/ml λ -carrageenan and sterile distilled water and toxicity test of λ -carrageenan	102

LIST OF ABBREVIATIONS

ABA	Abscisic acid
ANOVA	Analysis of variance
AOS	Allene oxide synthase
AzA	Azelaic acid
α -LA	α -linolenic acid
BA2H	Benzoic acid-2-hydroxylase
Cas9	CRISPR associated protein 9
CAT	Catalase
CBEL	Cellulose binding elicitor lectin
cm	Centimeter
COI1	Coronatine Insensitiveq1
CPS	Crude polysaccharide
CRISPR	Clustered regularly interspaced short palindromic repeats
CUL3	Cullin 3
DA	Dihydroabetalinal
DAB	3,3'-diaminobenzidine
DEAE	Diethylaminoethyl
$^{\circ}$ C	Degree Celsius
DNA	Deoxyribonucleic acid
DS	Disease severity index
DW	Distilled water
EDS1	Enhanced disease susceptibility 1
Em	Emission
EPS	Exo-polysaccharide
ET	Ethylene
ETI	Effector-triggered immunity
ETS	Effector-triggered susceptibility
Ex	Excitation
FTIR	Fourier-transform infrared

LIST OF ABBREVIATIONS

(Continued)

g	Gram
G3P	Glycerol-3-phosphate
GFP	Green fluorescent protein
GH12	Glycoside hydrolase family 12
GP42	Glycoprotein 42
GPC	Gel Permeation Chromatography
h	Hour
HPLC	High performance liquid chromatography
HR	Hypersensitive response
ICS	Isochorismate synthase
IPL	Isochorismate pyruvate lyase
ISR	Induced systemic resistance
JA	Jasmonic acid
JA-Ile	Jasmonoyl-isoleucine
JAZ	Jasmonate zim domain
JMT	Jasmonic acid carboxyl methyltransferase
kDa	Kilodalton
LC-MS/MS	Liquid chromatography tandem mass spectrometry
LOX2	Lipoxygenase 2
m	Meter
M	Molar
MAMPS	Microbial-associated molecular patterns
MeSA	Methyl salicylic acid
mg/ml	Milligram/milliliter
min	Minute
ml/min	Mililiter/minute
mm	Millimeter
mM	Milimolar
μ L	Microlitter

LIST OF ABBREVIATIONS

(Continued)

μM	Micromolar
MPK4	Mitogen-activated protein kinase 4
NADPH	Nicotinamide Adenine Dinucleotide Phosphate
NB-LRR	Nucleotide binding-leucine rich repeat receptor
NINJA	Novel interactor of jasmonate zim domain
NPR1	Nonexpressor of Pathogenic-related gene 1
PAL	Phenylalanine ammonia lyase
PAMPs	Pathogen-associated molecular patterns
PAS	Periodic acid-Schiff
%	Pecent
PCD	Program cell death
PDA	potato dextrose agar
PDF1.2	Plant defensins 1.2
Pep-13	13 amino acid
POD	Peroxidase
PRRs	Pattern recognition receptors
PS I	Photosystem I
PTI	PAMP-triggered immunity
PVDF	Polyvinylidenedifluoride
PVPP	Polyvinylpyrrolidone
	Quantitative reverse-transcriptase polymerase chain
qRT-PCR	reaction
R gene	Resistance gene
ROS	Reactive oxygen species
rpm	Round per minute
s	Second
SA	Salicylic acid
SAR	Systemic acquired resistance
Scp	Scopoletin

LIST OF ABBREVIATIONS

(Continued)

SDS-PAGE	Sodium dodecyl sulfate-polyacrylamide gel electrophoresis
SE	Standard error
sgRNA	Single guide ribonucleic acid
SPS	Sulphated polysaccharides
THI2.1	Thionin 2.1
TF	Transcription factor
TMV	Tobacco Mosaic Virus
TPL	Topless
UTR	Untranslated region
v/v	Volume/volume
VSP	Vegetative storage protein
w/v	Weight/volume
WT	Wild-type

CHAPTER 1

INTRODUCTION AND LITERATURE REVIEW

1.1 Introduction

Hevea brasiliensis (Wild.) Muell.-Arg or Para rubber is classified in the Euphorbiaceae family and *Hevea* genus. More than 90 fungal species are known to infect rubber tree such as *Colletotrichum heveae*, *Botryodiplodia elactica*, *B. theobromae* causing leaf spot, *Gloeosporium heveae* causing die-back, *Fomes lamaensis* causing brown root rot, *Polystichus occidentalis* and *P. personii* causing white spongy rot, and *Phytophthora palmivora* causing leaf-fall, fruit rot, die-back and black stripe. It is also infected by bacteria (Lieberei *et al.*, 2007). The black stripe and leaf-fall diseases in *H. brasiliensis* are often found in Thailand which can reduce the yield and quality of the rubber latex.

A thousand or more plant species including horticultural, agricultural and ornamental crops are infected by *P. palmivora*. It infects more than 200 plant species in the tropics and subtropics (Erwin and Ribeiro 1996) which are economically important hosts such as cacao, papaya, pineapple, durian, rubber tree, and oil palm. *P. palmivora* is a hemibiotrophic pathogen which can survive in dead tissue and acts as a necrotrophic pathogen. At the beginning of infection, it commonly grows as a biotroph and then switches to a necrotroph at later stages of infection. *P. palmivora* is classified as oomycetes which has characteristics distinct from the true fungi. Oomycete cell wall mainly consists of beta-1,3 glucan, whereas the fungal cell wall is chitin (Werner *et al.*, 2002; Latijnhouwers *et al.*, 2003).

P. palmivora spores may directly or indirectly cause infection. Sporangia produced on infected roots, stems, leaves or fruits are able to directly germinate on the plant surface. They can also produce small zoospores which can swim in soil, water or on a wet surface of plants until they germinate and enter the plants. Sporangia and zoospores are spread by wind or water. Zoospores can reach the plant surface, attach to the plant surface by secretion of adhesion molecules then encyst (Hardham and Shan 2009). After attachment of the host, the zoospore germinates a germ tube; in

addition, an appressorium is developed in order to penetrate the host surface (Latijnhouwers *et al.*, 2003). When penetration succeeded, intercellular hyphae form haustoria which are used to penetrate and obtain nutrients from the adjacent plant cells (Mendgen and Hahn 2002). *Phytophthora* spp. use appressoria and haustoria as the infection structures to reach the host cell (Fawke *et al.*, 2015). Cell wall-degrading enzymes are also expressed in germ tubes and infection hyphae to facilitate penetration (Pryce-Jones *et al.*, 1999).

Responses to infection of plants use a two-branched innate immune system. One of the two branches of important plant immune system is transmembrane pattern recognition receptors (PRRs) which are responded to microbial- or pathogen-associated molecular patterns (MAMPS or PAMPs) such as flagellin (Zipfel and Felix, 2005). The other acts inside the cell detected by the polymorphic nucleotide binding-leucine rich repeat (NB-LRR) proteins which were encoded by resistance (R) genes (Dangl *et al.*, 2001). PAMPs (or MAMPS) are recognized by PRRs resulting in PAMP-triggered immunity (PTI) that can inhibit further colonization. Successful pathogens produce effectors to promote pathogen pathogenicity. Effectors can interfere with PTI that is called effector-triggered susceptibility (ETS). A secreted effector is subsequently perceived by NB-LRR proteins leading to activation effector-triggered immunity (ETI). ETI is an amplified and accelerated PTI response resulting in plant resistance and it usually is a hypersensitive cell death response (HR) occurring at the infection site. Pathogens try to avoid ETI by acquiring additional effectors to suppress ETI (Jones and Dang 2006). Characterization of two important factors, elicitors and effectors on plant-pathogen interaction is significant to understand their effects.

A state of enhanced defensive capacity established by plants in response to appropriate stimuli is well known as induced resistance. This plant defense mechanism is highly effective defense responses against a wide range of subsequent pathogen infection (Van Loon *et al.*, 1998). Systemic acquired resistance (SAR) and induced systemic resistance (ISR) are two forms of induced resistance. SAR depends on accumulations of pathogenesis-related proteins and salicylic acid (SA) (Pieterse *et al.*, 1996), whereas ISR involves jasmonic acid (JA) and ethylene (ET) signaling

pathways (Pieterse *et al.*, 1998). Elicitors are biofactors or chemicals from many sources that are able to enhance physiological changes of targeted organisms. In plants, elicitors are chemical obtained from many sources that are able to induce morphological and physiological responses and phytoalexin accumulation. Elicitors have been considered and utilized as alternative substances to induce important economic crop resistance against pathogen infections.

Oligo- or polysaccharides are the most well characterized important signal molecules in elicitation such as chitosan, chitin, xyloglucans, oligogalacturonide and β -glucan. They have elicitor activity in many plant species and highly activate phytoalexin accumulation in plants (Zhao *et al.*, 2005). Many marine macroalgae are usually respected as an important source of unique polysaccharide elicitors and environmental friendly plant stimulants which can not be found in land plants (Klarzynski *et al.*, 2000). Algal polysaccharides have been characterized for their plant immunity enhancement and already applied for pest and disease preventions of economic crop plants (Klarzynski *et al.*, 2000; Klarzynski *et al.*, 2003). Vera *et al.*, (2011) showed that seaweed oligosaccharides and polysaccharides can induce plant defense responses and enhance defense response against subsequent pathogen infections.

This study was divided into three parts. The first part is in search for potential elicitors from culture filtrate of *P. palmivora*. I identified a secreted glycoprotein of 15 kDa, designated as Ppal15kDa which plays an important role in *P. palmivora* development and pathogenicity. Transient expression of Ppal15kDa in *Nicotiana benthamiana* enhanced *P. palmivora* infection. *Ppal15kDa* mutants generated via CRISPR/Cas9-mediated gene editing were lost in infectivity on both *N. benthamiana* and *papaya*, which corresponded to their reduced sporangium sizes, impaired germ tube elongation and appressorium formation. *Ppal15kDa* was found to be highly expressed in appressorium-forming cysts, which is consistent with its role in infection structure development and pathogenicity. This part has been shown in Chapter 2.

The second part is identification the new cell death-inducing elicitors from the culture filtrate of *P. palmivora*. The crude elicitor showed cell death-inducing activity

in tobacco leaves and promoted *P. palmivora* infection in rubber tree leaves. I purified the crude cell death-inducing elicitor into four fractions, beta-glucan (F1), high-molecular-weight glycoprotein (F2), broad-molecular-weight glycoprotein (F3) and 42 kDa protein (F4). F2, F3 and F4 fractions were novel compound and no one has reported their effect before. They induced SA accumulation and cell death, but the beta-glucan (F1) induced SA accumulation without cell death. Interestingly, the high-molecular-weight glycoprotein (F2), broad-molecular-weight glycoprotein (F3) and 42 kDa protein (F4) significantly promoted *P. palmivora* infection on rubber tree leaves. This part has been shown in Chapter 3.

The last part involved in finding of the potential elicitor which can induce rubber tree response against *P. palmivora* infection. Since crude polysaccharide (CPS) from *A. spicifera* has not yet been reported to be used as a plant biostimulant, in this study, the effects of polysaccharide extracted from *A. spicifera* on the rubber tree defense responses were investigated. CPS of this seaweed was utilized as a bioelicitor to induce the disease resistance of *H. brasiliensis* against *P. palmivora* infection. In addition, the levels of SA and Scp and expressions of *HbPR-1*, *HbGLU*, and *HbASI* were measured. The CPS was further purified and identified as λ -carrageenan. This λ -carrageenan was also used to test for responsive enzyme (catalase and peroxidase) and cell death inductions. This part has been shown in Chapter 4.

1.2 Review of Literature

1.2.1 *Hevea brasiliensis*

Hevea brasiliensis (Wild.) Muell.-Arg or Para rubber is classified in the Euphorbiaceae family and *Hevea* genus. It is a native tree of the Amazon Basin in Brazil and adjoining countries. *H. brasiliensis* is taken out from the Amazon area to grow in many tropical regions of the world such as South East Asia including Thailand by the British Colonial office (Reed, 1976).

Taxonomic classification of rubber tree is:

Kingdom: Plantae

Subkingdom: Viridiaeplantae

Infrakingdom: Streptophyta

Division: Tracheophyta

Subdivision: Spermatophytina

Infradivision: Angiospermae

Class: Magnoliopsida

Superorder: Rosanae

Order: Malpighiales

Family: Euphorbiaceae

Genus: *Hevea*

Species: *Hevea brasiliensis* (Willd.) Müll. Arg.

From: http://www.itis.gov/servlet/SingleRpt/SingleRpt?search_topic=TSN&search_value=506431

Hevea plants are usually grown at temperatures of 20 to 28°C with a well distribution of annual rainfall of 1,800 to 2,000 mm. *H. brasiliensis* is a quick-growing tree which has 25 m in height. It is a straight and branchless tree which has 50 cm in diameter. Its bark surface is smooth (Fig. 1.1) (Orwa *et al.*, 2009). Each branch of young *H. brasiliensis* tree has 3 leaflets. Seeds are ovoid and shiny which have 2 to 3.5 x 1.5 to 3 cm in sizes. The seed shape is determined by the pressures of the capsule. Seeds weigh is 2 to 4 g (Fig. 1.2) (Orwa *et al.*, 2009).



Fig. 1.1 Rubber tree plantations (<https://siamrath.co.th/n/70707>)

Tapping is usually performed by removal of a thin cut of the bark about 2 to 3 mm deep. Opening of latex vessels in the bark facilitates latex secretion. Trees are always tapped early in the morning because the flow of latex is highest.



Fig. 1.2 Leaf and seed of rubber tree (http://en.wikipedia.org/wiki/Hevea_brasiliensis)

More than 90 fungal species are known to infect rubber tree such as *Colletotrichum heveae*, *Botryodiplodia elactica* and *B. theobromae* causing leaf spot, *Gloeosporium heveae* causing die-back, *Fomes lamaensis* causing brown root rot, *Pellicularis salmonicolor* causing pink disease, *Oidium heveae* causing powdery mildew, *Polystichus occidentalis* and *P. personii* causing white spongy rot, and

Phytophthora palmivora causing leaf-fall, fruit rot, die-back and black stripe (Fig 3). It also is infected by bacteria (Lieberei *et al.*, 2007).

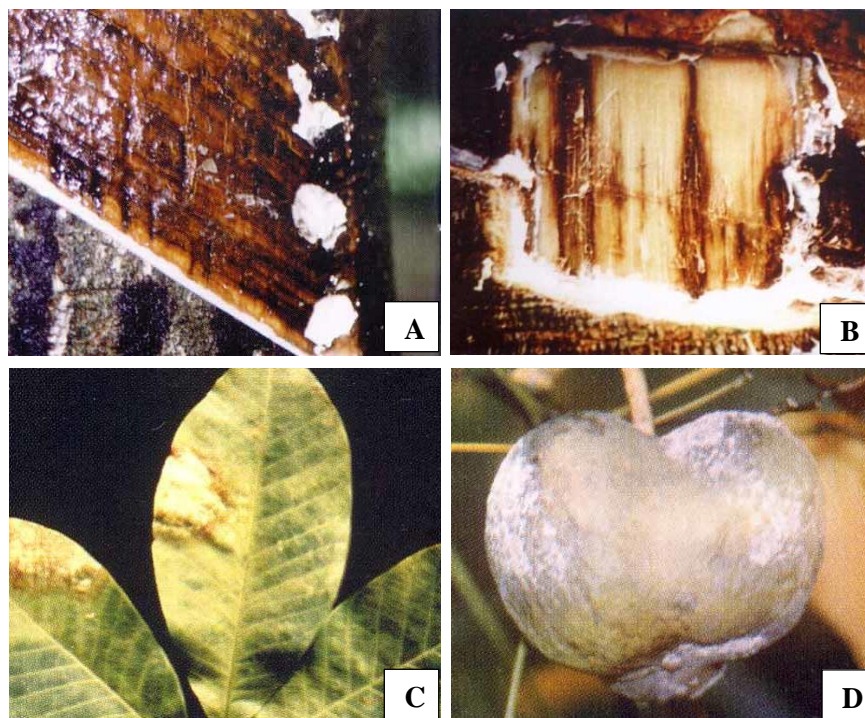


Fig. 1.3 Black stripe (A and B), leaf-fall (C) and fruit rot (D) of rubber tree caused by *P. palmivora* (http://pnpandbest.com/rubber/pnp_problems/pnp_problems07.html)

The black stripe and leaf-fall in *H. brasiliensis* are usually found in Thailand which can reduce the yield and quality of the rubber latex. The early symptoms of the black stripe are not clear. Appearances of slightly discolored area above the cutting surface and vertical fissures in the renewing bark are frequently observed (Fig. 1.3A). When bark is removed, dark vertical lines are visible (Fig. 1.3B). In the infection progresses, broad lesions are formed and finally spread covering all of tapping panel. Infection can occur on untapped area resulting in a wound called canker. In the early stage, the canker symptoms are not obvious, but in the severe stage, the bursting of bark and oozing out of latex are found. Incidence of black stripe is associated with persisting long periods of prolonged rainy season. In areas where abnormal leaf fall occurred, the sporangia can be washed from the tree canopy. Canker appearance is common disease in leaf fall areas by spreading from the canopy.

1.2.2 *Phytophthora palmivora*

P. palmivora infects a thousand or more plant species including agricultural, horticultural and ornamental crops. It infects more than 200 plant species in the tropics and subtropics (Erwin and Ribeiro 1996). For example, economically important hosts include papaya, cacao, pineapple, durian, rubber tree, citrus, and oil palm.

Taxonomic classification of *P. palmivora* is:

Phylum: Oomycota

Class: Oomycetes

Order: Pythiales

Family: Pythiaceae

Genus: *Phytophthora*

Species: *Phytophthora palmivora*

From <http://ippc.acfs.go.th/pest/G001/T008/FUNGI105>

P. palmivora is a hemibiotrophic pathogen. It can survive in dead tissue and acts as a necrotrophic pathogen. At the beginning of infection, it commonly grows as a biotroph then switches to a necrotroph at later stages of infection. *P. palmivora* is classified among the oomycetes which has characteristics distinct from the true fungi. Oomycete cell wall mainly consists of beta-1,3 glucan, whereas the fungal cell wall is chitin (Werner *et al.*, 2002; Latijnhouwers *et al.*, 2003). In Thailand, *P. palmivora* causes stem rot in both the durian tree (*Durio zibethinus*) and the rubber tree (*Hevea brasiliensis*), with resultant crop losses.

P. palmivora spores may directly or indirectly cause infection. Sporangia produced on infected roots, stems, leaves or fruits are able to directly germinate on the plant surface (Fig. 1.4). They can also produce small zoospores which can swim in soil, water or on a wet surface of plants until they germinate and enter the plants. Sporangia and zoospores are spread by wind and water. Zoospores can reach the plant surface, attach to the plant surface by secretion of adhesion molecules and encyst (Hardham and Shan 2009). After reach and attachment of the host, the zoospore germinates a germ tube; in addition, an appressorium is developed in order to penetrate the host surface (Fig. 1.4) (Latijnhouwers *et al.*, 2003). When penetration

succeeded, intercellular hyphae form haustoria which are used to penetrate and obtain nutrients from the adjacent plant cells (Mendgen and Hahn 2002). *Phytophthora* spp. use appressoria and haustoria as the infection structures to reach the host cell (Fawke *et al.*, 2015). Cell wall-degrading enzymes are also expressed in germ tubes and infection hyphae to facilitate penetration (Pryce-Jones *et al.*, 1999).

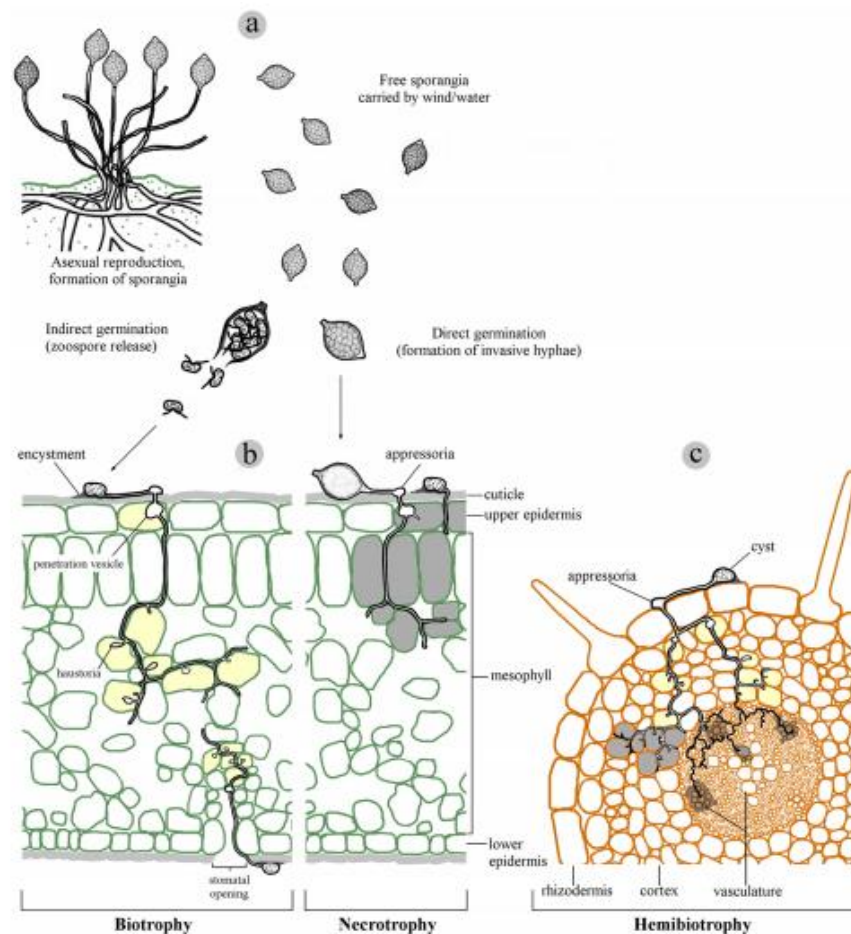


Fig. 1.4 Infection strategies and lifestyles of oomycetes. (a) Typical asexual *Phytophthora* dispersal structures. (b) Leaf colonization. (c) Root colonization (Fawke *et al.*, 2015).

Phytophthora spp. can produce secreted extracellular proteins, some of them are called elicitors which trigger plant defense reaction. Many elicitors produced by *Phytophthora* spp. have been identified and characterized. The 10 kDa extracellular, INF1 elicitor produced by *P. infestans* induces a hypersensitive response in plants. INF1-deficient *P. infestans* strains induce disease lesions when inoculated on *N.*

benthamiana (Kamoun *et al.*, 1998). The OPEL protein from *P. parasitica* causes cell death, callose deposition, production of reactive oxygen species and salicylic acid (SA)-responsive gene expression. Furthermore, *N. benthamiana* leaves infiltrated with the OPEL before challenging with *P. parasitica* display disease resistance (Chang *et al.*, 2015). *P. parasitica* also produces a 34 kDa glycoprotein elicitor (CBEL) which induces necrosis. Moreover, tobacco leaves pretreatment with this elicitor result in prevention of *P. parasitica* infection (Mateos *et al.*, 1997; Gaulin *et al.* 2006). The 32 kDa glycoprotein secreted by *P. megasperma* induces hypersensitive response (HR), SA accumulation and defense-related gene expression in tobacco (Baillieul *et al.*, 1995). An extracellular 42 kDa *P. megaspermaa* glycoprotein induces phytoalexin accumulation and defensive gene expression in cell culture and protoplasts of parsley (Parker *et al.*, 1991). The soybean pathogen *P. sojae* produces a glycoside hydrolase family 12 (GH12) protein which acts as xyloglucanase and beta-glucanase, induces cell death in *N. benthamiana* and exhibits as a crucial virulence factor during its infection (Ma *et al.*, 2015). An oligopeptide of 13 amino acid (Pep-13) within the cell wall glycoprotein (GP42) of *P. sojae* triggers phytoalexin accumulation, an oxidative burst and defensive gene expression in parsley (Nürnberg *et al.*, 1994; Hahlbrock *et al.*, 1994; Brunner *et al.*, 2002). For *P. palmivora*, a new protein 75 kDa and elicitor induce total phenolic compound and scopoletin accumulations in cell suspension and leaves of *H. brasiliensis* (Churngchow and Rattarasarn, 2000; Dutsadee and Churngchow, 2008). Many elicitors display the different activity on plant defense responses. That is significant and challenging to discover the new elicitors and their effects on plant defense response for better understanding of plant-microbe interaction.

Microorganisms, however, are known for their ability to synthesize polysaccharides with different structural complexities (Seviour *et al.*, 1992; Sutherland, 1994). These polysaccharides either remain attached to the cell surface or are found in the extracellular medium (Banik *et al.*, 2000). Woodward *et al.*, (1980) studied the structures and properties of wilt-inducing polysaccharides from *Phytophthora* species. Valepyn *et al.*, (2014) showed that the water soluble exopolysaccharide (EPS) from *Syncephalotrium racemosum* induces the phenylalanine ammonia lyase activity and H₂O₂ synthesis in *A. thaliana* cell suspensions. EPS

production from fungi has been studied over the last two decades. It has been showed that many fungi can produced different EPS which have different and interesting biological activities (Yang and He, 2008). In *P. palmivora*, the biological activity of its ESP has not been reported.

1.2.3 Carrageenan

Carrageenan is sulphated linear polysaccharides of D-galactose and 3,6-anhydro-D-galactose extracted from certain species of red seaweeds (Rhodophyta). It is evident that carrageenan is a large molecule being made up of 1000 residues. There are three main types, kappa, iota, and lambda carrageenans. In a kappa-type seaweed extract, some of the D-galactose contains 4-sulphate ester groups. Iota carrageenan is characterized by having 4-sulphate ester groups on D-galactose residues and 2-sulphate ester groups on 3,6-anhydro-D-galactose residues. The λ -carrageenan structure consists of a repeating dimer of D-galactose (A unit) having a sulphate group in C2, linked to a D-galactose (B unit) which is sulphated in C2 and C6 (Fig. 1.5). The position of sulphate ester group is determined with an infrared spectrophotometer (Table 1.1).

Table 1.1 Absorbance of carrageenans determined with an infrared spectrophotometer

Wave number(cm^{-1})	Functional group	Absorbance		
		Kappa	Iota	Lambda
1210 -1260	Ester sulphate	very strong	very strong	very strong
1010 -1080	Glycosidic linkage	very strong	very strong	very strong
928 – 933	3,6-anhydro-D-galactose	strong	strong	absent- low
840 – 850	D-galactose-4-sulphate	medium	medium	absent
820 – 830	D-galactose-2-sulphate	absent	absent	medium
810 – 820	D-galactose-6-sulphate	absent	absent	medium
800 – 805	3,6-anhydro-D-galactose-2-sulphate	absent- low	medium	absent

From carrageenan book in www.cpkelco.com

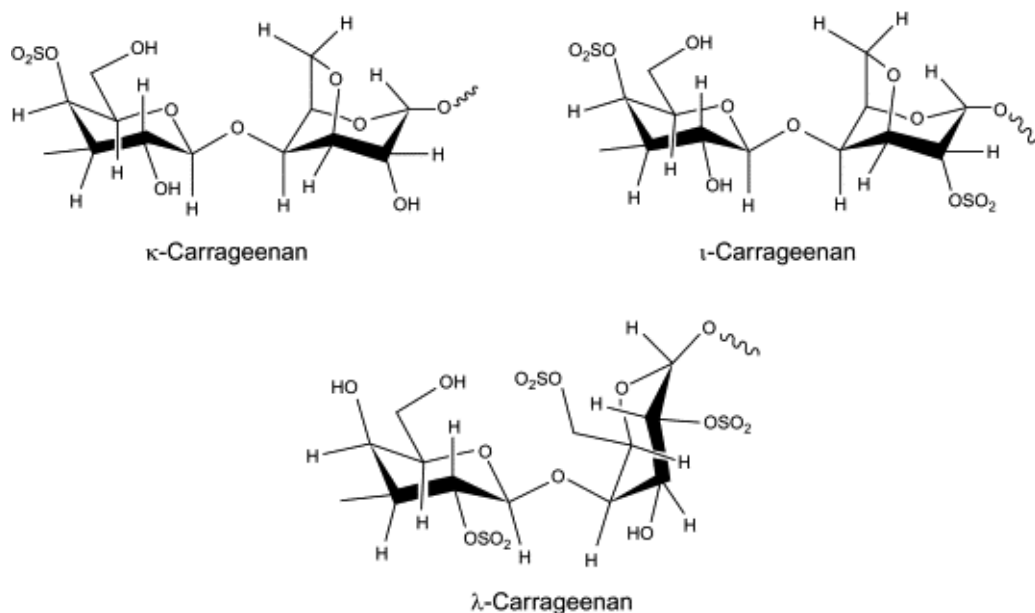


Fig. 1.5 Structure of carrageenans (Kariduraganavar *et al.*, 2014)

1.2.4 *Acanthophora spicifera*

A. spicifera is a red seaweed of the Rhodomelaceae family (order Ceramiales). Parekh *et al.*, (1989) reported that the structure of carrageenan extracted from *A. spicifera* is a λ -type-carrageenan.

Taxonomic classification of *A. spicifera* is:

Kingdom: Plantae

Phylum: Rhodophyta

Subphylum: Eurhodophytina

Class: Florideophyceae

Subclass: Rhodymeniophycidae

Order: Ceramiales

Family: Rhodomelaceae

Genus: *Acanthophora*

Species: *Acanthophora spicifera*

From http://www.algaebase.org/search/species/detail/?species_id=3309

The λ -carrageenan structure consists of a repeating dimer of D-galactose (A unit) having a sulphate group in C2, linked to a D-galactose (B unit) which is sulphated in C2 and C6. It has been reported that the sulphated polysaccharide from *A. spicifera* composed of A and B units of galactose molecules. In addition, some of the B unit

was 3,6-anhydro- α -L-galactose (Duarte *et al.*, 2004) which resulted in the loss of C6-sulphate. However, applications and an alternative purification method of *A. spicifera* extract in plant induced resistance have rarely been reported.

1.2.5 Elicitors

Elicitors are biofactors or chemicals from many sources that are able to induce physiological changes of targeted living organisms. In plants, elicitors are chemical obtained from many sources that are able to trigger morphological and physiological responses and phytoalexin accumulation. Elicitors are classified into two types, biotic elicitors from fungi, bacteria, viruses or herbivores and plant cell components as well as chemicals that are released at the attack site by plants upon pathogen invasion and abiotic elicitors such as metal ions.

Oligo- or polysaccharides are the most well characterized signal molecules in elicitation such as chitosan, chitin, xyloglucans, oligogalacturonide and β -glucan. They have elicitor activity in many plant species and highly activate phytoalexin accumulation in plants (Zhao *et al.*, 2005). Elicitors have been used as alternative substance to induce economic crop resistance against pathogen infection. A main class of plant defense inducers is oligosaccharides which can be released from fungal and oomycete cell walls during the interaction with their host plants (Felix *et al.*, 1991). Many marine macroalgae have been respected as a source of important polysaccharidic elicitors and environmental friendly biostimulants which can not be found in land plants (Klarzynski *et al.*, 2000). Broad spectra of algal polysaccharides have been characterized for their plant defense response enhancing activity and already utilized on economic crop plants to induce defense responses against diseases and pests (Klarzynski *et al.*, 2000; Klarzynski *et al.*, 2003). For example, laminarin, a carbohydrate extracted from the brown algae, *Laminaria digitata*, can enhance defence responses in cell suspensions of tobacco (*Nicotiana tabacum*) (Klarzynski *et al.*, 2000), grapevine (*Vitis vinifera*) (Aziz *et al.*, 2003), alfalfa (*Medicago sativa*) (Cardinale *et al.*, 2000). Moreover, many carrageenans and other sulphated polysaccharides from red alga act as inducer of defense response in several plants. The algal polysaccharide carrageenans can elicit plant defense responses possibly through the sulphate content (Mercier *et al.*, 2011). Kappa-carrageenan extracted from red alga, *Tichocarpus crinitus*, enhances tobacco leaves against local infection by

tobacco mosaic virus (Nagorskaia *et al.*, 2008). Plants treated with ι - and κ -carrageenan exhibit reduction of leaf damage caused by *Trichoplusia ni*, whereas those treated with λ -carrageenan cannot (Sangha *et al.*, 2011). Vera *et al.*, (2011) showed that seaweed oligosaccharides and polysaccharides can stimulate host defense responses and enhance defense response against plant pathogen infections.

Many experiments in plant and animal systems elucidated that oligo- and polysaccharides having sulphate residues show high biological elicitor activity. It has been suggested that polysaccharides which is chemically sulphated can increase their elicitor activity (Bouarab *et al.*, 1999; Sangha *et al.*, 2010). Recent reports explained that after chemical sulfation of laminarin, it becomes a stronger inducer of the salicylic acid (SA) signaling pathway in tobacco leaves. This higher elicitor activity is determined by the induction of a broad spectrum of defense responses (Ménard *et al.*, 2004).

1.2.6 The plant immune system

Responses to infection of plants use a two-branched innate immune system. Although plants lack a somatic adaptive immune system and mobile defender cells but they have the innate immunity of each cell and systemic signals translocated from infection sites (Dangl *et al.*, 2001; Ausubel, 2005; Chisholm *et al.*, 2006). One of the two branches of plant immune system is transmembrane pattern recognition receptors (PRRs) used to respond microbial- or pathogen-associated molecular patterns (MAMPS or PAMPs) such as flagellin (Zipfel and Felix, 2005). The other acts inside the cell detected by the polymorphic nucleotide binding-leucine rich repeat receptor (NB-LRR) proteins which are encoded by resistance (R) genes (Dangl *et al.*, 2001).

Jones and Dang (2006) showed that plant immune system can be represented as a four phased 'zigzag' model (Fig. 1.6). In phase 1, PAMPs (or MAMPs) are recognized by PRRs resulting in PAMP-triggered immunity (PTI) that can inhibit further colonization. In phase 2, successful pathogens produce effectors to promote pathogen virulence. Effectors can interfere with PTI that is called effector-triggered susceptibility (ETS). In phase 3, a secreted effector is specifically recognized by NB-LRR proteins leading to activate effector-triggered immunity (ETI). ETI is an accelerated and amplified PTI response resulting in disease resistance and it usually is

a hypersensitive cell death response occurring at the infection site. In phase 4, pathogens try to avoid ETI by acquiring additional effectors to suppress ETI.

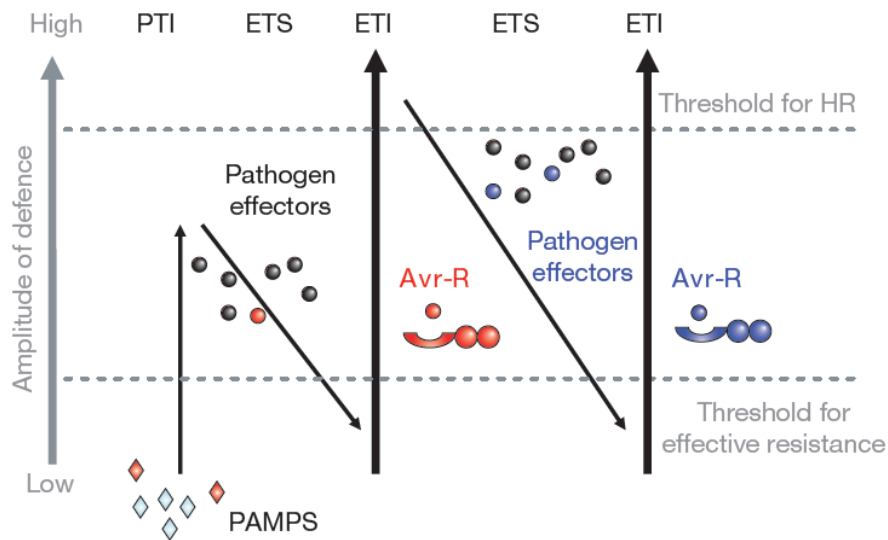


Fig. 1.6 A zigzag model illustrates the quantitative output of the plant immune system (Jones and Dang, 2006).

An important process in plant defenses against pathogens is hypersensitive response cell death. It is induced by accumulations of O_2^- and H_2O_2 which finally trigger a protein kinase-mediated cell death process similar to program cell death (PCD) (Mehdy 1994; Levine *et al.*, 1996). Accumulation of H_2O_2 inhibits the growth of biotrophic pathogens (Thordal-Christensen *et al.*, 1997), whereas production of H_2O_2 promotes the growth of necrotrophic pathogens (Govrin and Levine 2000). Lee and Rose (2010) suggested that the hemibiotrophic pathogen *P. infestans* facilitates the development of infection by secreting a cell death suppressor during its biotrophic phase and producing cell death inducers in its necrotrophic phase. The virulence of *Botrytis cinerea*, a necrotrophic pathogen, is conducted by a number of lytic enzymes, toxins, high levels of reactive oxygen species and necrosis-inducing factors (van Kan 2006; Choquer *et al.*, 2007). Govrin and Levine (2000) concluded that *B. cinerea* induces the accumulation of H_2O_2 to kill *Arabidopsis thaliana* cells and facilitate its invasion. HR cell death resists biotroph infection by disconnecting nutrient supplies resulting in limiting pathogen growth, however, it may provide growth substrates for invasive necrotrophs (Govrin and Levine 2000). Hemibiotrophs, meanwhile, establish

a biotrophic stage within the plant, kill host cells and then switch to a necrotrophic fungal phase (Horbach *et al.*, 2011).

HR cell death is activated by the salicylic acid (SA) signaling pathway. Torres *et al.* (2005) and Lu *et al.* (2009) showed that a high level of SA facilitated PCD in *A. thaliana*. SA and jasmonic acid (JA) are secondary messengers involved in PAMP-triggered immunity and effector-triggered immunity (van Loon *et al.* 2006; Bent and Mackey 2007). The SA-signaling pathway activated by biotrophs can suppress the JA-signaling pathway which is involved in blocking necrotrophic pathogen infection (Spoel *et al.*, 2007; Koornneef *et al.*, 2008; Pieterse *et al.*, 2012). PCD is the effective defense against biotrophic pathogens which is regulated by the SA-dependent pathway. On the other hand, necrotrophic pathogens benefit from host cell death and therefore are not restricted by the SA-dependent pathway but are controlled by the JA-signaling pathway (Glazebrook 2005). Some pathogens can mimic signaling pathways to suppress defense responses. For example, *B. cinerea* produces a beta-glucan elicitor which activates the SA-signaling pathway and suppresses the JA-signaling pathway (El Oirdi *et al.*, 2011). The phytotoxin coronatine, a JA mimic produced by the biotrophic pathogen *Pseudomonas syringae*, promotes its infection by suppressing the SA-signaling pathway (Brooks *et al.*, 2005; Cui *et al.*, 2005)

1.2.7 Cell death in plants

The reduction of oxygen gives rise to accumulation of reactive oxygen species (ROS) including superoxide, hydrogen peroxide and hydroxyl radical which can be produced by chloroplasts, mitochondria and peroxisomes. Superoxide radical occurred due to reduction of electron transport components involving in photosystem (PS) I and a reaction associated with the photorespiratory cycle in the peroxisome. NADPH-dependent oxidases, plasma membrane enzyme, can reduce oxygen to superoxide. Inhibition of this oxidase impairs ROS production (Allan and Fluhr, 1997). The mitochondrial electron transport chain can also produce ROS transferring of a single electron to oxygen producing superoxide. The high level of ROS causes photooxidative damage to DNA, proteins and lipids resulting in cell death. At high concentrations (oxidative stress), the various ROS can react indiscriminately with almost all cellular components provoking, for example, destruction of protein and DNA strand breaks (Beckman and Ames, 1997; Berlett and Stadtman, 1997).

ROS can act as signaling molecules which are involved in growth and developmental processes, stress hormone production, pathogen defense responses (Apel and Hirt, 2004). Cell death is also described during incompatible plant-pathogen interactions including hypersensitive response (Pennell and Lamb, 1997). Although necrosis and PCD have been quite well defined in animals, in plants, there are some overlaps of the phenotypic and molecular hallmarks between them. It is hard to discriminate between the two events in plants (Van Breusegem and Dat, 2006). They propose that necrosis is caused by extrinsic factors such as phytotoxic accumulation of specific molecules (Van Breusegem and Dat, 2006).

ROS-dependent PCD is associated with increase of both salicylic acid (SA) and ethylene levels having a positive feed-back that can promote ROS-dependent cell death (Fig. 1.7) (de Jong *et al.*, 2002; Moeder *et al.*, 2002; Danon *et al.*, 2005). On the other hand, jasmonic acid plays an antagonistic effect in this oxidative-dependent cell death cycle. The short H_2O_2 induction is sufficient to induce PCD in leaves, in contrast, the continuous H_2O_2 accumulation leads to necrosis and ROS-mediated lipid peroxidation (Montillet *et al.*, 2005)

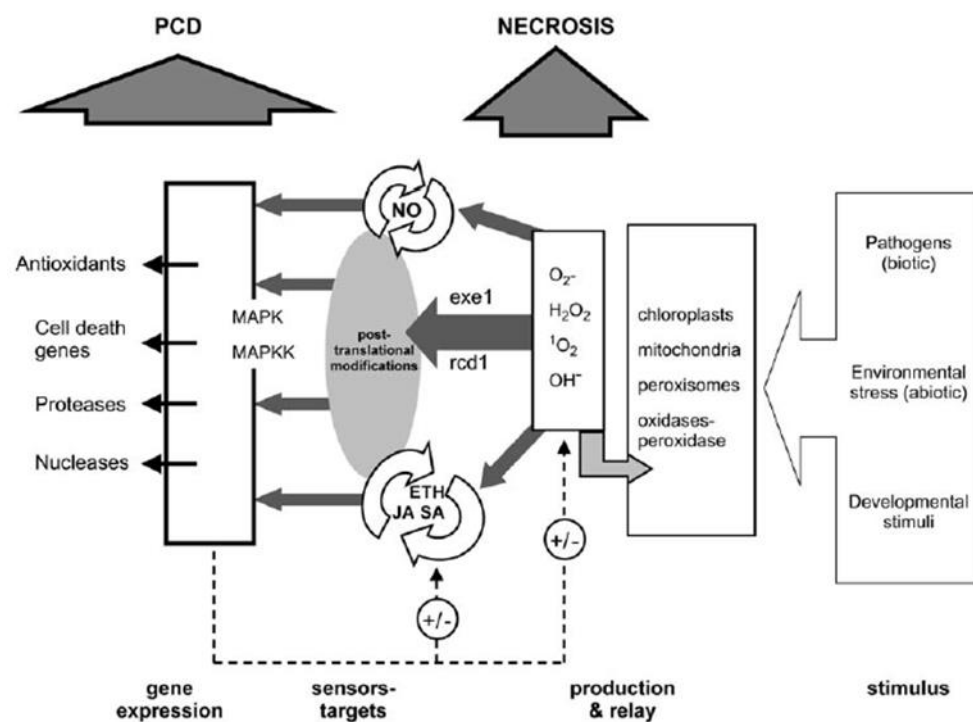


Fig. 1.7 Schematic representation of ROS-dependent cell death pathways (Van Breusegem and Dat, 2006).

Fu *et al.* (2012) explained why high SA levels can cause cell death in plants: the level of SA affected NPR3 and NPR4, the cullin 3 (CUL3) adapters for degradation of NPR1 (a cell death suppressor). At high concentrations, SA binds to NPR3 and mediates the degradation of NPR1, which induces cell death. But at low concentrations, SA cannot bind to NPR3 and connects instead to NPR4, which blocks NPR1 degradation, resulting in cell survival (Fig. 1.8).

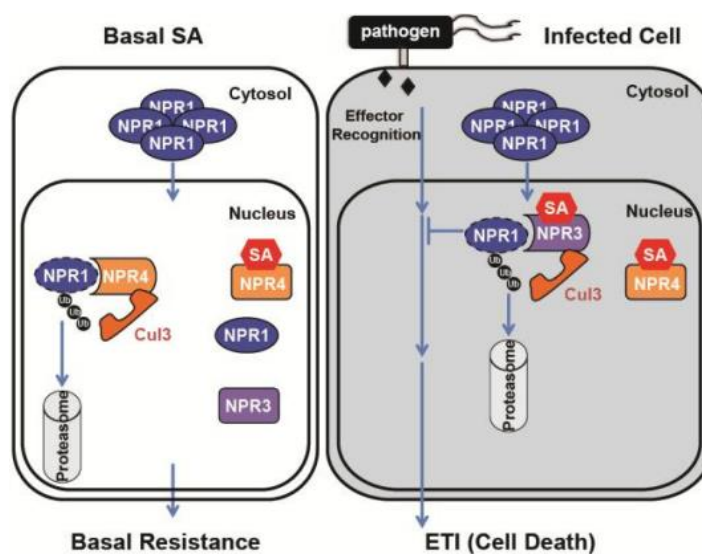


Fig. 1.8 Schematic representation the level of SA affected NPR3 and NPR4 (Fu *et al.* 2012).

1.2.8 Induced resistance

A state of enhanced defensive capacity established by plants in response to appropriate stimuli is known as induced resistance. This plant defense mechanism is highly effective defense responses against a wide range of subsequent pathogen infection (Van Loon *et al.*, 1998). Systemic acquired resistance (SAR) and induced systemic resistance (ISR) are two forms of induced resistance. SAR depends on accumulations of pathogenesis-related proteins and salicylic acid (SA) (Pieterse *et al.*, 1996), whereas ISR involves jasmonic acid (JA) and ethylene (ET) signaling pathways (Pieterse *et al.*, 1998).

An extremely desirable form of resistance that provides broad-spectrum resistance and long-lasting in plants is SAR (Ross, 1961; Kuc, 1987) which involves the generation of mobile signals within 4 to 6 hours in the primary infected tissues

and then it rapidly translocate to systemic uninfected tissues in order to prepare the systemic tissue for following infections from related/unrelated pathogens. Mobile signals in SAR include the methyl SA (MeSA), a dicarboxylic acid as a azelaic acid (AzA), an abietane diterpenoid, dihydroabietinal (DA), and a phosphorylated sugar derivative, glycerol-3-phosphate (G3P). SAR signal generation of AzA, DA, and G3P translocate to the systemic tissue within 6 to 12 hours post primary infection (Chanda *et al.*, 2011; Chaturvedi *et al.*, 2012; Yu *et al.*, 2013). MeSA has been previously shown to accumulate during SAR and suggested to induce defense via its conversion to SA (Shulaev *et al.*, 1987).

1.2.9 Signal transduction

1.2.9.1 Salicylic acid signaling

SA is synthesized from phenylalanine (Fig. 1.9). In addition, there is the alternative pathway for SA biosynthesis which SA can be synthesized from chorismate through isochorismate. Some bacteria synthesize SA from chorismate through isochorismate. The enzymes isochorismate synthase (ICS) and isochorismate pyruvate lyase (IPL) catalyze the two steps from chorismate to SA (Serino *et al.*, 1995). Recently, several studies have shown that overexpression of these two bacterial enzymes in transgenic plants enhances SA accumulation (Mauch *et al.*, 2001; Verberne *et al.*, 2000).

SA plays a significant role in various plant-pathogen interactions. It activates defense responses and is generally involved in defense against biotrophs (Glazebrook, 2005; Spoel *et al.*, 2007). In response to hemibiotrophs, SA has an early role during the biotrophic stage of the pathogen infection (Halim *et al.*, 2007) which is important for hypersensitive response leading to induce the death of cells and inhibit infection of the cell containing pathogens.

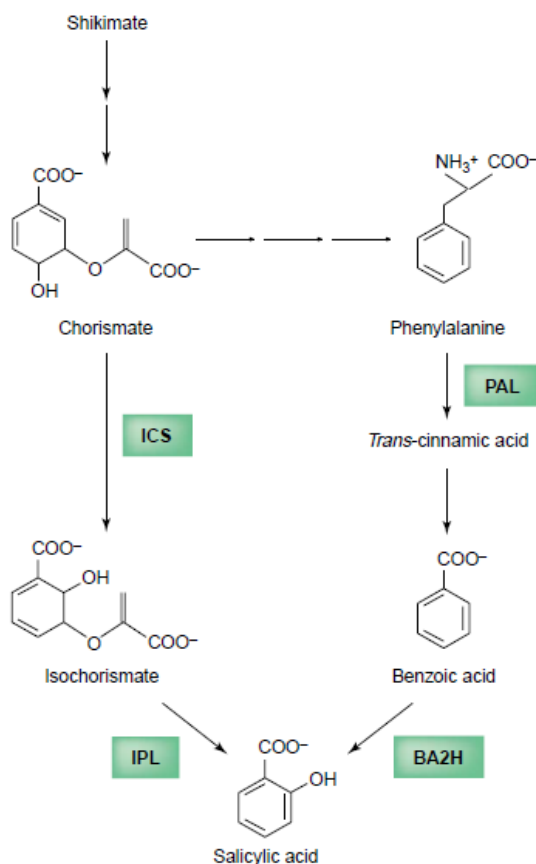


Fig. 1.9 Proposed pathways for the biosynthesis of SA in plants (Shah, 2003)

(ICS:isochorismate synthase, IPL: isochorismate pyruvate lyase, PAL: phenylalanine ammonia lyase, BA2H: benzoic acid-2-hydroxylase)

The cellular redox balance is changed by increase of SA levels leading to partial reduction of the key transcriptional regulator of nonexpressor of PR gene 1 (NPR1) and releasing monomeric NPR1 from cytoplasmic oligomers through thioredoxin-mediated reduction of intermolecular disulfide bridges (Tada *et al.*, 2008). Monomerization of NPR1 enhances its translocation to the nucleus where NPR1 binds SA through NPR1 cysteine residues coordinated by copper leading to a conformational change and releasing of NPR1 C-terminal transactivation domain from the N-terminal autoinhibitory domain (Wu *et al.*, 2012). Nuclear NPR1 can interact with the TGA transcriptional factors that are able to act as activators or repressors, and promote the transcriptional activation of SA-responsive genes such as PR-1 (Fig. 1.10) (Despres *et al.* 2000; Fan and Dong, 2002)

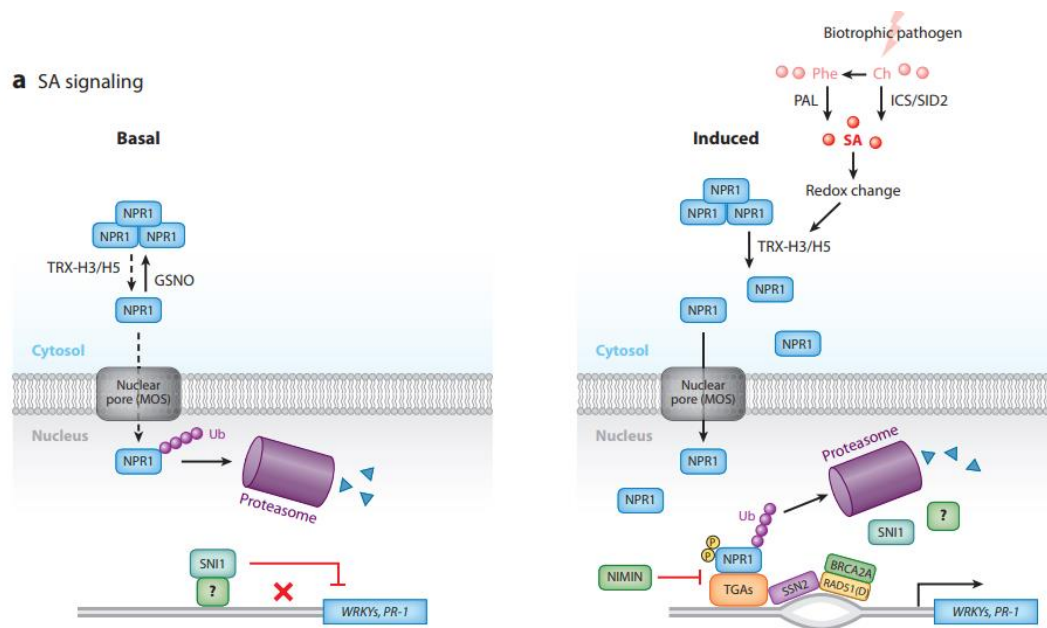


Fig. 1.10 Schematic overview of the salicylic acid (SA) signaling pathway (Pieterse *et al.*, 2012)

Many marker genes including pathogenesis-related genes PR-1, PR-2, and PR-5 are frequently used to illustrate a SA-responsive plant defense (Linthorst and Van Loon, 1991). These genes are partially regulated by NPR1, a key regulatory gene in the SA signaling pathway (Cao *et al.*, 1994; Delaney *et al.*, 1994; Shah *et al.*, 1997). The NPR family consists of NPR1 and NPR1-like genes such as NPR3. NPR1 plays an important role in downstream of SA and is specifically important for systemic acquired resistance induction. It can interact with the TGA family of transcription factors involving in SA signaling. Lossing of this interaction leads to impair of SAR induction (Deprés *et al.*, 2000).

SA induces gene expression which is related to biosynthesis and production of some plant secondary metabolites (Taguchi *et al.*, 2001) such as phytoalexins, low-molecular-weight antimicrobial compounds that accumulate in plants in response to pathogen infection or abiotic stress (Ahuja *et al.*, 2012). Induction of these compounds is important for enhancement of disease resistance to pathogens and pests.

1.2.9.2 JA signaling

JA is lipid-derived compounds that are synthesized rapidly via the oxylipin biosynthesis pathway upon pathogen or insect attack (Gfeller *et al.*, 2010). JA biosynthesis starts with the release of α -linolenic acid (α -LA) from membrane lipids. Upon synthesis, JA can be readily metabolized to MeJA through the activity of JA carboxyl methyltransferase (JMT) (Seo *et al.*, 2001) or conjugated to amino acids such as isoleucine via the JA conjugate synthase JAR1 (Staswick and Tiryaki, 2004) which lead to synthesis of jasmonoyl-isoleucine (JA-Ile), a biologically highly active compound (Fig. 1.11) (Fonseca *et al.*, 2009).

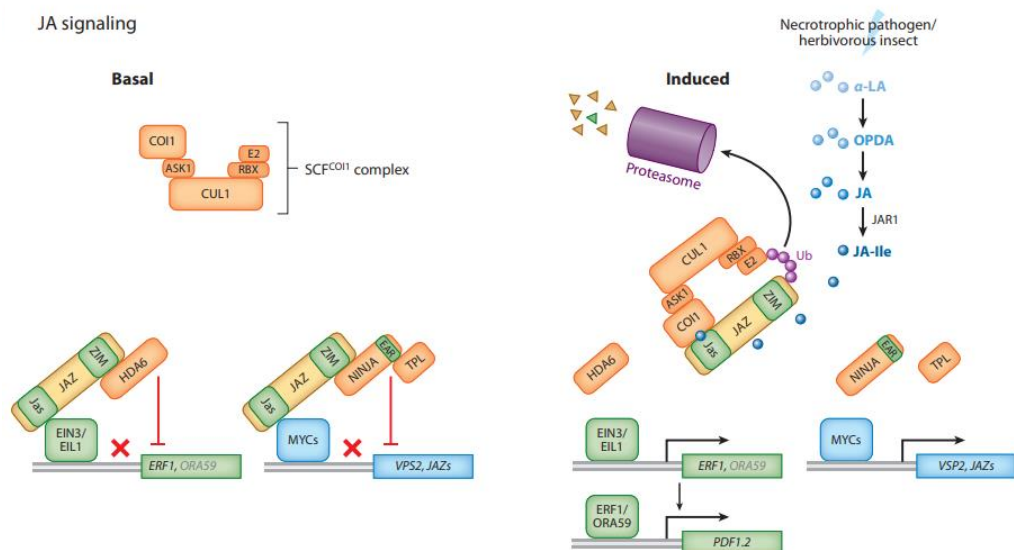


Fig. 1.11 Schematic overview of the jasmonic acid (JA) signaling pathway (Pieterse *et al.*, 2012)

JA is generally thought to play a larger role in defense against necrotroph infection (Glazebrook *et al.*, 2005; Spoel *et al.*, 2007). JA-Ile, the bioactive hormone is recognized by a receptor complex consisting the F-box component Coronatine Insensitive1 (COI1) of the SCF (Skp1/Cullin/F-box)-type E3 ubiquitin ligase COI1 and a member of the Jasmonate Zim domain (JAZ) protein family (Fig. 1.11) (Fonseca *et al.*, 2009; Sheard *et al.*, 2010). Before their co-receptor function, JAZ proteins are also repressors of TFs regulating JA responses such as MYC2, MYC3 and MYC4 (Fernandez-Calvo *et al.*, 2011), and required the general co-repressors TOPLESS (TPL) through the adaptor protein of Novel Interactor of JAZ (NINJA) (Pauwels *et al.*, 2010). After JA-Ile recognition, JAZ are ubiquitinated and targeted

for proteasomal degradation (Pauwels and Goossens, 2011) which releases TFs freely and activates transcription of JA-responsive genes (Memelink, 2009). Degradation of JAZ proteins lead to induce JA pathway-related defense genes (Table 1.2).

1.2.9.3 Abscisic acid signaling

Abscisic acid (ABA) can be synthesized by protein from ABA synthesis genes (Table 1.2). It plays a role in regulating of physiological processes including seed germination and dormancy, lateral root elongation, seedling development as well as responses to environmentally abiotic stresses such as drought (Ton *et al.*, 2004; Adie *et al.*, 2007). ABA has been reported to be negative and positive regulators of disease resistance including ROS generation, callose deposition and synergistic effects with JA (Asselbergh *et al.*, 2008).

Table 1.2 The marker genes of SA, JA, ethylene, and ABA signaling pathways (Derksen *et al.*, 2013).

Pathway	Genes
Salicylic acid	Phenylalanine ammonia lyase (PAL) Pathogenesis-related protein 1 (PR-1) endo-1,3- β -d-glucanase (PR-2); thaumatin-like (PR-5)
Jasmonic acid/Ethylene	Ethylene response factor 1 (ERF1) Lipoxygenase (POTLX3) ACS (Ethylene synthesis gene) Thionin (THI2.1) Defensin (PDF1.2); chitinase (PR-3) Hevein-like protein (PR-4) Proteinase inhibitor (PR-6) Peroxidase (PR-9)
Abscisic acid	ABA transcription factors (ABREs/ABFs) ABA synthesis genes

1.2.10 Crosstalk among signaling pathways

1.2.10.1 Suppression of JA pathways by SA pathway

The antagonism between SA and JA pathway frequency occurs via NPR1, the regulatory protein playing as transcriptional factor (Spoel *et al.*, 2003). It is associated to both ISR and SAR and required for a SA signaling pathway. Interestingly, NPR1 mutant leads to enhancement of the lipoxygenase 2 (LOX2) expression (Spoel *et al.*, 2003), an important enzyme in the octadecanoid pathway involving in the JA biosynthesis. In many studies showed that decrease of SA levels and having a higher JA expression lead to enhance disease susceptibility in many plants (Dewdney *et al.*, 2000; Brodersen *et al.*, 2006)

The PR-genes related to the JA pathways have been shown to be a target for analysis of antagonism by SA such as plant defensins (PDF1.2). They are associated with the JA pathways presenting at higher levels in SA-deficient than wild-type plants (Penninckx *et al.*, 1996). Other PR-genes such as proteinase inhibitors induced by the JA pathways are also inhibited by SA and derivatives (Doares *et al.*, 1995).

A transcription factor, WRKY70 is affected by both SA and JA pathways. WRKY70 is induced by SA and suppressed by JA. It activates genes involved in the SA pathway including PR-2 and PR-5, and represses genes responding to JA such as Vegetative Storage Protein (VSP) and PDF1.2 (Li *et al.*, 2004).

1.2.10.2 Suppression of SA by JA pathways

JA can negatively affect the SA pathway, even though the examples of this event are rarely reported (Derksen *et al.*, 2013). Mitogen-activated protein kinase 4 (MPK4) acts as a negative regulator of SAR and is controlled by the SA pathway (Petersen *et al.*, 2000). In addition, it is also required for PDF1.2 and thionin 2.1 (THI2.1) expressions through the JA and/or ET pathways. Brodersen *et al.* (2006) showed that Enhanced Disease Susceptibility 1(EDS1) acts as a SA pathway inducer and a JA and/or ET pathways repressor (Fig. 1.12), whereas MPK4 can act the opposite effects (Fig. 1.12).

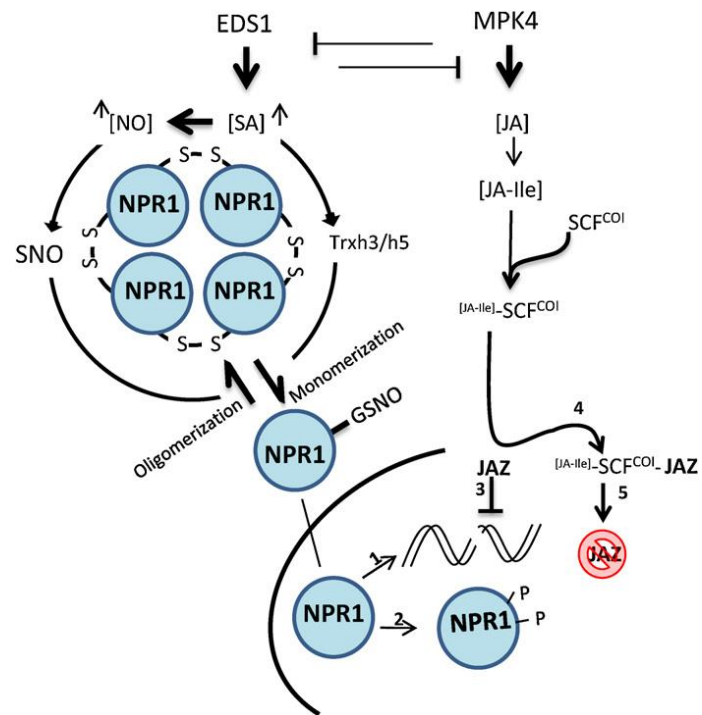


Fig. 1.12 Crosstalk between SA and JA/ET pathway through EDS1 and MPK4 (Derksen *et al.*, 2013).

CHAPTER 2

A SECRETED PROTIEN OF 15 kDa PLAYS AN IMPORTANT ROLE IN *PHYTOPHTHORA PALMIVORA* DEVELOPMENT AND PATHOGENICITY

2.1 Introduction

Oomycetes are fungal-like microorganisms belonging to the kingdom Straminipila (Baldauf 2003; Kamoun 2003). Their characteristics are distinct from true fungi since oomycetes are diploid or polyploid whereas fungi are haploid for most of the life cycles (Sansome 1977; Judelson 1997; Kamoun 2003). In addition, cell walls of oomycetes mainly consist of 1,3-beta-glucan, while the major cell wall constituent of fungi is chitin (Erwin and Ribeiro 1996). Oomycetes include many destructive plant pathogens, among which are over 100 species in the genus *Phytophthora* that severely threaten agricultural production and natural ecosystems (Erwin and Ribeiro 1996; Kamoun *et al.*, 2015).

Phytophthora palmivora is a hemibiotrophic oomycete pathogen that infects more than 200 plant species in the tropics and subtropics (Erwin and Ribeiro 1996). Examples of economically important hosts include papaya, cacao, pineapple, durian, rubber tree, citrus, and oil palm. In addition, it also infects model plant species, such as *Nicotiana benthamiana* and *Medicago truncatula* (Huisman *et al.*, 2015; Rey *et al.*, 2015; Ekchaweng *et al.*, 2017). Similar to other *Phytophthora* spp., plant infection by *P. palmivora* starts with motile zoospores, which encyst after contacting plant surfaces, followed by formation of germ tubes and then appressoria to penetrate the plant surface (Judelson and Blanco 2005; Huisman *et al.*, 2015; Carella *et al.*, 2018). During infection, *P. palmivora* initially grows as a biotroph by forming haustoria inside the host cells to get nutrients, and then switches to necrotrophy in the later stages of infection (Le Fevre *et al.*, 2016; Evangelisti *et al.*, 2017). Evidence suggests that establishment of the biotrophic stage and transition to necrotrophic stage require the functions of effector proteins (Lee and Rose 2010; Ali *et al.*, 2017).

Effector proteins are secreted proteins that pathogens produce to suppress plant immunity and to alter host cell physiology to promote infection (Hogenhout *et*

et al., 2009). Based on subcellular localization in the host plants, oomycete effectors are broadly classified into two categories, apoplastic effectors and cytoplasmic effectors (Kamoun 2006). Apoplastic effectors function in the plant extracellular space, and include hydrolytic enzymes, enzyme inhibitors, lipid transfer proteins and necrotizing toxins (Wawra *et al.*, 2012; Ali *et al.*, 2017). Cytoplasmic effectors are translocated inside host cells functioning at various subcellular compartments, such as RxLR-effectors and crinklers (Wawra *et al.*, 2012). Many putative effector proteins have been found in *P. palmivora* transcriptomic and genomic sequences (Ali *et al.*, 2017; Evangelisti *et al.*, 2017). Characterization of these effectors is critical to our understanding of the diversity of molecular mechanisms of *P. palmivora* pathogenicity, which remain largely unknown.

During pathogen infection, plants are able to recognize pathogen-associated molecular patterns (PAMPs) or microbe-associated molecular patterns (MAMPs) to activate defense responses called PAMP-triggered immunity (PTI) (Jones and Dangl 2006). PAMPs or MAMPs often derive from conserved components essential for pathogen survival and include a variety of proteins and other molecules (Newman *et al.*, 2013). Due to their defense-eliciting activities, they are also known as elicitors (Newman *et al.*, 2013). Many proteinaceous elicitors produced by *Phytophthora* spp. have been identified and characterized from culture filtrate. They are secreted proteins and some of them are also glycoproteins. Well-characterized examples include *P. infestans* elicitor INF1 (Kamoun *et al.*, 1998b), *P. parasitica* (current name: *P. nicotianae*) 34 kDa glycoprotein elicitor (CBEL) (Sejalón-Delmas *et al.*, 1997; Mateos *et al.*, 1997), two glycoproteins of 32 kDa and 42 kDa from *P. megasperma* (Sacks *et al.*, 1993; Baillieul *et al.*, 1995), an oligopeptide of 13 amino acids (Pep-13) within the cell wall glycoprotein (GP42) of *P. sojae* (Brunner *et al.*, 2002a), and *P. sojae* glycoside hydrolase family 12 (GH12) protein XEG1 (Ma *et al.*, 2015). In *P. palmivora*, the elicitor palmivorein and a 75 kDa protein were identified as elicitor proteins (Churngchow and Rattarasarn, 2000; Dutsadee and Churngchow 2008). Treatment of these elicitor proteins induces a range of plant defense responses on non-host and/or host plants, such as hypersensitive response (HR) which is characterized by rapid cell death, phytoalexin accumulation and defense-related gene

expression (Sacks *et al.*, 1993; Baillieul *et al.*, 1995; Sejalon-Delmas *et al.*, 1997; Mateos *et al.*, 1997; Kamoun *et al.*, 1998b; Churngchow and Rattarasarn 2000; Brunner *et al.*, 2002a; Dutsadee and Churngchow 2008; Ma *et al.*, 2015). As plants pretreated with elicitor proteins were shown to exhibit high level of resistance (Mateos *et al.*, 1997; Liu *et al.*, 2016), identification of elicitor proteins has the potential to develop novel disease control. In addition, since some elicitor proteins, such as XEG1, also play an important role in virulence (Ma *et al.*, 2015), identifying proteins from cultrate filtrate of *Phytophthora* spp. may be able to reveal novel pathogenicity factors.

The application of CRISPR/Cas9-mediated gene editing technology has revolutionized oomycete functional genomics, which used to be very challenging due to their genetic features, such as being diploid or polyploid and heterothallic (Fang *et al.*, 2017; Gumtow *et al.*, 2018). Since Fang and Tyler (2016) adapted this technology to oomycete genome editing, it has been successfully used to edit the genomes of three *Phytophthora* spp., including *P. sojae*, *P. capsici* and *P. palmivora* (Fang and Tyler 2016; Gumtow *et al.*, 2018; Miao *et al.*, 2018). *P. palmivora*'s functional genomic studies particularly benefit from this technology as genome analyses of a cacao isolate suggested that *P. palmivora* is tetraploid (Ali *et al.*, 2017). Gumtow *et al.*, (2018) used a simple and efficient *Agrobacterium*-mediated transformation method to express Cas9 and single guide RNA (sgRNA) to achieve effective gene editing in *P. palmivora*. With this system, *P. palmivora* extracellular cystatin-like protease inhibitor *PpalEPIC8* mutants were successfully generated, which allowed the genetic identification of its role in pathogen virulence (Gumtow *et al.*, 2018). This system is expected to accelerate functional identification of many other *P. palmivora* effector proteins.

In this study, in search for potential elicitors from culture filtrate of *P. palmivora*, I identified a secreted glycoprotein of 15 kDa, designated as Ppal15kDa. I found that it plays an important role in *P. palmivora* development and pathogenicity. Transient expression of Ppal15kDa in *N. benthamiana* enhanced *P. palmivora* infection. *Ppal15kDa* mutants generated via CRISPR/Cas9 were compromised in infectivity on both *N. benthamiana* and papaya, which corresponded to their reduced

sporangium sizes, impaired germ tube elongation and appressorium formation. *Ppal15kDa* was found to be highly expressed in appressorium-forming cysts, which is consistent with its role in infection structure development and pathogenicity.

2.2 Objectives

2.2.1 To identify the gene encoding the 15 kDa protein

2.2.2 To characterize the function of the 15 kDa protein

2.3 Materials and Methods

2.3.1 *P. palmivora* growth and zoospore preparation

P. palmivora P1 strain isolated from a naturally infected papaya plant (Wu *et al.*, 2016) was used throughout this study. It was routinely cultured on 10% unclarified V8 agar (10% V8 juice, 0.1% CaCO₃, 1.5% agar) at 25°C for 7 days. For preparing zoospore suspensions used in various assays, the 7-day-old culture in a 100 mm Petri dish was flooded with twelve milliliters of cold (4°C) sterile distilled water. The plate was incubated at 4°C for 15 min and then at room temperature for 15 min to release zoospores. The concentration of zoospores was measured using a haemocytometer under a light microscope.

2.3.2 *N. benthamiana* growth

N. benthamiana plants were grown in a growth chamber at 25°C, 60% humidity, under 12h-light and 12h-dark cycle. 6-week-old *N. benthamiana* plants were used for all agroinfiltration experiments and infection assays with wild-type (WT) and mutant *P. palmivora*.

2.3.3 Identification of Ppal15kDa in *P. palmivora* culture filtrate

For preparation of *P. palmivora* culture filtrate, 7-day-old *P. palmivora* on 10% V8 agar was cut with a cork borer, and then cultured in Henniger medium (Henniger 1963) at 25°C, 100 rpm for 14 days. The culture filtrate was filtered through Whatman filters (No. 1), dialyzed with a dialysis membrane with a cutoff of 12 kDa, and then lyophilized. The culture filtrate proteins were separated on 15% SDS-PAGE and stained with InstantBlue™ Protein Stain kit (Expdeon, U.K.)

following the manufacturer's protocol. The protein band of around 15 kDa was cut and subsequently identified by liquid chromatography tandem mass spectrometry (LC-MS/MS) using a database generated from *P. palmivora* transcriptomic sequences (Evangelisti *et al.*, 2017). In order to stain glycoproteins, periodic acid-Schiff staining (Zacharius *et al.*, 1969) was performed by soaking the gel in 7.5% (v/v) acetic acid for 1 hour, and then in 1% (w/v) periodic acid for 45 min at 4°C in the dark, followed by washing in 7.5% acetic acid for 10 min (6 times), staining with the periodic acid-Schiff reagent for 1 hour at 4°C in the dark and then washing with 0.5% (w/v) sodium metabisulfite.

2.3.4 Bacterial strains and plasmids

Agrobacterium tumefaciens strains GV3101 (Koncz and Schell 1986) and EHA105 and *E. coli* strain DH5 α (Invitrogen, CA, USA) were grown on Luria-Bertani (LB) agar or broth supplemented with appropriate antibiotics (Sambrook *et al.*, 1989) at 28°C or 37°C, respectively. The pGEM[®]-T vector (Promega, Madison, WI, USA) was used to clone *Ppal15kDa*. pJL-TRBO, a Tobacco Mosaic Virus (TMV)-based binary vector that allows high levels of expression of foreign proteins in plants (Lindbo 2007), was used to transiently express *Ppal15kDa* in *N. benthamiana* leaves. pCB301TOR-CRISPR (Gumtow *et al.*, 2018) was used for CRISPR/Cas9-mediated gene editing of *Ppal15kDa* in *P. palmivora*.

2.3.5 Bioinformatics analysis

Protein translation was performed using the translate tool (ExpASY; <http://web.expasy.org/translate/>). Prediction of signal peptide was conducted using SignalP version 4.1 (<http://www.cbs.dtu.dk/services/SignalP/>) (Petersen *et al.*, 2011). Potential O- and N-glycosylation sites were predicted using DictyOGlyc version 1.1 (<http://www.cbs.dtu.dk/services/DictyOGlyc/>) (Gupta *et al.*, 1999) and NetNGlyc version 1.0 (<http://www.cbs.dtu.dk/services/NetNGlyc/>) (Gupta *et al.*, 2002), respectively. BLASTP and TBLASTN were performed using tools and databases in NCBI BLAST server (<https://blast.ncbi.nlm.nih.gov/Blast.cgi>) (Altschul *et al.*, 1990) and FungiDB (<https://fungidb.org/fungidb/>) (Stajich *et al.*, 2012). Conserved or functional domain search was performed using NCBI Conserved Domain search engine

(<https://www.ncbi.nlm.nih.gov/Structure/cdd/wrpsb.cgi>) (Marchler-Bauer *et al.*, 2017) and InterProScan (<http://www.ebi.ac.uk/interpro/search/sequence-search>) (Jones *et al.*, 2014). Phylogenetic analysis of Ppal15kDa and homologous sequences was performed using the BLOSUM series matrix of ClustalW alignments and the neighbor-joining method (Nei and Saitou 1987) with 1000 bootstrap replicates by the Molecular Evolutionary Genetics Analysis (MEGA) version 6.0 software (Tamura *et al.*, 2013).

2.3.6 Isolation and cloning of *Ppal15kDa*

P. palmivora mycelium was ground to a fine powder with liquid nitrogen in a mortar with a pestle. Total RNA was isolated using the RNeasy® Plant Mini Kit (Qiagen, CA, USA) according to the manufacturer's protocol. The contaminating genomic DNA was removed using an on-column RNase-free DNase I digestion set (Qiagen, CA, USA) according to the instruction manual of the RNeasy® Plant Mini Kit. First-strand cDNA synthesis was conducted using the Superscript™ III (Invitrogen, CA, USA).

The *oligos Ppal15kDa-F* (5'-GTGCGTAGATAACCAACAGACTG-3') and *Ppal15kDa-R* (5'-GGTTGGGCTCGTTTCATACTAC-3') targeting 5' and 3' untranslated region (UTR) were designed based on the sequence of *PLTG_02159* (Evangelisti *et al.*, 2017). The PCR reaction was performed using Emerald Amp® GT PCR Master mix (Takara, Otsu, Shiga, Japan). The PCR product was separated on 2% (w/v) agarose gel and purified using the Gel/PCR DNA Fragments Extraction Kit (Geneaid, New Taipei City, Taiwan), and ligated into pGEM®-T vector (Promega, Madison, WI, USA). The recombinant plasmids were isolated using the AccuPrep® plasmid DNA extraction kit (Bioneer, Alameda, CA, USA) and subjected to Sanger sequencing by MacroGen DNA sequencing service (Seoul, South Korea).

2.3.7 Transient expression of *Ppal15kDa* in *N. benthamiana* via agroinfiltration

The pJL-TRBO-*Ppal15kDaA* and pJL-TRBO-*Ppal15kDaB* plasmids were constructed by cloning DNA fragments of the open reading frames of *Ppal15kDaA* and *Ppal15kDaB* fused with the hexahistidine (His)-tag encoding sequence at the C-terminus into the pJL-TRBO (Lindbo 2007). The primers, *Ppal15kDa-FPacI*

(5'-GCGttaattaaATGCGTATGMTTCAGGTCGTGTTC-3') and *Ppal15kDa*-RAvrII (5'GCGcctaggTCAGtgggatgggatgggCTCTTGTCTGAAGAAGACGCGATG -3') were used to amplify the DNA fragments. The introduced PacI and AvrII restriction sites were underlined. The italic letters represent the His-tag sequence. The PCR amplification was performed using Phusion[®]High-Fidelity DNA polymerase (New England BioLabs, MA, USA) by preheating at 98°C for 30 s, followed by 35 cycles of denaturing at 98°C for 15 s, annealing at 58°C for 15 s and extension at 72°C for 30 s, and a final extension step at 72°C for 10 min. The amplified fragments were digested with PacI and AvrII restriction enzymes and ligated into the pJL-TRBO vector (Lindbo 2007). The ligation products were transformed into *E. coli* strain DH5 α (Invitrogen, CA, USA). The pJL-TRBO-*Ppal15kDaA* and pJL-TRBO-*Ppal15kDaB* plasmids containing the correct *Ppal15kDaA* and *Ppal15kDaB* nucleotide sequences were used to transform *A. tumefaciens* strain GV3101 by electroporation.

Transient protein expression in *N. benthamiana* was performed using *A. tumefaciens* GV3101 carrying the above plasmids or pJL-TRBO-G expressing GFP (Lindbo 2007) (as a control) as described previously by Khunjan *et al.*, (2016).

2.3.8 Detection of Ppal15kDa transiently expressed in *N. benthamiana* by Western blot.

The agrobacterium-infiltrated leaf tissues were collected using a No.7 cork borer, flash frozen with N₂ liquid, and then ground to fine powders using a FastPrep[®]-24 homogenizer (MP Biomedicals). The ground samples were extracted with 2x Laemmli buffer, boiled for 5 min and subsequently centrifuged at 13,000 rpm for 5 min. The supernatant was loaded onto 12% SDS-PAGE and transferred onto a polyvinylidenedifluoride (PVDF) membrane (Thermo Scientific). The His-tagged Ppal15kDa proteins were detected using HRP conjugated anti-His monoclonal antibody His-probe (H-3) (sc-8036 HRP, Santa Cruz Biotechnology, INC) and 1-Step Ultra TMB-Blotting Solution (Thermo Scientific).

2.3.9 Infection of *P. palmivora* on *N. benthamiana* leaves expressing *Ppal15kDa*

Forty-eight hours after agroinfiltration, two 10- μ L drops of zoospore suspensions (1×10^4 /ml) were inoculated on each *N. benthamiana* leaf with one drop on the half expressing the *Ppla15kDa* and another drop on the other half expressing *GFP* (control). The lesions were photographed at 4 days after inoculation and the lesion areas were measured using Photoshop (Adobe Systems, CA, USA).

2.3.10 Generation of *Ppal15kDa* mutants using CRISPR/Cas9 gene editing

Generation of *Ppal15kDa* mutants via CRISPR/Cas9 gene editing was performed essentially as described by Gumtow *et al.*, (2018). A 20-nt sequence G151F (5'-GCCAAGCAGAACAACAACA-3'), which is on the forward coding strand of *Ppal15kDa* and immediately upstream of 5'-CGG-3', was selected as the sgRNA target sequence. The potential off-targets of G151F were not found in *P. palmivora* genome (Ali *et al.*, 2017). Two oligo-nucleotides, *Ppal15kDa*-Crisper_F1 (5'-
ctagcCTTGGCCTGATGAGTCCGTGAGGACGAAACGAGTAAGCTCGTCGCCA
AGCAGAACAACAACA-3') and *Ppal15kDa*-Crisper_R1 (5'-
aacTTGTTGTTGTTCTGCTTGGCGACGAGCTTACTCGTTTCGTCCTCACGGA
CTCATCAGGCCAAGg-3', which consist of the 20 nt sgRNA target sequence (shaded) jointed together with the HH-ribozyme sequence (underlined) and necessary nucleotides for cloning (in lower case), were annealed and cloned to *Nhe*I and *Bsa*I sites of pCB301TOR-CRISPR (Gumtow *et al.*, 2018). The resulted plasmid was named pCB301TOR-CRISPR-*Ppal15kDa*. *A. tumefaciens* strain EHA105 containing pCB301TOR-CRISPR-*Ppal15kDa* was used to transform *P. palmivora* papaya isolate P1 via *Agrobacterium*-mediated transformation (Wu *et al.*, 2016). Single zoospore transformants were isolated from the initial G418-resistant transformants as described by Ho and Ko 1997. Briefly, zoospore suspensions (1 μ l) at a concentration of 1500 zoospores/ml were dropped onto Plich agar. The agar pieces with a single zoospore were transferred onto new Plich agar for growth. The growing mycelium was transferred and grown on 10% unclarified V8 agar containing 15 μ g/ml G418 under 12h-light and 12h-dark cycle at room temperature for 5 to 7 days.

To detect the *Ppal15kDa* mutations in single zoospore-derived transformants, genomic DNA was extracted using DNeasy[®] PowerLyzer[®] Microbial Kit (Qiagen, Germany) according to the manufacturer's protocol. The *Ppal15kDa* from both WT and transformants was amplified with primers, *Ppal15kDa*-FPacI (5'-GCGgtaattaaATGCGTATGMTTCAGGTCGTGTTC-3') and *Ppal15kDa*-RKpnl (5'-GCGggtaccTCACTCTTGTCGAAGAAGACGC-3') using Phusion high-fidelity DNA polymerase (New England Biolabs, Ipswich, MA, USA). The PCR products were purified using ExoSAP-IT[™] PCR Product Cleanup reagents (Applied biosystems, Thermo Fisher scientific, US) and sequenced using the same primers. *Ppal15kDa* was also amplified using *Ppal15kDa*-FPacI (5'-GCGgtaattaaATGCGTATGMTTCAGGTCGTGTTC-3') and *Ppal15kDa*-RAvrII (5'GCGgctaggTCAgtggtgatggtgatggtgCTCTTGTCGAAGAAGACGCGATG -3'), and cloned into the pJL-TRBO (Lindbo 2007) through PacI and AvrII sites as described above. The recombinant plasmids were extracted using QIAprep[®] Spin Miniprep Kit (Qiagen, Germany) and subsequently used for sequencing.

2.3.11 Virulence assays of *Ppal15kDa* mutants on *N. benthamiana* leaves and papaya fruits

6-week-old *N. benthamiana* plants and green mature Sunrise papaya fruits were inoculated with 15 µl droplets of *P. palmivora* zoospore suspensions (1×10^5 /ml). To accurately compare the virulence between WT and mutants, the mutants were inoculated with WT side-by-side. On each *N. benthamiana* leaf (separated by the midvein), one drop of WT zoospores was inoculated on one half and the same amount of zoospores from a mutant on another half. For inoculation on papaya fruits, three drops of WT zoospores were inoculated on one half of the fruit with a mutant on the other half. The inoculated plants/fruits were kept in clear plastic trays with lids on to maintain high humidity for 1 day. Photos were taken, and the lesion areas and lesion diameters were measured from *N. benthamiana* leaves and papaya fruits, respectively, at 4 days post inoculation.

2.3.12. Sporangium size measurement

Sporangia of 7-day-old WT and mutant *P. palmivora* strains growing on 10% unclarified V8 agar were collected with the 1 ml pipette tips, smeared into 15 µl drops of sterile distilled water on glass slides and covered with cover slips. The sporangia were photographed under a light microscope. The sporangium length was measured using INFINITY ANALYZE software.

2.3.13 Zoospore germination and germ tube growth assay

For zoospore germination assay, 1-cm diameter circles were drawn on the back of the petri dish containing Plich agar. A 15 µl drop of zoospore suspension (5×10^3 zoospore/ml) of WT and mutants was dropped on Plich agar medium within each circle. Germinating zoospores were counted and photographed twice under light microscope after growing on Plich agar for 4 hours and 24 hours, respectively.

2.3.14 Appressorium induction

Zoospores from WT and mutants were harvested from 10-day-old 10% unclarified V8 agar plates and resuspended to 5×10^4 zoospores/ml in H₂O. 30-µl droplets of zoospore suspensions were placed on a plastic cover slip and covered with another one and incubated on Plich agar in petri dish at room temperature for 4 hours. Appressorium formation of WT and mutants was observed and photographed under a light microscope. More than 200 zoospores were counted.

2.3.15 Gene expression analyses of *Ppal15kDa*

For vegetative hyphae, agar plugs of 7-day-old *P. palmivora* culture were grown in liquid Plich medium (Kamoun *et al.*, 1993) at room temperature in the dark for 7 days. The vegetative hyphae were collected by vacuum filtration (Ambikapathy *et al.*, 2002). For sporulating hyphae, agar plugs of 7-day-old *P. palmivora* culture were grown in 10% V8 broth for 3 days in the dark and subsequently transferred to 12 h light/ 12 h dark condition for 4 days (Ambikapathy *et al.*, 2002). Zoospore suspensions were prepared as described above and zoospores were collected by centrifugation at 13,000 rpm for 1 min. Cysts were prepared by vigorously vortexing the tube containing zoospore suspension on a mixer for 30 seconds (Chen *et al.*, 2014). Germinating cysts were prepared by incubating zoospores on water-treated

cellophane membrane and collected when about 80% of cysts germinated (Chen *et al.*, 2014). For preparation of appressorium-forming cysts, appressorium induction was performed as described above in this study. After induction for 4 hours, appressorium-forming cysts were collected by centrifugation at 13,000 rpm for 1 min. The vegetative hyphae, sporulating hyphae, zoospores, cysts, germinating cysts, and appressorium-forming cysts were crushed to fine powder in liquid nitrogen. The powders were used for RNA isolation using RNeasy® Plant Mini Kit (Qiagen, CA, USA). Contaminating genomic DNA was removed with DNA-free™ kit (Ambion). One µg of total RNA was used to synthesize first-strand cDNAs using SuperScript II reverse transcriptase (Invitrogen, CA, USA). qPCR was performed using SsoAdvanced™ Universal SYBR® Green Supermix (Bio-rad) as previously described (Gumtow *et al.*, 2018). The oligos *Ppal15kDaqPCR-F* (5'-TCAGGTCGTGTTTCATGCTTC-3') and *Ppal15kDaqPCR-R* (5'-TCTGCTTGGCATCTTCTGTG-3') were used for specific amplification of *Ppal15kDa* gene. Amplification of *P. palmivora* β -tubulin gene using primers described by Gumtow *et al.*, (2018) was used as an internal control to normalize the expression of *Ppal15kDa*. The fold change of *Ppal15kDa* expression at various developmental stages relative to *in vitro* grown mycelium was calculated using $2^{-\Delta\Delta C_T}$ method (Schmittgen and Livak 2008).

2.3.16 Statistical analysis

For analyzing the differential expression of *Ppal15kDa* at various developmental stages and sporangium size measurements of *P. palmivora* WT and mutant strains, the one-way analysis of variance (ANOVA) according to Duncan's multiple range tests was utilized to determine significance with $P \leq 0.05$ and performed by using SPSS Statistics 17.0 software. The lesion area data derived from *P. palmivora* infection on *N. benthamiana* leaves with one half transiently expressing *Ppal15kDaA* or *Ppal15kDaB* compared to another half expressing GFP gene, and the lesion area data obtained from *N. benthamiana* leaves or papaya fruits with one half infected with WT *P. palmivora* compared to another half infected with mutant *P. palmivora* were analyzed by paired t-test (P -value ≤ 0.05) using SPSS Statistics 17.0 software.

2.4 Results

2.4.1 Identification of a 15 kDa glycoprotein from culture filtrate of *P. palmivora*.

To identify potential elicitors, culture filtrate of *P. palmivora* grown in Henniger medium (Henniger 1963) was collected, dialyzed and lyophilized, and then separated on 15% SDS-PAGE. Two replicative gels were stained with InstantBlue™ Coomassie Protein Stain (Expedeon) and periodic acid-Schiff reagent for visualization of total proteins and glycoproteins, respectively. A strong protein band of about 15 kDa appeared on the gel stained with InstantBlue™ Coomassie Protein Stain (Fig. 2.1A). A band of similar size also appeared on the gel stained with periodic acid-Schiff reagent (Fig. 2.1B). These suggest that there is a 15 kDa glycoprotein abundantly present in the culture filtrate of *P. palmivora*.

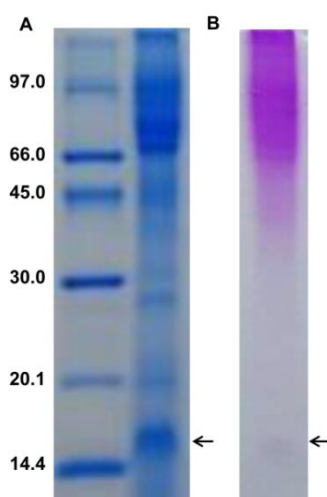


Fig. 2.1 Detection of the 15 kDa glycoprotein from culture filtrate of *P. palmivora*. The crude extract was separated by 15% SDS-PAGE and stained with InstantBlue Protein Staining (A) and periodic acid-Schiff reagent (B). The arrows indicate the 15 kDa protein.

To identify this protein, the 15 kDa band on the gel stained with InstantBlue™ Coomassie Protein Stain was cut and subjected to LC-MS/MS analyses using the *P. palmivora* transcriptome (Evangelisti *et al.*, 2017) as the database. Multiple proteins (peptide score) were matched, including PLTG_02159.1 (68), PLTG_04166.1 (30),

PLTG_11937.1 (29), PLTG_07335.1 (28), PLTG_10394.1 (24), PLTG_10965.2 (23), PLTG_11247.2 (21) and PLTG_04306.1 (21). However, the threshold peptide score of a protein with 95% identity should be higher than 31 (identity threshold). Only PLTG_02159.1 showed peptide score (68) higher than identity threshold (>31) and its molecular weight was 14.83 kDa. Two peptides VVTPASSDEER and ASTSVAAAGEGAR matched PLTG_02159.1 with 100% identity (Fig. 2.2). Consequently, the PLTG_02159.1 protein was designated as Ppal15kDa.

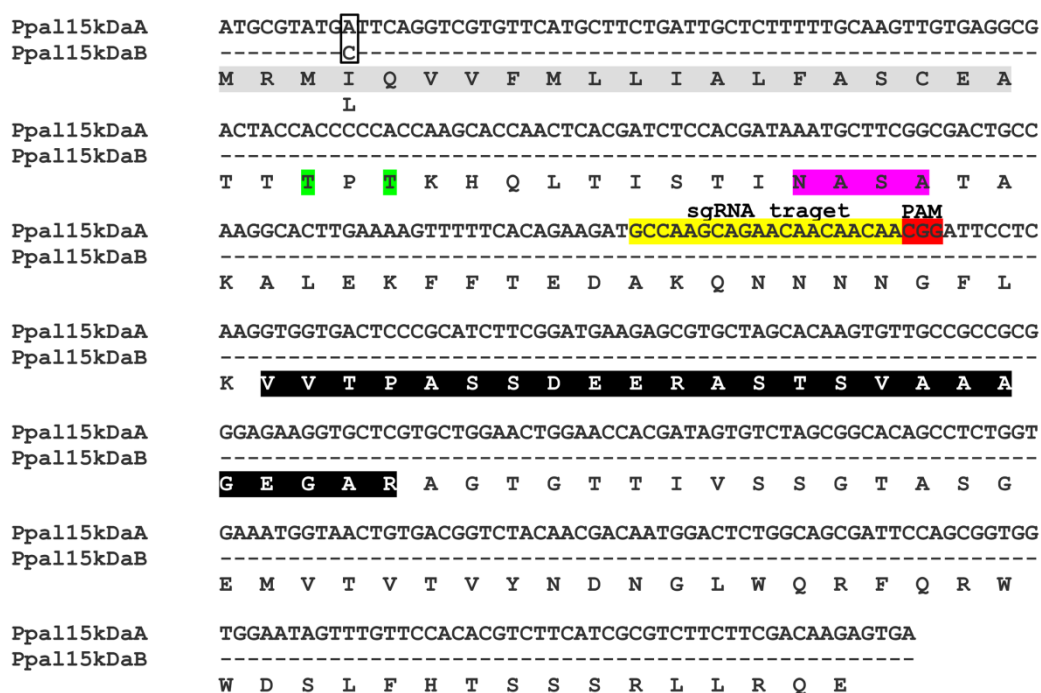


Fig. 2.2 The nucleotide and amino acid sequences of *Ppal15kDaA* and *Ppal15kDaB* with the sgRNA target sequence used for CRISPR/Cas9-mediated gene editing. The dashed lines represent the same nucleotides in *Ppal15kDaA* and *Ppal15kDaB*. The single nucleotide polymorphism (SNP) leading to the substitution of isoleucine (I) and leucine (L) is shown in the box. The sgRNA target sequence together with its downstream protospacer adjacent motif (PAM) CGG is shown. The signal peptide sequence is shown in gray shade. The matching peptide sequences identified by LC-MS/MS are shown in black shade. The potential N-glycosylation (35 NASA) and O-glycosylation (Thr23 and Thr25) sites are highlighted in pink and green, respectively.

I amplified and cloned *Ppal15kDa* from *P. palmivora* papaya isolate P1 using primers designed based on the nucleotide sequence of PLTG_02159.1 (Evangelisti *et al.*, 2017). I found two variants of *Ppal15kDa*, A and B forms (Fig. 2.2). A single nucleotide variation led to an amino acid change at the 4th amino acid from the N-terminus with isoleucine in A and leucine in B form (Fig. 2.2).

The translated amino acid of the *Ppal15kDa* had 136 residues with a putative signal peptide of 20 amino acids predicted using Signal P 4.0 (Maximal C- and Y-score at position 21= 0.817 and 0.876, respectively; D-score for 1-20 amino acids = 0.915, which is much higher than the cut-off score of 0.450) (Fig. 2.2). There were one potential N-glycosylation (Asn-X-Ser/Thr) site (35 NASA) and two potential O-glycosylation sites (Thr23 and Thr25) (Fig. 2.2). I found multiple single nucleotide polymorphisms (SNPs) between *Ppal15kDaA* and *Ppal15kDaB* in the 5' untranslated region (Fig. 2.3)

```

Ppal15kDaA      GTGCGTAGATAACCAACAGACTGCTGCTCTATCCAACAGACGAGGTCTGGCTACAACCTGA 60
Ppal15kDaB      GTGCGTAGATAACCAACAGACTGCT-GCCTACCCAACAGACGAGGTCTGGCTACAACCTGA 59
*****
*****          *** *****

Ppal15kDaA      TGGCCTAACTTGCCGTGTCATCTTTGATTGGGATCCGCCTCAGCTCTTCGATCATTTCGCA 120
Ppal15kDaB      TGGCCTAACTTGCCGTGTCATCTTTGATTGGGATCCGCCTCAGCTTTTCGATCATTTCGCA 119
*****
*****

Ppal15kDaA      AACTGCACTCGACTACCAACACCTGAACTTGTGCTCTCAAGAAAAATGCGTATGATT 180
Ppal15kDaB      AACTGCACTCGACTACCAACACCTGAACTTGTGCTCTCAAGAAAAATGCGTATGATT 179
*****
*****          Start codon

Ppal15kDaA      CAGGTCGTGTTTCATGCTTCTGATTGCTCTTTTGGCAAGTTGTGAGGCGACTACCACCCC 240
Ppal15kDaB      CAGGTCGTGTTTCATGCTTCTGATTGCTCTTTTGGCAAGTTGTGAGGCGACTACCACCCC 239
*****

Ppal15kDaA      ACCAAGCACCAACTCAGATCTCCACGATAAATGCTTCGGCGACTGCCAAGGCACCTTGAA 300
Ppal15kDaB      ACCAAGCACCAACTCAGATCTCCACGATAAATGCTTCGGCGACTGCCAAGGCACCTTGAA 299
*****

Ppal15kDaA      AAGTTTTTCACAGAAGATGCCAAGCAGAACAACAACAACGGATTCCCTCAAGGTGGTGACT 360
Ppal15kDaB      AAGTTTTTCACAGAAGATGCCAAGCAGAACAACAACAACGGATTCCCTCAAGGTGGTGACT 359
*****

Ppal15kDaA      CCCGCATCTTCGGATGAAGAGCGTGTAGCACAAGTGTTCGCCCGCGGGAGAAGGTGCT 420
Ppal15kDaB      CCCGCATCTTCGGATGAAGAGCGTGTAGCACAAGTGTTCGCCCGCGGGAGAAGGTGCT 419
*****

Ppal15kDaA      CGTGCTGGAAGTGAACACGATAGTGTCTAGCGGCACAGCCTCTGGTGAATGGTAACT 480
Ppal15kDaB      CGTGCTGGAAGTGAACACGATAGTGTCTAGCGGCACAGCCTCTGGTGAATGGTAACT 479
*****

Ppal15kDaA      GTGACGGTCTACAACGACAATGGACTCTGGCAGCGATTCCAGCGGTGGTGAATAGTTTG 540
Ppal15kDaB      GTGACGGTCTACAACGACAATGGACTCTGGCAGCGATTCCAGCGGTGGTGAATAGTTTG 539
*****
*****          Stop codon

Ppal15kDaA      TTCCACACGCTTTCATCGCGTCTTCTTCGACAAGAGTGA      579
Ppal15kDaB      TTCCACACGCTTTCATCGCGTCTTCTTCGACAAGAGTGA      578
*****

```

Fig. 2.3 Multiple single nucleotide polymorphisms (SNPs) at 5' untranslated region (UTR) of *Ppal15kDaA* and *Ppal15kDaB*.

The homologs of Ppal15kDa appeared to be broadly present in plant pathogenic *Phytophthora* spp (Fig. 2.4). Using BLASTP and TBLASTN against NCBI non-redundant database, and the protein, transcript, EST and PopSet databases in FungiDB (<https://fungidb.org/fungidb/>), homologous sequences of Ppal15kDa were found in *P. megakarya*, *P. cactorum*, *P. parasitica* (current name: *P. nicotianae*), *P. sojae*, *P. cinnamomi* and *P. capsici* with identify higher than 50% and E-value below 1e-22 (Fig. 2.4).

```

P. sojae      XP_009519869.1   1  MSRTIQVLLVVMVALLASCNA-DIATKNQFTIATTNAAATKALOKFFAEDSKONKKNQV
P. cinnamomi PHYCI_93984T0 1  MMRMLQVLLVIMVALLASCDAADTPTKNHLLTISTTNAGATAKALOKFFADDAKONKKNQV
P. palmivora POM75182.1      1  -MRMIEVLFVFLVASFASCAGAVAPTKNQLTISTKDGSTATAKALOKFFVEDAKNNKNNAR
P. capsici   PHYCA_14775T0   1  -MRMAQAFLLVLLVALLSLWNCEAAATKNQLVISTTNNGIATAKALOKFFVEDAKONNDKGF
P. cinnamomi PHYCI_81820T0   1  MLHLLRVLVLLVLLVLLANCGEGTGTATKSOLTIAITTNADATAKALOKFFVEDAKONKSNQV
P. megakarya OWZ12090.1   1  ---MFEVPLVFLVLLVSCVHGTTITPTKNQLTISTTNSTATAKALOKFFVEDAKONKDSGF
P. parasitica XP_008909746.1 1  MRVLFQALLVLLVALLVSCNEAANPTKHOLTIVTTNSTATAKALOKFFNDDAKQNESNGF
P. cactorum RAW38577.1  1  MRMLFQVHLVFLVALFASCNEAATPTKNQLVSTTNSTATAKALOKFFAEDAKONNNNGF
P. palmivora Ppal15kDaA      1  -MRMIEVVFMLLIALFASCNAAATPTKNQLTISTTNASATAKALOKFFVEDAKONNNNGF
P. megakarya OWZ12091.1  1  -MHIEQVVFVFLVLLVFTSCVSTTAPTRHOLTISTTNASTATAKALOKFFVEDAKONKNGF
P. parasitica XP_008909747.1 1  -MLLIQVLLVFLVALFVSCVAAA--TONQLTITTTDSTATAKALOKFFVEDAKONRNNNGF
P. cactorum RAW38578.1  1  -MRMSQVLLVFLVLLVSCVATA--AQNQLTIAITTNSTATAKALOKFFVEDSKONQNNNGF

P. sojae      XP_009519869.1   60  LKVVLSGSAADDEERVSA--GAIAAAEGARAGAGTTVVSSSTSGTTRVTVTVIYNNNGLWQR
P. cinnamomi PHYCI_93984T0 61  LKVVLTVTSAADDEERVSA--GAIAAAEGARAGAGTTVVSSQSGSTQTVTVTVIYNNNGLWQR
P. palmivora POM75182.1      60  DKVKKRRPCL-D-----EACYGTTVVSSDRESGGEVTVTVYNNNGLWQR
P. capsici   PHYCA_14775T0   60  LKVVITPSSS-DEERASA--GAI AAGEGARAGAGTTVSSGSPSSGELF-----
P. cinnamomi PHYCI_81820T0   61  LKMMNVSSA-DGEERGA--GALASGOGPRVVGAGTTVVSDGTGSSQTVTVTVIYNNNGLWQR
P. megakarya OWZ12090.1   58  LKVVTLSSS-KEERV----IASGOGPRAGAGTTVVSSDAGIGETVTVTVYNNNGLWQR
P. parasitica XP_008909746.1 61  LKVVTLSSS-NEERASA--GAI TSGOGPRAGAGTTVVVANDASSGETVTVTVYNNNGLWQR
P. cactorum RAW38577.1  61  LKVVTLSSS-NEERASA--GAM TSGOGPRAGAGTTVVANDAPSGETVTVTVIYNNNGLWQR
P. palmivora Ppal15kDaA      60  LKVVTPASS-DEERAST--SVA AAGEGARAGTGTIVSSGTASGEMVTVTVYNNNGLWQR
P. megakarya OWZ12091.1  60  LKVVTPSSS-GEERAST--SAITAGEGARAGTGTIVVSSDTPSGEMVTVTVYNNNGLWQR
P. parasitica XP_008909747.1 58  LKVVTLFSS-EEERAST-SGAI TAGEGARAGTGTIVVSSDTPSGETVTVTVYNNNGLWQR
P. cactorum RAW38578.1  58  LKVVTLSSS-EEERASTSGAITAGEGARVAAGTTVVVANDPFLGETVTVTVYNNNGLWQR

P. sojae      XP_009519869.1   118  FORWWNSLFARRRLRHASN-----
P. cinnamomi PHYCI_93984T0 119  FORWWNRLFRNDSTRRLRVAASGANN
P. palmivora POM75182.1      102  FORWWNRLNLNGSTRRLRHPITGEQ--
P. capsici   PHYCA_14775T0   -----
P. cinnamomi PHYCI_81820T0   118  FORWWNRLFHRSSSSARRL-R-----
P. megakarya OWZ12090.1   111  FORWWNRLFNR-----
P. parasitica XP_008909746.1 118  FORWWNRLFVGSAA NSTRLRTDN--
P. cactorum RAW38577.1  118  FORWWNRLFVGSAA NSTRLRTDN--
P. palmivora Ppal15kDaA      117  FORWWNSLFHTSSS---RLLRQE---
P. megakarya OWZ12091.1  117  FORWWNRLFHTSSS---RLLRPS---
P. parasitica XP_008909747.1 116  FORWWNRLFHVSSN---RLLREGGKK
P. cactorum RAW38578.1  117  FORWWNRLFHVSSS-STRLLREKV--

```

Fig. 2.4 Amino acid sequence alignment of Ppal15kDa and its homologs in *Phytophthora* spp.

All these sequences were annotated as hypothetical proteins. The phylogenetic dendrogram revealed that Ppal15kDa was most closely related to the hypothetical protein OWZ12091.1 from *P. megakarya* (Fig. 2.5). No functional domain indicative of Ppal15kDa's biochemical function was identified using NCBI Conserved Domain Search and InterProScan by searching multiple databases that make up the InterPro consortium (Jones *et al.*, 2014).

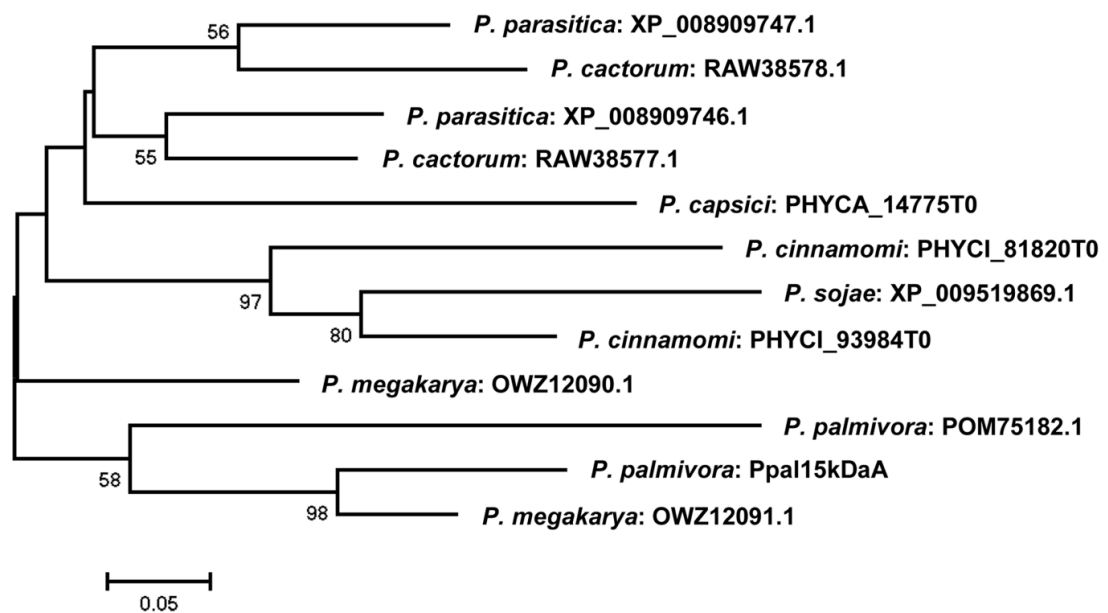


Fig. 2.5 Phylogenetic analyses of Ppal15kDa and its homologs in *Phytophthora* spp. Construction of the phylogenetic tree was performed with the amino acid sequences using the neighbor-joining (NJ) method built in MEGA version 6.0. Bootstrap values were obtained with 1000 replicates and values higher than 50% are shown. The scale bar represents 0.05 amino acid substitutions per site.

2.4.2. Expression of *Ppal15kDa* in *N. benthamiana* enhances *P. palmivora* infection

To assess the roles of Ppal15kDa in pathogen virulence, I expressed Ppal15kDa in *N. benthamiana* via *Agrobacterium*-mediated transient expression. The *Ppal15kDaA* and *Ppal15kDaB* coding sequences fused to the hexahistidine (His)-tag at the C-terminus were cloned into pJL-TRBO plasmid (Lindbo 2007) and transiently expressed in *N. benthamiana* leaves by agroinfiltration. The expression of

Ppal15kDaA and Ppal15kDaB proteins were analyzed in total proteins extracted from agroinfiltrated *N. benthamiana* leaves by Western blot with HRP conjugated anti-His monoclonal antibody. Two bands of approximately 15 kDa and 17 kDa were detected in leaves infiltrated with *Agrobacteria* carrying pJL-TRBO-Ppal15kDaA or pJL-TRBO-Ppal15kDaB, but not in leaves infiltrated with *Agrobacteria* carrying pJL-TRBO-GFP for expression of GFP (Fig. 2.6), demonstrating the successful expression of 15kDa. The two bands of 15 kDa and 17 kDa may represent different modifications of the proteins.

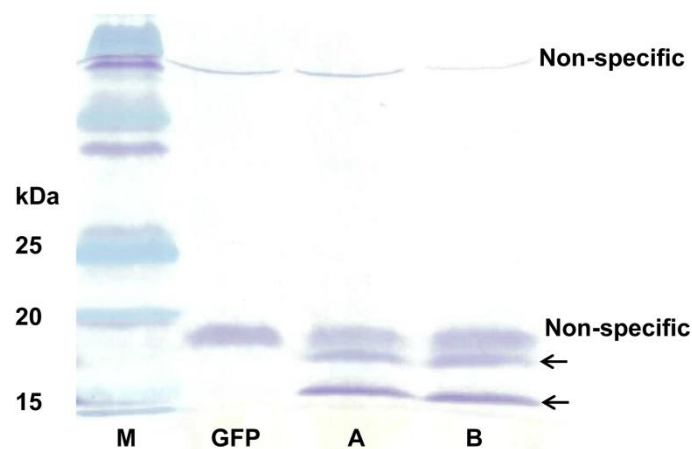


Fig. 2.6 Agrobacterium-mediated transient expression of *Ppal15kDa* in *N. benthamiana*. Total proteins were extracted from infiltrated *N. benthamiana* leaves and subjected to SDS-PAGE followed by Western blot with HRP conjugated anti-His monoclonal antibody. Lane M represents the protein standard and lane GFP represents *N. benthamiana* leaves infiltrated with *A. tumefaciens* GV3101 carrying pJL-TRBO-G. Lane A and B represent *N. benthamiana* leaves infiltrated with *A. tumefaciens* GV3101 carrying pJL-TRBO-*Ppal15kDaA* and pJL-TRBO-*Ppal15kDaB*, respectively. The arrows indicate two forms of *Ppal15kDa*.

N. benthamiana leaf halves expressing the *Ppal15kDa* or GFP were inoculated with zoospore suspensions and lesions were measured at 4 days post inoculation. Lesions on *N. benthamiana* half leaves expressing *Ppal15kDaA* or *Ppal15kDaB* were much larger than the ones expressing GFP (Fig. 2.7A, B). Average lesion sizes of *N. benthamiana* leaf halves expressing *Ppal15kDaA* and *Ppal15kDaB* were 3.9 and 4.5

cm², respectively, which were about 4 folds higher than the control (Fig. 2.7B). This result indicated that Ppal15kDa contributed to *P. palmivora* virulence during infection.

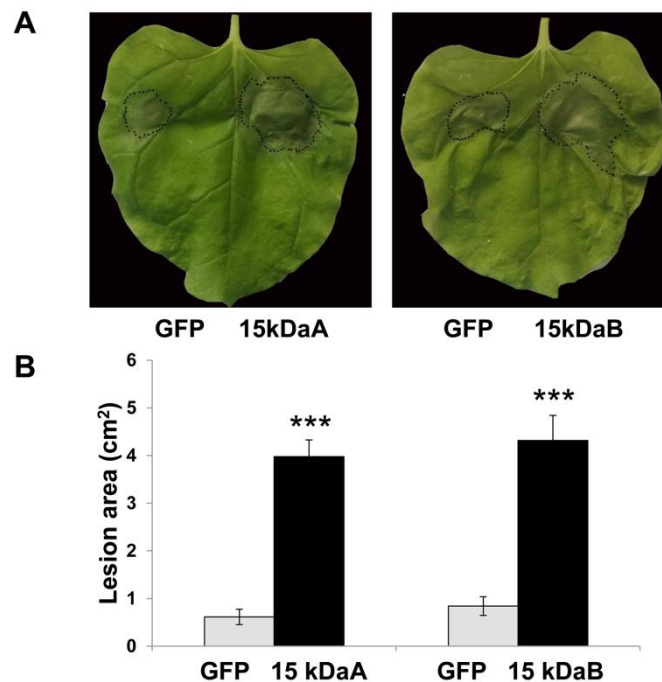


Fig. 2.7 Expression of Ppal15kDa in *N. benthamiana* leaves enhanced *P. palmivora* infection. A, Infection symptoms of *P. palmivora* on a representative *N. benthamiana* leaf with one half transiently expressing Ppal15kDaA or Ppal15kDaB and the other half expressing GFP. The photograph was taken at 4 days post inoculation (dpi). B, The average lesion areas caused by *P. palmivora* at 4 dpi on *N. benthamiana* leaves treated as in A. The histograms correspond to the mean \pm standard errors (SE) of lesion areas calculated from independent leaves (n = 28). Three asterisks (***) indicate statistically significant differences (P -value < 0.001) in the lesion areas on leaf halves expressing Ppal15kDaA or Ppal15kDaB compared to the other halves expressing GFP determined by paired t-test.

2.4.3 Generation of *Ppal15kDa* mutants by CRISPR/Cas9-mediated gene editing.

To further confirm the role of Ppal15kDa in *P. palmivora* virulence, I generated Ppal15kDa mutants using CRISPR/Cas9-mediated gene editing. A 20-nt sgRNA target sequence targeting the upstream of Ppal15kDa central region was

selected (Fig. 2.2), which together with the HH ribozyme sequence (Fang *et al.*, 2017) were cloned into pCB301TOR-CRISPR. The resulted plasmid pCB301TOR-CRISPR-*Ppal15kDa* was used to transform *P. palmivora* via *A. tumefaciens*-mediated transformation. I isolated single zoospore-derived transformants from 20 initial transformants and sequenced *Ppal15kDa* to identify the mutations. In *Ppal15kDa* sequencing chromatograms, I observed mixed peaks immediately after the Cas9 cleavage site in six single zoospore lines T1-2, T3-1, T9-4, T11-10, T13-2 and T17-5, but not in WT (Fig. 2.8), suggesting that mutations occurred in these lines.

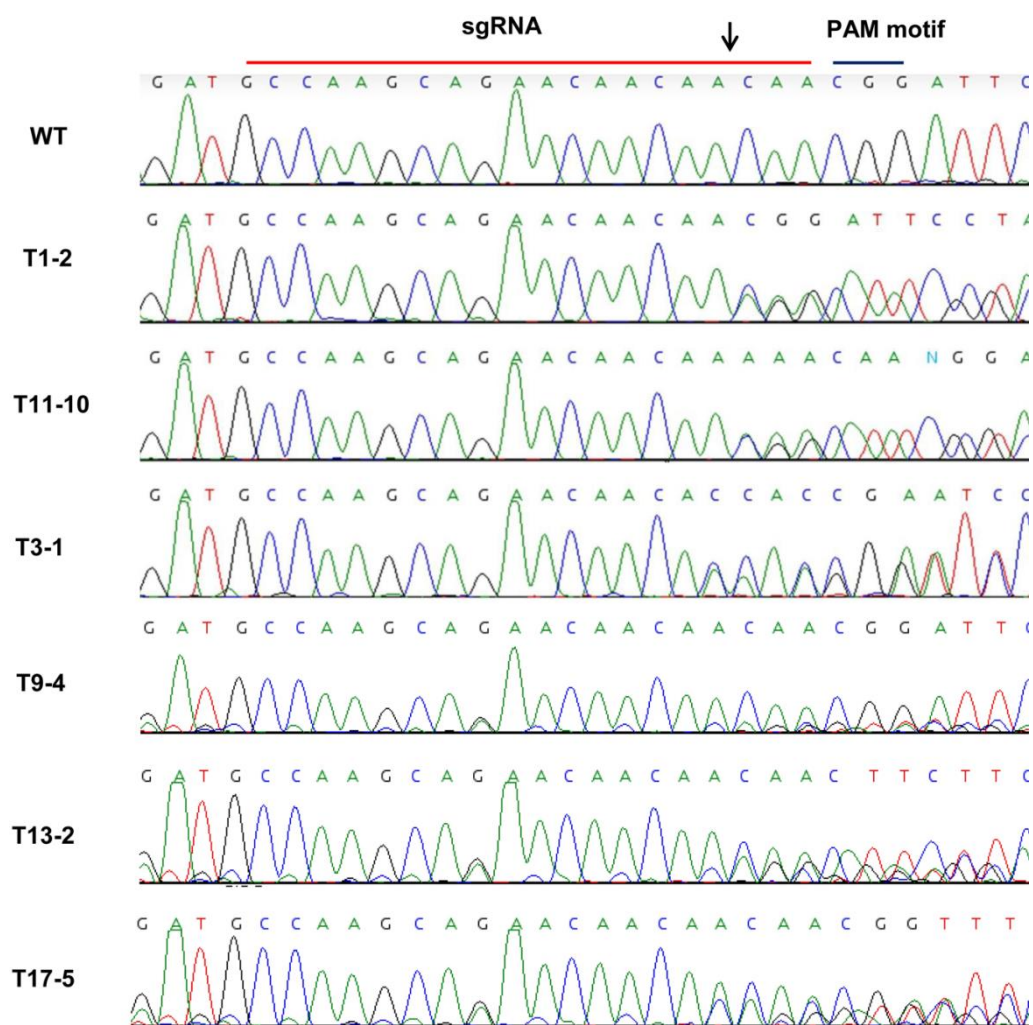


Fig. 2.8 Chromatograms of the partial sequences of *Ppal15kDa* gene in mutants generated using CRISPR/Cas9 gene editing. The mutant lines exhibited mix peaks. The putative Cas9 cleavage site is shown by an arrow.

These lines originated from six initial transformants T1, T3, T9, T11, T13 and T17 and therefore represent independent transformation events. The mixed sequence chromatograms suggested that not all copies of *Ppal15kDa* in the genome got mutated and/or different mutations occurred at different copies (Fig. 2.8).

To determine the types of mutations in the above transformants, I cloned the PCR products of *Ppal15kDa* from these transformants and performed Sanger sequencing. The number of sequenced clones for each transformant varied from 12-24. Two types of mutations were observed in T1-2 and T11-10 transformants, including a 3 bp insertion leading to the addition of lysine (K) and a 3 bp deletion leading to the loss of asparagine (N) (Fig. 2.9).

```

WT      GATGCCAAGCAGAAACAACAACAACGGATTTCCTCAAGG
        D A K Q N N N N G F L K V
T1-2/T11-10 GATGCCAAGCAGAAACAACA---CGGATTTCCTCAAGG
        D A K Q N N N N G F L K V
        GATGCCAAGCAGAAACAACAAAACAACGGATTTCCTCAAGG
        D A K Q N N K N N G F L K
T3-1/T13-2/ T17-5 GATGCCAAGCAGAAACAACAACAACGGATTTCCTCAAGG
        D A K Q N N N N G F L K V
        GATGCCAAGCAGAAACAACA---CGGATTTCCTCAAGG
        D A K Q N N N N G F L K V
        GATGCCAAGCAGAAACAACAAAACAACGGATTTCCTCAAGG
        D A K Q N N K N N G F L K
        GATGCCAAGCAGAAACAACA-CAACGGATTTCCTCAAGG
        D A K Q N N T T D S S R
T9-4     GATGCCAAGCAGAAACAACAACAACGGATTTCCTCAAGG
        D A K Q N N N N G F L K V
        GATGCCAAGCAGAAACAACA---CGGATTTCCTCAAGG
        D A K Q N N N N G F L K V
        GATGCCAAGCAGAAACAACAAAACAACGGATTTCCTCAAGG
        D A K Q N N K N N G F L K

```

Fig. 2.9 The *Ppal15kDa* nucleotide mutations and the resulted amino acid changes in *P. palmivora* mutants generated via CRISPR/Cas9 gene editing. The sgRNA target sequence in WT is underlined and PAM motif is shown in the box. The inserted nucleotides are shown in green italic and the deleted nucleotides are indicated with dashed lines. The deleted, inserted and changed amino acids are shown in red, green and blue, respectively.

T3-1, T13-2 and T17-5 had the wide-type (WT) copy and three types of mutations, including the two types that occurred in T1-2 and T11-10 and 1 bp deletion resulting in frame shift (Fig. 2.9). T9-4 had the WT copy and the two types of mutations in T1-2 and T11-10 (Fig. 2.9).

2.4.4 *Ppal15kDa* mutants are compromised in pathogenicity

To investigate the effect of *Ppal15kDa* mutations on *P. palmivora* pathogenicity, six *Ppal15kDa* mutants were inoculated on *N. benthamiana* leaves and papaya fruit side-by-side with WT. Inoculation of *N. benthamiana* leaf halves with WT consistently produced big lesions. In contrast, the *N. benthamiana* leaf halves inoculated with different mutants produced lesions of varying sizes that were smaller than WT (Fig. 2.10A). T1-2, T3-1 and T11-10 showed either no infection or very small lesions (Fig. 2.10A). The average lesion areas caused by T1-2/WT, T3-1/WT and T11-10/WT were 0.1/13.5, 0/14.7 and 0.3/13.7 cm², respectively (Fig. 2.10B). T9-4 and T17-5 caused bigger lesions on *N. benthamiana* leaves than T1-2, T3-1 and T11-10, but significantly smaller than WT. The average lesion areas of T9-4/WT and T17-5/WT were 1.6/13.8 and 3.4/12.6, respectively (Fig. 2.10B). The lesions caused by T13-2 were only slightly smaller than WT (Fig. 2.10A and B).

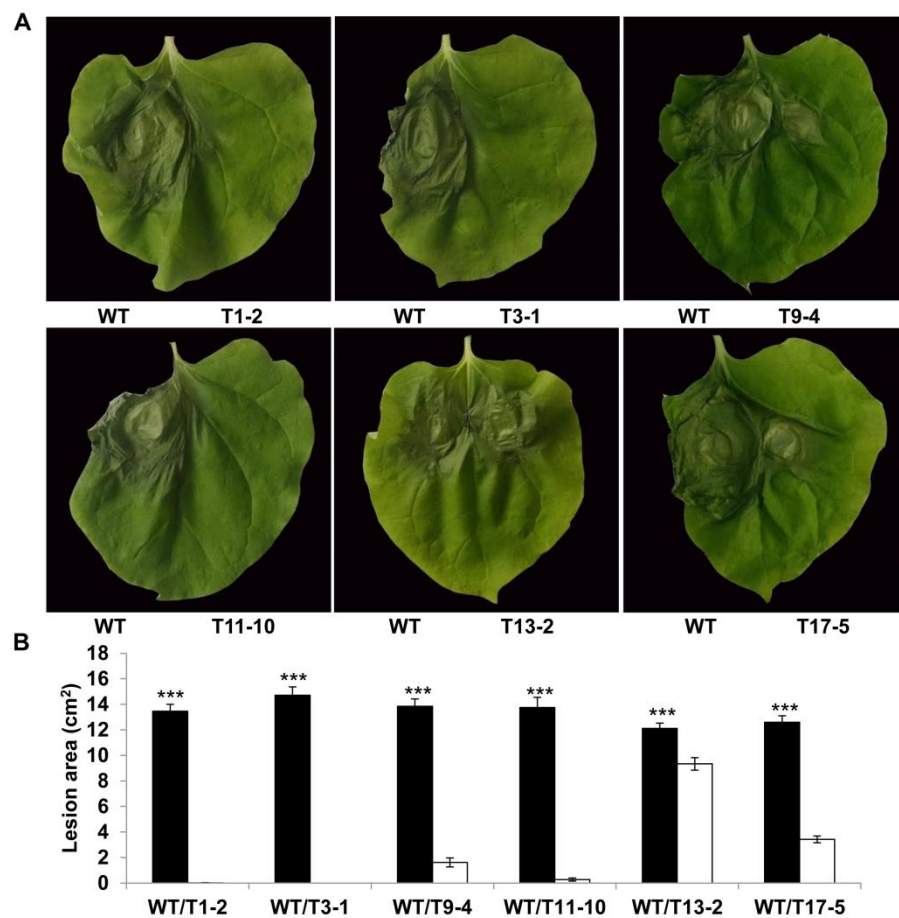


Fig. 2.10 Infection assays of *N. benthamiana* leaves with *P. palmivora* wild-type (WT) strain and *Ppal15kDa* mutants. A, Symptoms of representative leaves infected with WT and mutant strains side-by-side at 4 days post inoculation (dpi). B, The average lesion areas at 4 dpi on *N. benthamiana* leaves inoculated as in A. The histograms correspond to the mean \pm standard errors (SE) of lesion areas calculated from independent leaves ($n = 20$). Three asterisks (***) indicate statistically significant differences (P -value < 0.001) in the lesion areas caused by WT compared to *Ppal15kDa* mutants determined by paired t-test. The experiment was repeated 3 times with similar results.

Similar results were obtained from infection assays of papaya fruit. The lesions caused by mutants T1-2, T3-1, T9-4 and T11-10 and T17-5 were significantly smaller than WT (Fig. 2.11A), with the average lesion diameters of mutant/WT of papaya fruits as 0.54/4.09, 0.55/4.15, 1.19/4.42, 0.8/3.96, and 2.31/4.22 respectively

(Fig. 2.11B). T13-2 produced lesions slightly smaller than WT, with the average lesion diameter of T13-2/WT as 2.94/3.85 (Fig 11B).

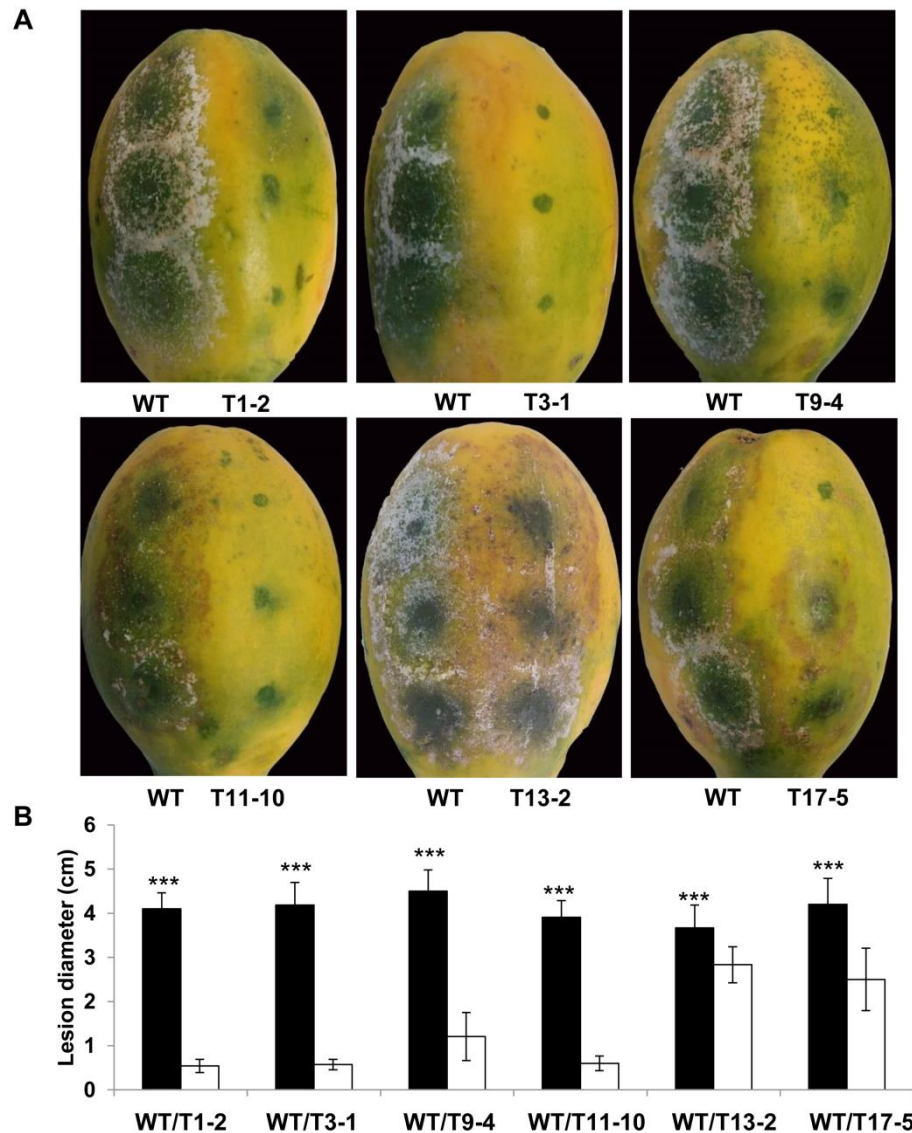


Fig. 2.11 Infection assays of papaya fruits with *P. palmivora* wild-type (WT) strain and *Ppal15kDa* mutants. A, Symptoms of representative papaya fruits infected with WT and mutant strains side-by-side at 4 dpi. B, The average lesion diameters at 4 dpi on papaya fruits inoculated as in A. The histograms correspond to the mean \pm standard errors (SE) of lesion diameters calculated from independent fruits ($n = 13$). Three asterisks (***) indicate statistically significant differences (P -value < 0.001) between WT and the indicated *Ppal15kDa* mutant determined by paired t-test. The experiment was repeated 3 times with similar results.

In summary, although the infectivity of different mutants varied, they all exhibited reduced virulence compared with WT with some mutants' virulence almost completely compromised. These results suggest that *Ppal15kDa* gene plays an important role in *P. palmivora* pathogenicity.

2.4.5 *Ppal15kDa* mutants produce smaller sporangia and are compromised in germ tube elongation and appressorium formation

Because *Ppal15kDa* mutants are compromised in pathogenicity on both *N. benthamiana* leaves and papaya fruits, I investigated whether mutations of *Ppal15kDa* affect *P. palmivora* development. I did not observe mutations of *Ppal15kDa* cause changes in mycelium growth (Fig. 2.12).

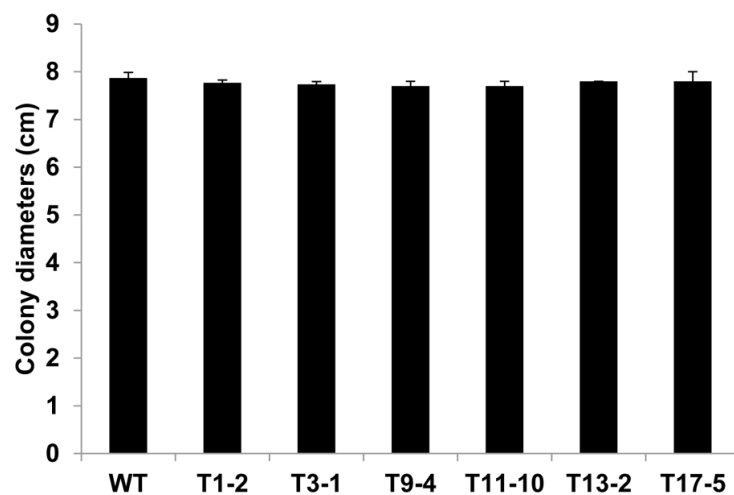


Fig. 2.12 Mycelium growth of WT and mutants. WT and mutants were cultured on 10% unclarified V8 agar. The colony diameters were measured after 5 days.

In addition, I did not observe mutations of *Ppal15kDa* cause changes in sporulation (all mutants could produce sporangia) and zoospore germination (Fig. 2.13).

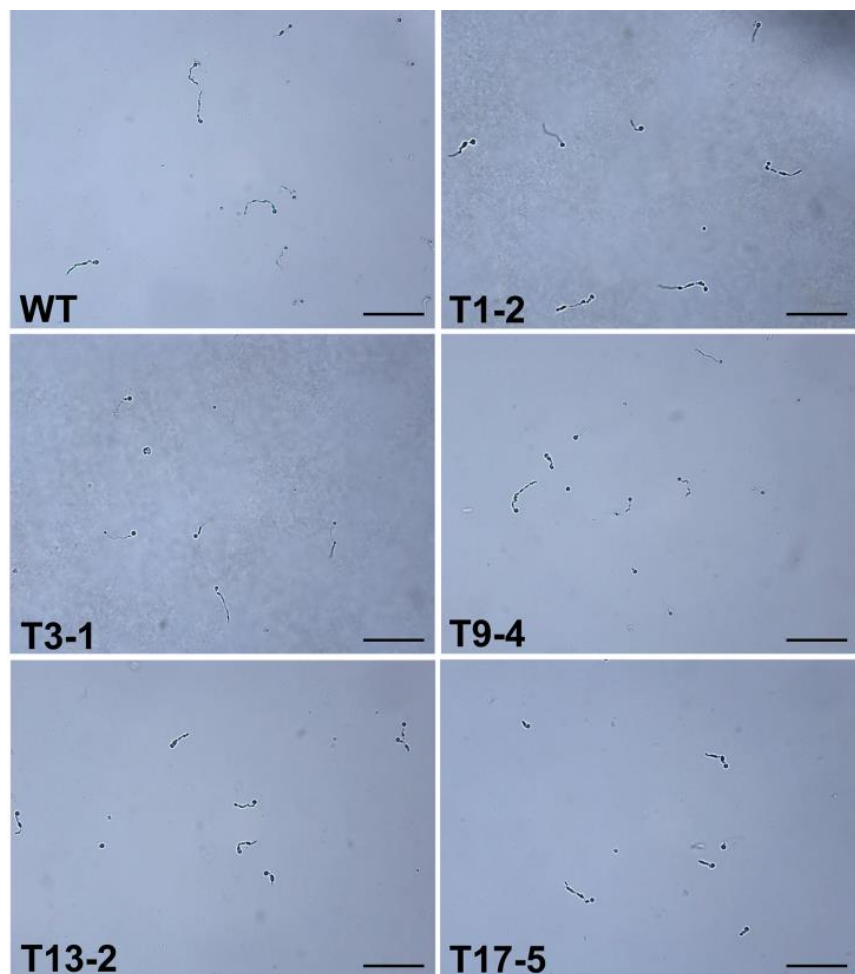


Fig. 2.13 Zoospore germination assay of *P. palmivora* wild-type (WT) strain and *Ppal15kDa* mutants. Zoospores were cultured on Plich agar for 4 hours and photographed under light microscope. Scale bars = 250 μ m.

However, I observed significant difference in sporangium sizes, germ tube lengths and appressorium formation between WT and *Ppal15kDa* mutants. I used five mutants (T1-2, T3-1, T9-4, T13-2 and T17-5) for these assays. As T1-2 and T11-10 exhibited similar genotype and virulence, I only included one of them (T1-2).

The sporangium sizes of all tested mutants were found to be significantly smaller than WT (Fig. 2.8). The average sporangium lengths of T1-2, T3-1, T9-4, T13-2 and T17-5 were 32, 29, 33, 37, 33 μ m, respectively, whereas the average sporangium length of WT was 42 μ m (Fig. 2.14).

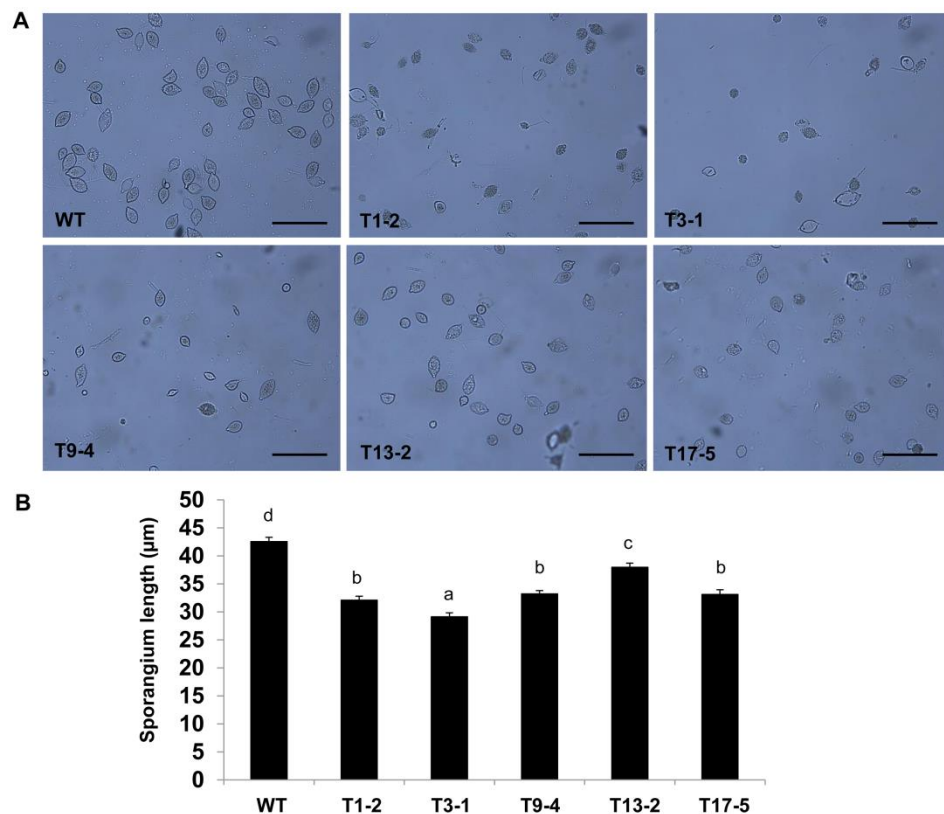


Fig. 2.14 Measurements of the sporangium sizes of *P. palmivora* WT strain and *Ppal15kDa* mutants. A, Representative micrographs of sporangia of WT and mutant strains (scale bars = 250 μm). B, The average sporangium length of wild-type (WT) strain and *Ppal15kDa* mutants. The histograms correspond to the mean ± standard errors (SE) of sporangium length calculated from independent sporangium (n=120). Different letters indicate significant differences, determined using Duncan's multiple range test (P -value < 0.05)

I observed the zoospore germination and germ tube elongation under light microscope at 4 and 24 hours after incubating zoospores on Plich agar. At 4 hours, it was not clearly different between WT and the mutants in zoospore germination rate and germ tube lengths (Fig. 2.13). However, at 24 hours, the germ tubes of *Ppal15kDa* mutant T1-2, T3-1 and T9-4 appeared to be significantly shorter than WT, whereas the germ tube elongation of T13-2 and T17-5 were not clearly affected (Fig. 2.15).

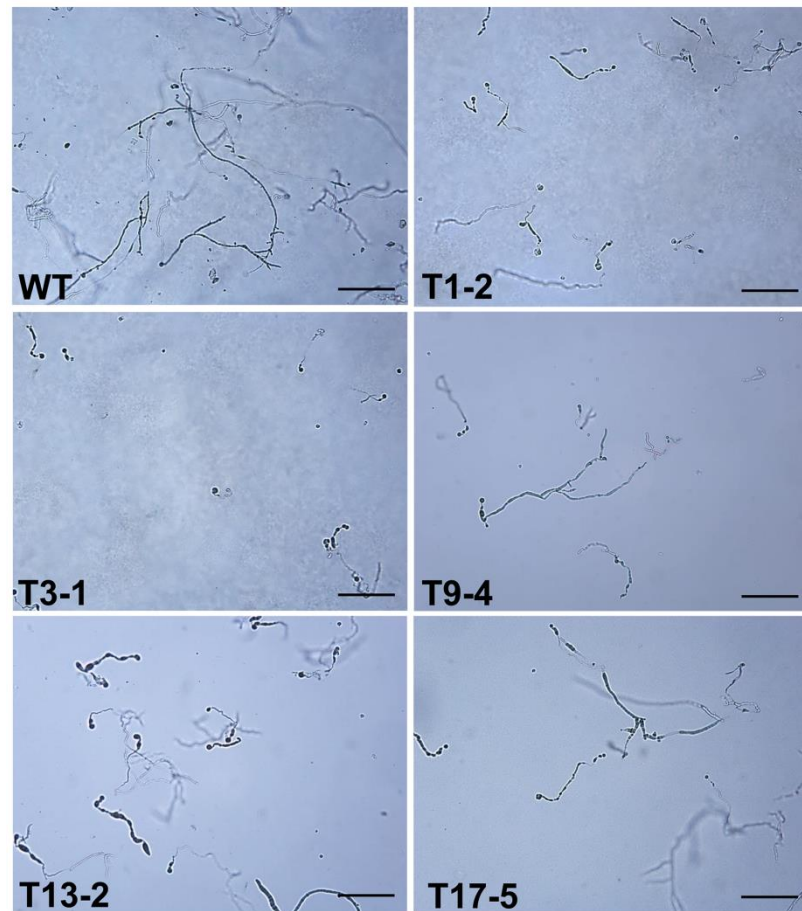


Fig. 2.15 Micrographs of germ tubes of *P. palmivora* WT strain and *Ppal15kDa* mutants. Zoospores were cultured on Plich agar for 24 hours and photographed under light microscope (scale bars = 250 μ m).

Appressoria were observed and counted under light microscope after 4 hours of induction by incubating zoospores between hydrophobic plastic cover slips, which were placed on Plich agar. The percentages of appressorium-forming cysts of T1-2, T3-1 and T9-4 were 8, 12 and 28%, which were much lower than WT with a percentage of 84% (Fig. 2.16). The percentages of appressorium-forming cysts of T13-2 and T17-5 were 74 and 63%, which were slightly lower than WT (Fig. 2.16).

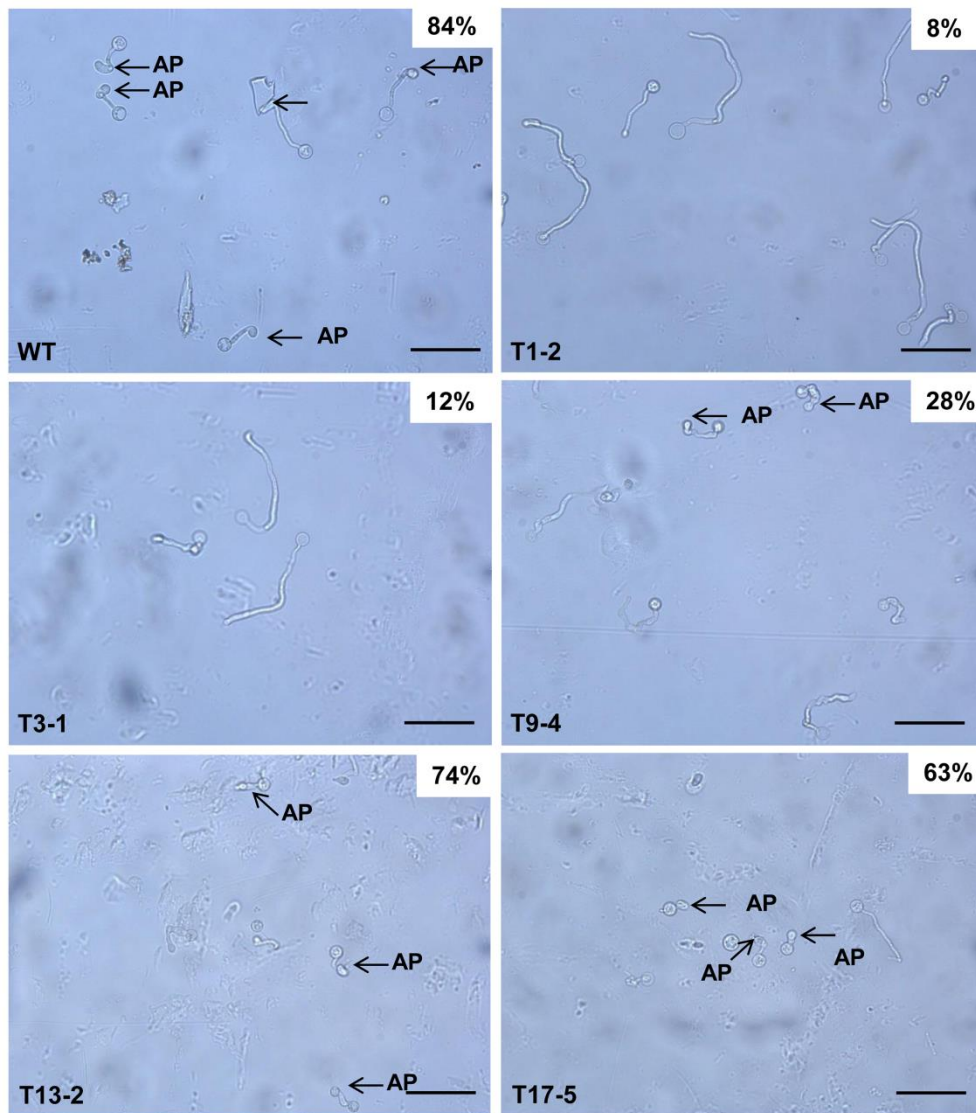


Fig. 2.16 Assays of appressorium formation of *P. palmivora* WT and *Ppal15kDa* mutants. Zoospores were incubated between two plastic cover slips placed on Plich agar at room temperature for 4 hours. Appressoria (AP) were observed and counted under light microscope. The percentage of more than 200 germinated cysts that developed appressoria was shown at the upper right corner of each micrograph. Scale bars = 50 μ m. The experiment was repeated 2 times with similar results.

Clearly, the extent to which germ tubes and appressoria in the mutants were affected was consistent with the level of reduced pathogenicity on plants. T1-2, T3-1 and T9-4 were dramatically compromised in pathogenicity on *N. benthamiana* and papaya (Fig. 2.10 and 11), and their germ tube elongation and appressorium formation were affected at a high level. Consistently, the pathogenicity of T13-2 and T17-5 was affected to a lesser extent, and correspondingly their germ tube elongation and appressorium formation were either not clearly affected or slightly affected. Altogether, the above data suggest that *Ppal15kDa* plays a significant role in sporangium formation and development of infection structures such as germ tubes and appressoria, and *Ppal15kDa* contributes to pathogenicity at least in part by functioning in normal development of *P. palmivora* infection structures.

2.4.6 *Ppal15kDa* is highly induced during appressorium formation.

I determined the expression of *Ppal15kDa* at various *P. palmivora* developmental stages, including zoospores, cysts, germinating cysts, appressorium-forming cysts, sporulating hyphae and vegetative hyphae, using quantitative reverse transcription PCR (RT-qPCR). The expression of *Ppal15kDa* in appressorium-forming cysts was the highest among all tested developmental stages (Fig. 2.17) and induced by about 40 folds compared to the expression in vegetative hyphae (Fig. 2.17). In addition, the expression of *Ppal15kDa* was also induced in cysts by about 8 folds. This result suggests that *Ppal15kDa* is expressed at early stage of infection, i. e. appressorium-forming cysts, a stage before and when penetration takes place.

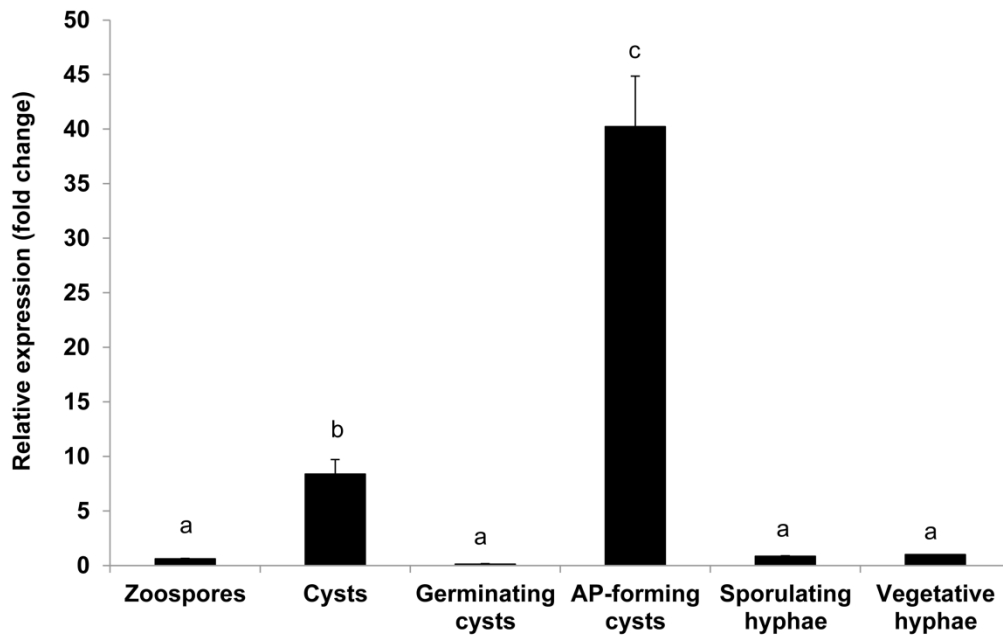


Fig. 2.17 Expression of *Ppal15kDa* in various development stages of *P. palmivora* by RT-qPCR. cDNAs were extracted from zoospores, cysts, germinating cysts, appressorium-forming cysts, sporulating hyphae, and vegetative hyphae of *P. palmivora*. The expression was normalized using *P. palmivora* β -tubulin gene and relative to vegetative hyphae with the expression level in vegetative hyphae calculated as 1. The error bars represent standard deviations from three technical replicates. Different letters indicate significant differences, determined using Duncan's multiple range test (P -value < 0.05).

2.5 Discussion

Many proteins that play important roles in plant-oomycete interactions were identified from culture filtrate of *Phytophthora* spp. (Sacks *et al.*, 1993; Nürnberger *et al.*, 1994; Baillieul *et al.*, 1995; Sejalon-Delmas *et al.*, 1997; Mateos *et al.*, 1997; Kamoun *et al.*, 1998a; Brunner *et al.*, 2002b; Ma *et al.*, 2015). For example, *P. sojae* glycoside hydrolase family 12 (GH12) protein, XEG1, identified from culture filtrate, acts as an important virulence factor during infection but also serves as a PAMP to trigger defense responses including cell death (Ma *et al.*, 2015). In this study, I identified a secreted protein of 15 kDa, Ppal15kDa, abundantly present in culture filtrate of *P. palmivora* using LC-MS/MS. By transient expression of Ppal15kDa in *N.*

benthamiana and generation of its *P. palmivora* mutants using CRISPR/Cas9 gene editing, I found that Ppal15kDa plays a significant role in *P. palmivora* infection structure development and pathogenicity. Ppal15kDa is a previously uncharacterized protein. Besides the signal peptide, it does not have a functional domain indicative of its biochemical function and its homologs were not found in organisms other than *Phytophthora* spp. Ppal15kDa homologs found in *Phytophthora* spp. were all annotated as a hypothetical protein. As such, this study identified a novel apoplastic effector involved in development and pathogenicity of *P. palmivora* and possibly many other *Phytophthora* spp as Ppal15kDa homologs appear to be broadly present in *Phytophthora* spp. In addition, as Ppal15kDa is an extracellular protein and its mutations almost completely crippled *P. palmivora* pathogenicity, it represents a potential ideal target for genetic and chemical control.

After landing and attaching to the host, *P. palmivora* zoospore germinates and produces a germ tube, which differentiates into an appressorium to penetrate the host surface (Le Fevre *et al.*, 2016; Evangelisti *et al.*, 2017). Our results showed that Ppal15kDa mutants were impaired in germ tube elongation and appressorium formation, which corresponded to their compromised pathogenicity, suggesting that Ppal15kDa contributes to infection at early stage by participating in infection structure development. In support of this, *PLTG_02159* which is the Ppal15kDa-encoding gene, was found to be induced at 6 hours post infection, but not at later hours (Evangelisti *et al.*, 2017).

Two specific bands of 15 and 17 kDa were detected by Western blot in *N. benthamiana* leaves expressing His-tagged Ppal15kDa (Fig. 2.6). They likely represent two different glycosylated forms of Ppal15kDa as Ppal15kDa can be stained using periodic acid-Schiff reagent (Fig. 2.1), which is used for staining of glycoproteins, and has potential N-glycosylation and O-glycosylation sites (Fig. 2.2). It is common for glycoproteins expressed in plants to have different glycosylation and therefore migrate as two or more bands on SDS-PAGE. For example, McGarvey *et al.*, (1995) expressed a glycoprotein (G-protein) that coats the outer surface of rabies virus in tomato using *A. tumefaciens*-mediated transformation, and Western blot detection revealed two distinct bands with apparent molecular weight of 60 and 62

kDa. After mixing the G-protein with extracts from normal tomato plant, the smaller size is observed. Their results suggest that a specific enzymatic cleavage of sugar or amino acid residues may be responsible for double bands (McGarvey *et al.*, 1995).

I do not have direct evidence suggesting that Ppal15kDaA and Ppal15kDaB are homoalleles or paralogs in *P. palmivora* genome, but indirect evidence suggests the former. The Ppal15kDa-encoding sequence was found in a single scaffold of the genome assembly of a tetraploid *P. palmivora* cacao isolate (Ali *et al.*, 2017) using BLAST search. In addition, in the Ppal15kDa mutants generated using CRISPR/Cas9 gene editing, the maximal number of different versions of Ppal15kDa observed in a single zoospore-derived transformant is four (Fig. 2.9).

I tested 6 independent single zoospore-derived Ppal15kDa mutants for their infectivity on *N. benthamiana* and papaya and analyzed their phenotypes at various developmental stages. Although overall these mutants were compromised in pathogenicity and affected in sporangium sizes, germ tube elongation and appressorium formation, the affected levels varied. In T1-2 and T11-10, all *Ppal15kDa* copies were mutated. Correspondingly, these two mutants almost completely lost pathogenicity and the development was considerably affected. In the remaining four mutants (T3-1, T13-2, T17-5, T9-4), there was at least one wide-type (WT) *Ppal15kDa* copy present, as a result, their pathogenicity and development were less affected than T1-2/T11-10 except T3-1. T3-1, T13-2 and T17-5 seem to have the same pattern of gene editing (Fig. 2.9), however, their phenotypes varied significantly. There are several factors that might contribute to the difference. When I sequenced the *Ppal15kDa* gene in the mutants, the primers used did not differentiate Ppal15kDaA and Ppal15kDaB versions. Therefore, although I observed the same pattern of mutations and WT copy, as these mutations (or WT) could be in either Ppal15kDaA or Ppal15kDaB, these mutants are very likely to be different. Ppal15kDaA and Ppal15kDaB do not seem to be functionally divergent at the protein level as both were equally effective in enhancing *P. palmivora* infection (Fig. 2.7). The difference contributed by these two versions may lie in their different transcription and/or translation efficiency. To support this, I found multiple single nucleotide polymorphisms (SNPs) between *Ppal15kDaA* and *Ppal15kDaB* in the 5'

untranslated region (Fig. 2.3). Their promoters might be divergent as well. Other factors that contribute to the differences among T3-1, T13-2 and T17-2 could be different integration sites of the T-DNA expressing Cas9 and Ppal15kDa-targeting sgRNA, which affected the phenotypes due to disruption or interference of the neighboring genes.

2.6 Conclusion

I provided the novel finding of a virulent factor from *P. palmivora*, Ppal15kDa and its effects at early stage of infection. The understanding of *Ppal15kDa* gene was reported including promoting infection, involving in germ tube elongation. Especially, the *Ppal15kDa* gene was involved in appressorium formation which was the first report in *Phytophthora* spp.

CHAPTER 3

NOVEL CELL DEATH-INDUCING ELICITORS FROM *PHYTOPHTHORA PALMIVORA* PROMOTE INFECTION ON *HEVEA BRASILIENSIS*

3.1 Introduction

Phytophthora palmivora is a hemibiotrophic pathogen. It can survive in dead tissue and acts as a necrotrophic pathogen. At the beginning of infection, it commonly grows as a biotroph then switches to a necrotroph at later stages of infection. *P. palmivora* is classified among the oomycetes which has characteristics distinct from the true fungi. Oomycete cell wall mainly consists of beta-1,3 glucan, whereas the fungal cell wall is chitin (Werner *et al.*, 2002; Latijnhouwers *et al.*, 2003). In Thailand, *P. palmivora* causes stem rot in both the durian tree (*Durio zibethinus*) and the rubber tree (*Hevea brasiliensis*), with resultant crop losses.

Elicitors containing a variety of molecules are able to activate defense responses in host plants. Because elicitors are structurally conserved components, they are mostly classified as pathogen-associated molecular patterns (PAMPs). Reported biologically active elicitors produced by *Phytophthora* spp. include the oligopeptide 13 amino acid (Pep-13) within cell wall glycoprotein (GP42) of *P. sojae* (Nürnberg *et al.*, 1994; Hahlbrock *et al.*, 1995; Brunner *et al.*, 2002), the OPEL protein encoded by the *OPEL* gene (Chang *et al.*, 2015) and the 34 kDa glycoprotein elicitor (CBEL) (Mateos *et al.*, 1997; Gaulin *et al.*, 2006) of *P. parasitica*. A new protein 75 kDa and elicitin (10 kDa) have been reported for *P. palmivora*. These proteins induce scopoletin (Scp), a plant phytoalexin, and total phenolic compound accumulations in the cell suspension of *H. brasiliensis* (Churngchow and Rattarasarn 2000; Dutsadee and Nunta 2008)

An important process in plant defenses against pathogens is hypersensitive response (HR) cell death. It is induced by accumulations of O_2^- and H_2O_2 which finally trigger a protein kinase-mediated cell death process similar to program cell death (PCD) (Mehdy 1994; Levine *et al.*, 1996). Accumulation of H_2O_2 inhibits the growth of biotrophic pathogens (Thordal-Christensen *et al.*, 1997), whereas

production of H₂O₂ promotes the growth of necrotrophic pathogens (Govrin and Levine 2000). Lee and Rose (2010) suggested that the hemibiotrophic pathogen *P. infestans* facilitates the development of infection by secreting a cell death suppressor during its biotrophic phase and producing cell death inducers in its necrotrophic phase. The virulence of *Botrytis cinerea*, a necrotrophic pathogen, is conducted by a number of lytic enzymes, toxins, high levels of reactive oxygen species and necrosis-inducing factors (van Kan 2006; Choquer *et al.*, 2007). Govrin and Levine (2000) concluded that *B. cinerea* induces the accumulation of H₂O₂ to kill *Arabidopsis thaliana* cells and facilitate its invasion. HR cell death resists biotroph infection by disconnecting nutrient supplies resulting in limiting pathogen growth, however, it may provide growth substrates for invasive necrotrophs (Govrin and Levine 2000). Hemibiotrophs, meanwhile, establish a biotrophic stage within the plant, kill host cells and then switch to a necrotrophic fungal phase (Horbach *et al.*, 2011).

HR cell death is activated by the salicylic acid (SA) signaling pathway. Torres *et al.*, (2005) and Lu *et al.*, (2009) showed that a high level of SA facilitated PCD in *A. thaliana*. SA and jasmonic acid (JA) are secondary messengers involved in PAMP-triggered immunity and effector-triggered immunity (van Loon *et al.*, 2006; Bent and Mackey 2007). The SA-signaling pathway activated by biotrophs can suppress the JA-signaling pathway which is involved in blocking necrotrophic pathogen infection (Spoel *et al.*, 2007; Koornneef *et al.*, 2008; Pieterse *et al.*, 2012). PCD is the effective defense against biotrophic pathogens which is regulated by the SA-dependent pathway. On the other hand, necrotrophic pathogens benefit from host cell death and therefore are not restricted by the SA-dependent pathway but are controlled by the JA-signaling pathway (Glazebrook 2005). Some pathogens can mimic signaling pathways to suppress defense responses. For example, *B. cinerea* produces a beta-glucan elicitor which activates the SA-signaling pathway and suppresses the JA-signaling pathway (El Oirdi *et al.*, 2011). The phytotoxin coronatine, a JA mimic produced by the biotrophic pathogen *Pseudomonas syringae*, promotes its infection by suppressing the SA-signaling pathway (Brooks *et al.*, 2005; Cui *et al.*, 2005)

Cell death and SA inductions are benefit for necrotrophic infections (Govrin and Levine 2000; Glazebrook 2005). Based on the nature of *P. palmivora*, it switches

into necrotroph; consequently, cell death- and SA-inducing elicitors could promote *P. palmivora* infection. Like a glycoside hydrolase family 12 (GH12) protein, XEG1 produced by the soybean pathogen *P. sojae* exhibits xyloglucanase and beta-glucanase activity, and can act as a PAMP. It induces cell death in *Nicotiana benthamiana* and plays an important role as a virulence factor during *P. sojae* infection. After the XEG1 in *P. sojae* was silenced, its virulence was reduced (Ma *et al.*, 2015). *B. cinerea* produces a cell death-inducing elicitor that promotes the Gray Mold Disease on *A. thaliana* leaves (Govrin *et al.*, 2006) and a beta-glucan elicitor that promotes its infection of tomato plants by activating the SA-signaling pathway and suppressing the JA-signaling pathway (El Oirdi *et al.*, 2011). Kliebenstein and Rowe (2008) suggested that the HR cell death caused by biotrophs could increase necrotrophic infection after being inoculated in the same area. *P. palmivora* acts as a biotroph then switches to a necrotroph. If the cell death response is activated at the biotrophic phase of *P. palmivora*, but the infection cannot be resisted; consequently, activated cell death may promote its infection in the necrotrophic phase.

However, the effects of cell death-inducing elicitors of *P. palmivora* have rarely been reported. To identify new elicitors and their effects on plant defense response, I isolated a crude elicitor from culture filtrate of *P. palmivora*. The crude elicitor showed cell death-inducing activity in tobacco leaves and promoted *P. palmivora* infection in rubber tree leaves. I fractionated the crude cell death-inducing elicitor into four fractions, beta-glucan (F1), high-molecular-weight glycoprotein (F2), broad-molecular-weight glycoprotein (F3) and 42 kDa protein (F4). F2, F3 and F4 fractions were novel compound and no one has reported their effect before. They induced SA accumulation and cell death, but the beta-glucan (F1) induced SA accumulation without cell death. Interestingly, the high-molecular-weight glycoprotein, broad-molecular-weight glycoprotein and 42 kDa protein significantly promoted *P. palmivora* infection of rubber tree leaves.

3.2 Objectives

3.2.1 To isolate cell death-inducing elicitors from culture filtrate of *P. palmivora*

3.2.2 To characterize the effect of cell death-inducing elicitors on *H. brasiliensis* defense responses

3.3 Materials and Methods

3.3.1. Pathogen and plants

P. palmivora isolated from rubber tree leaves was generously given by the Songkhla Rubber Research Center, Songkhla, Thailand. The *P. palmivora* mycelium was grown on potato dextrose agar (PDA) at 25°C for 1 week. PDA plugs containing *P. palmivora* were cut with a 5 mm diameter cork borer and transferred onto V8 juice agar for 1 week. To trigger the release of zoospores from sporangia, 1-week *P. palmivora* on V8 juice agar was layered with sterile distilled water, further incubated at 4°C for 15 min, and then shaken at 25°C for 15 min. Petroff Hausser (Boeco, Germany), a cell counter, was utilized to count zoospores under a light microscope. To prepare the elicitor, 1-week *P. palmivora* on V8 juice agar was cut with a cork borer, transferred into Henninger medium (Henniger 1963) and cultured in an incubator at 25°C, with shaking at 100 rpm for 14 days. The culture filtrate was drained through Whatman filter paper (No.1).

Rubber plant seedlings of cultivar RRIM600 at the developmental B2C stage and 8-week tobacco plants (*Nicotiana tabacum*) were maintained in a temperature-controlled room with photoperiod regulation (12 hours light: 12 hours dark: 25°C).

3.3.2 Elicitor isolation and fractionation

Culture filtrate (100 ml) was precipitated with 3 volumes of cool 80% ethanol then the pellet was collected by centrifugation at 10,000 rpm, for 10 min at 4°C. The pellet was re-dissolved with distilled water and subsequently fractionated once for 5 min by the Sevage method (Chloroform : n-butanol = 4:1) to remove proteins. To obtain the crude elicitor, the aqueous phase was collected, dialyzed and lyophilized.

The obtained crude elicitor was dissolved in 20 mM Tris-HCl at pH 7.5 to achieve a final concentration of 0.0125 mg/ml. A 25 ml aliquot of the elicitor solution was loaded into a DEAE-Sepharose column (GE Healthcare, USA, 25 ml gel volume) at a static flow rate of 0.75 ml/min. After collecting ten tubes (2.5 ml of each) of the unbound component (F1), the column was washed with 25 ml of 20 mM Tris-HCl pH 7.5 and then eluted with 25 ml of 20 mM Tris-HCl pH 7.5 containing 0.1 M NaCl. Ten tubes of a second fraction (F2) were collected. The elution was repeated for a third (F3) and fourth (F4) fractions, eluting respectively with 0.15 and 0.3 M NaCl in

25 ml of 20 mM Tris-HCl pH 7.5. Ten tubes of the third (F3) and fourth (F4) fractions were collected. Every tube was measured using the phenol-sulfuric acid method for polysaccharide detection and with absorption at 280 nm for protein content. The target fractions with a high polysaccharide or protein content were pooled and checked for purity by sodium dodecyl sulfate-polyacrylamide gel electrophoresis (SDS-PAGE). For further utilization, the elicitors were desalted in a PD-10 column (GE Healthcare, USA) and then lyophilized.

For size exclusion chromatography, Sephadex-G75 (GE Healthcare, USA) was utilized to purify the 42 kDa protein. Briefly, lyophilized powder of the F4 fraction was re-dissolved with 20 mM Tris-HCl pH 7.5 buffer. The elicitor solution (250 μ l) was loaded into the Sephadex-G75 column (11 x 520 mm, 49 ml of gel volume) using the invariable flow rate at 0.15 ml/min. Each tube (0.75 ml) was collected for 65 tubes. 100 μ l of each separated tube was infiltrated into tobacco leaves to detect the cell death induction. Fractions causing cell death were collected and further analyzed by SDS-PAGE. Three times for Sephadex-G75 purification were performed.

3.3.3 Cell death induction in tobacco leaves

Crude elicitor solution at a concentration of 250 μ g/ml was infiltrated into tobacco leaves. After 24 hours, visual evident of cell death was photographed with a digital camera (Canon EOS 1100D). Sterile distilled water was the control.

After desalting and lyophilizing, F1, F2, F3 and F4 were re-dissolved in 1 ml sterile distilled water and 100 μ l of each solution were infiltrated into tobacco leaves to observe for cell death induction. Five independent biological replicates were performed.

3.3.4 Histochemical staining on tobacco leaves

Cell death was monitored at 12 hours post infiltration. At this time point, cell death on treated tobacco leaves was not visible, so visualization was attempted with Trypan blue staining following a method adapted from Leite *et al.*, (1999). At the designated time points, the tobacco leaves were placed in 0.1% (v/v) Triton X-100 for 10 min and transferred into a 0.4% (w/v) Trypan blue solution (Sigma Aldrich, USA) for 30 min. The unbound dye was rinsed out with sterile distilled water and the leaves were digitally photographed under light microscopy.

To determine the localization of hydrogen peroxide (H₂O₂) at 12 hours post infiltration, the tobacco leaves were stained with 3,3'-diaminobenzidine (DAB) (Sigma Aldrich, USA) according to a procedure adapted from Thordal-Christensen *et al.*, (1997). Briefly, the leaves were immersed in 0.1% (v/v) Triton X-100 for 20 seconds, placed in 1 mg/mL (w/v) DAB and incubated at room temperature. After 8 hours, the leaves were cleared by boiling for 30 min in 95% ethanol to stop the reaction and to remove chlorophyll from the leaf tissue. Five independent biological replicates were performed.

3.3.5 High performance liquid chromatography (HPLC) analysis

Rubber tree and tobacco leaves were respectively sprayed and infiltrated with the elicitor and then collected at designated time points to measure levels of SA, Scp, and ABA by HPLC. The samples were extracted according to the method of Ederli *et al.*, (2011) with modification. The treated leaves (0.5 g) were ground to a fine powder in a mortar with liquid nitrogen and mixed with 750 µl of 90% MeOH. The suspensions were transferred into 1.5 ml Eppendorf tubes, centrifuged at 12,000 rpm for 5 min, and the supernatants were collected. Pellets were re-suspended with 500 µl of 90% MeOH and centrifuged again at 12,000 rpm for 5 min. The supernatants were pooled and added with 50% (w/v) trichloroacetic acid to a final concentration of 5% (w/v) then filtered through a 0.2 µm nylon membrane. The extracted samples were analyzed using HPLC (Agilent series 1100, Waldbronn, Germany) with Eclipse XDB-C18 column (ZORBAX, 4.6 x 150 mm, 5 micron particle size). The mobile phases consisted of 2 solutions, 0.1% formic acid and acetonitrile (ACN), used in gradient elution system, increasing the percentage of ACN. Briefly, I used static 20% ACN

from 0 to 2 min; after 2 min, the ACN content was increased from 20 to 40% until 8.50 min; after 8.50 min, I used static 40% ACN until 10 min and then increased ACN from 40% to 60% until 13 min. A diode array detector was used to detect ABA at 254 nm and fluorescence detectors were used to analyze the levels of Scp (337 nm Ex and 425 nm Em) and SA (294 nm EX, 426 nm EM). Three independent biological replicates were performed.

3.3.6 Functional identification

Infrared (IR) spectra of the crude elicitor and F1 fraction were produced using FTIR spectroscopy. One gram of each was mixed with spectroscopic grade KBr powder, dispersed in a KBr disc and then pressed into 1 mm pellets for FTIR measurement in a wave-range from 600 to 4000 cm^{-1} (Bruker: Vertex70).

3.3.7 Gel staining

After SDS-PAGE, gels were stained with a silver nitrate staining kit (GE Healthcare, Bio-Sciences) according to the manufacturer's protocol for protein detection. Glycoprotein was stained by periodic acid-Schiff staining (Zacharius *et al.*, 1969). Briefly, after fixing in 7.5% (v/v) acetic acid for 1 hour, the gel was immersed in 1% (v/v) periodic acid for 45 min at 4°C in darkness, washed in 7.5% acetic acid for 10 min (6 times) then stained with the periodic acid-Schiff reagent for 1 hour at 4°C in the dark. Finally, the gel was washed with a 0.5% (w/v) sodium metabisulfite solution.

3.3.8 Cell death neutralization

A crude elicitor aliquot of 50 μg in 1 ml of 100 mM sodium acetate buffer at pH 5.0 was digested with 100 μl of beta-1,3-glucanase (0.6 U/ml) for 8 hours at 20°C. After centrifugation for 5 min at 12,000 rpm, the digested solution was infiltrated into tobacco leaves. In addition, 500 μg of the crude elicitor in 1 ml 20 mM Tris-HCl pH 7.5 was treated with 20 μg of Proteinase K for 30 min at 37°C, centrifuged for 5 min at 12,000 rpm then infiltrated into tobacco leaves. Three independent biological replicates were performed.

3.3.9 Infection of rubber tree leaves by *P. palmivora*

Initially, a droplet method was used to apply crude elicitor to rubber tree leaves by co-treatment with zoospores of *P. palmivora*. The ventral side of the leaves was wetted with drops (25 μ l) of a mixture solution containing 1×10^4 zoospores/ml of *P. palmivora* in crude elicitor at a concentration of 250 μ g/ml. The leaves were monitored for disease development at 5 days post treatment. A mixture solution containing 1×10^4 zoospores/ml of *P. palmivora* in sterile distilled water was used as the control.

Exposing rubber tree leaves to infection by spraying required pre-treatment of the leaves with 250 μ g/ml of crude elicitor solution, which was sprayed onto the leaves for 24 hours. After that time, the treated leaves were sprayed with 1×10^4 zoospores/ml of *P. palmivora*. Besides this pre-treatment spraying method, rubber tree leaves were also co-sprayed with crude elicitor, at 250 μ g/ml, and *P. palmivora* zoospores at 1×10^4 zoospores/ml. The severity of infection was evaluated according to the method described by Yang *et al.*, (1996). Five grades of symptom were taken into consideration. If no infection spot was visible, the leaf was classified as grade 0: no symptom. Grade 1 described slight symptoms (1-20 infection spots/leaf); grade 2 described medium disfigurement (21-40 infection spots/leaf); grade 3: rather serious disfigurement (41-60 infection spots/leaf) (41-60 infection spots/leaf) and grade 4: very serious symptoms (more than 60 infection spots/leaf) (Fig. 3.3E). The disease severity index was calculated using the following formula:

Disease severity index (DSI)

$$= \frac{\sum(\text{disease grade} \times \text{no. of leaves in each grade} \times 100)}{(\text{total no. of leaves} \times \text{highest disease grade})}$$

Three independent biological replicates were performed and each replicate consisted of 42 leaves. For testing disease induction by the F1, F2, F3 and F4 fractions, 100 μ l elicitor solutions were mixed with 100 μ l of *P. palmivora* zoospores at a concentration of 2×10^4 zoospores/ml and rubber tree leaves were wetted with drops (20 μ l) of the mixtures. Five days post treatment, lesion diameters were measured. Four independent biological replicates were performed.

3.3.10 Statistical analysis

The presented values were mean value \pm standard error (SE) from the results of at least three independent biological replicates. SPSS Statistics 17.0 software was used to determine significance at $P \leq 0.05$ by one-way analysis of variance (ANOVA) according to Duncan's multiple range tests. Pairwise comparisons with lower numbers of treatments were conducted according to Student's t-test at $P \leq 0.05$.

3.4 Results

3.4.1 Isolation of cell death-inducing elicitor

Our goal was to identify a new cell death-inducing elicitor from the culture filtrate of *P. palmivora*, growing in Henninger medium (Henninger 1963), by ethanol precipitation. The obtained elicitor caused cell death on tobacco leaves at 24 hours post infiltration (Fig. 3.1A). This elicitor did not cause cell death in rubber tree leaves, either by the droplet or the spraying methods, but after making a wound in the leaf to facilitate diffusion into the cells, it could cause chlorotic cell death (Fig. 3.1B).

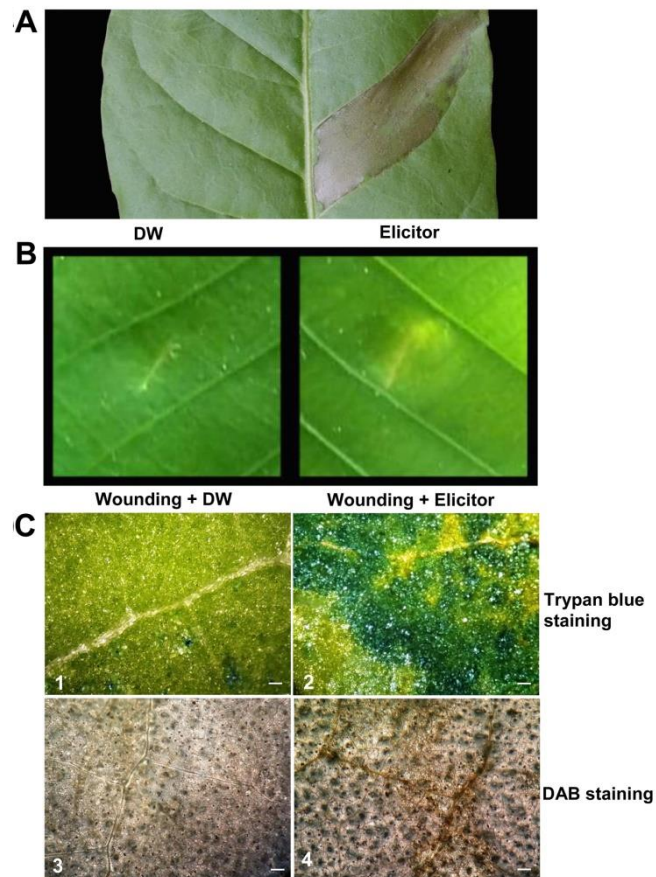


Fig. 3.1 Cell death induced by the crude elicitor on tobacco leaves at 24 hours post infiltration (A). The representatives of chlorotic cell death on wounded rubber tree leaves at 5 days after droplet method treatment with the cell death-inducing elicitor (B). Trypan blue staining of infiltrated areas on tobacco leaves treated with sterile distilled water (C1) and 250 $\mu\text{g}/\text{ml}$ of elicitor solution (C2) and DAB staining of infiltrated areas on tobacco leaves treated with sterile distilled water (C3) and 250 $\mu\text{g}/\text{ml}$ of elicitor solution (C4) at 12 hours post infiltration. Figure 1C-1, C-2, C-3 and C-4 were photographed under a light microscope (scale bars = 200 μm). The pictures are representative of five independent biological replicates and all replicates showed the same results.

In tobacco leaves, cell death induced by this elicitor was not visible at 12 hours post infiltration. However, it could be observed after Trypan blue staining (Fig. 3.1C-2). Cell death requires the accumulation of reactive oxygen species (ROS), O_2^- and H_2O_2 (Mehdy 1994; Levine *et al.*, 1996). Interestingly, at 12 hours post infiltration, accumulation of H_2O_2 was detected using DAB staining method (Fig. 3.1C-4). The results suggested that the obtained elicitor might cause cell death on tobacco leaves through the accumulation of H_2O_2 .

3.4.2 Effects of the cell death-inducing elicitor

3.4.2.1 Tobacco leaves: inductions of SA, Scp and ABA

After infiltrating the crude elicitor into tobacco leaves, SA, Scp, and ABA levels were measured by HPLC. SA generally facilitates cell death in plants (Torres *et al.*, 2005; Lu *et al.*, 2009). The levels of SA was significantly increased at 4 hours post infiltration compared to the control leaves and was continuously induced throughout 12 hours (Fig. 3.2A). Scp, a tobacco phytoalexin, also gradually increased at 4 hours post infiltration and synthesized abundantly at 12 hours (Fig. 3.2B). In a previous work, cell death initiated by wounding was significantly induced by ABA (Cui *et al.*, 2013). Our results showed that the level of ABA was significantly increased at 12 hours, which correlated with the occurrence of cell death (Fig. 3.2C). These results indicated that our elicitor might induce cell death not only through H_2O_2 accumulation, but also through SA and ABA accumulations.

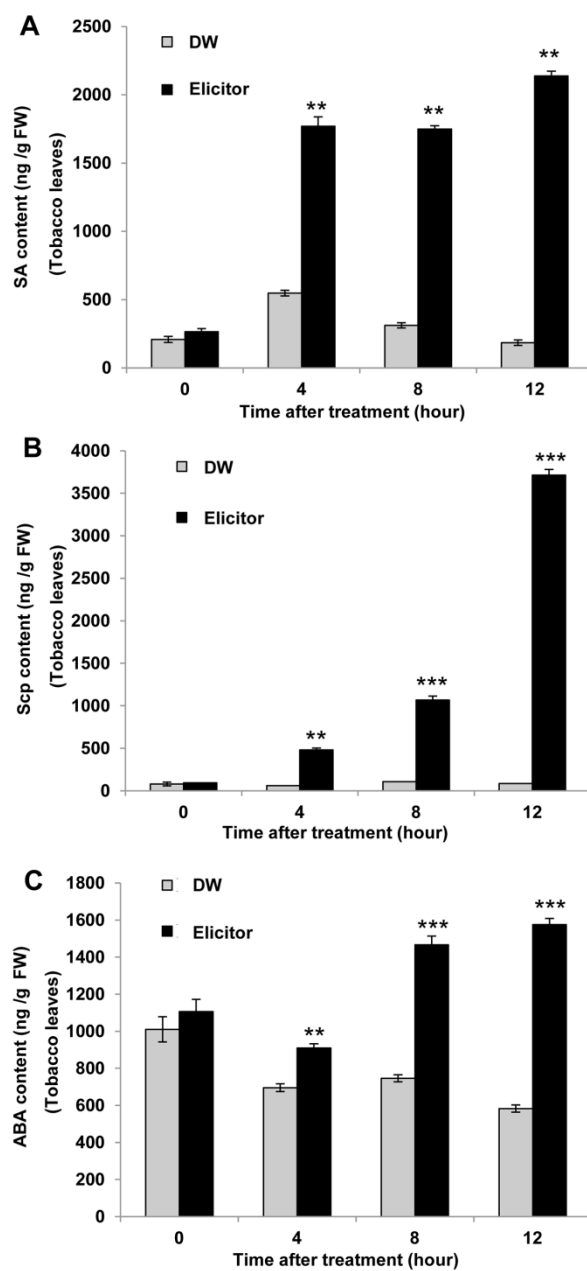


Fig. 3.2 High-performance liquid chromatography analysis of time-related concentrations of SA (A), Scp (B), and ABA (C) in tobacco leaves after infiltration with the cell death-inducing elicitor and sterile distilled water (DW). Data bars are the means (\pm SE) of three independent biological replicates. Two and three asterisks (** and ***) indicate statistically significant differences of cell death-inducing elicitor-treated tobacco leaves compared with sterile distilled water-treated tobacco leaves as a control (P -value ≤ 0.05 and P -value ≤ 0.01 , respectively) determined by Student's t -test.

3.4.2.2 Rubber tree leaves: induction of SA, Scp and ABA

After spraying rubber tree leaves with a concentration of 250 µg/ml of the cell death-inducing elicitor, the levels of SA, Scp, and ABA were analyzed by HPLC. It was found that the SA level at 48 hours post treatment had significantly increased compared to the level in control leaves (Fig. 3.3A) and that the level of Scp had significantly increased at 24 hours post treatment and remained high until 96 hours post treatment (Fig. 3.3B). In addition, the level of ABA had significantly increased at 72 and 96 hours post treatment (Fig. 3.3C). These results indicated that our cell death-inducing elicitor increased SA, Scp and ABA accumulations not only in tobacco leaves but also in rubber tree leaves.

3.4.2.3 Rubber tree leaves: promotion of *P. palmivora* infection

To determine whether the cell death-inducing elicitor facilitated *P. palmivora* infection in rubber tree leaves, I performed co-treatments with *P. palmivora* zoospores and the cell death-inducing elicitor by both droplet and spraying methods. Infection from co-treatment by the droplet method was clearly more severe than it was in leaves co-infected with *P. palmivora* zoospores and sterile distilled water (Fig. 3.3D). After treatment by spraying, the infection levels were classified into five categories (Fig. 3.3E). Rubber tree leaves pre-treated with the cell death-inducing elicitor and infected with *P. palmivora* showed a more severe level of infection than controls (Fig. 3.3F). In addition, the severity of the symptoms significantly increased after co-treatment with the cell death-inducing elicitor and *P. palmivora* zoospores (Fig. 3.3F). The results suggested that our cell death-inducing elicitor enhanced *P. palmivora* infection on rubber tree leaves.

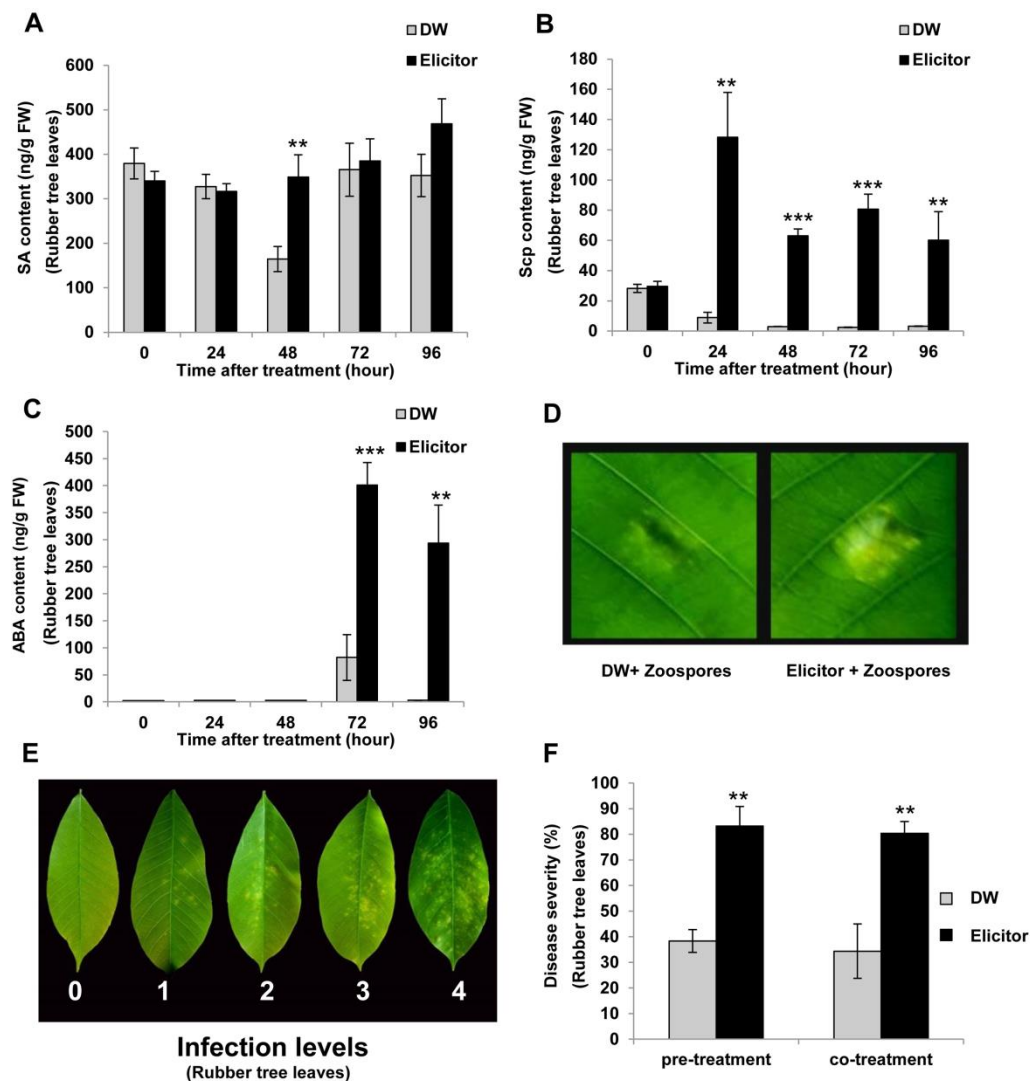


Fig. 3.3 High-performance liquid chromatography analysis of SA (A), Scp (B) and ABA (C) in rubber tree leaves after treatment with the cell death-inducing elicitor by spraying method. The representatives of disease symptom from five independent biological replicates caused by co-infection with cell death-inducing elicitor and *P. palmivora* by a droplet method (D) at 5 days after infection and all replicates showed the same result. The images of symptoms of *P. palmivora* infection on rubber tree leaves from spraying treatment were used to evaluate the disease severity index (level 0-4) (E). The disease severity of *P. palmivora* infection on rubber tree leaves after pre-treatment and co-treatment with the cell death-inducing elicitor using spraying method (F). Data bars are the means (\pm SE) of three independent biological replicates. Two and three asterisks (** and ***) indicated statistically significant differences of

cell death-inducing elicitor-treated rubber tree leaves compared with sterile distilled water-treated rubber tree leaves as a control (P-value \leq 0.05 and P-value \leq 0.01, respectively) determined by Student's t-test.

3.4.3 Identification and characterization of the cell death-inducing elicitor

3.4.3.1 By FTIR and SDS-PAGE

Since this elicitor induced cell death and promoted *P. palmivora* infection, it merited further characterization. The FTIR spectrum of the cell death-inducing elicitor presented many absorption bands which were characteristic of polysaccharides (Fig. 3.4A). I detected a broad and strong absorption band at 3387 cm^{-1} and a band at 2927 cm^{-1} . The bands near 3405 and 2930 cm^{-1} indicated stretching of the OH group and CH bond, respectively (Šandula *et al.*, 1999). A strong and broad absorption band, detected between 950 and 1200 cm^{-1} was assigned to CO vibration (Šandula *et al.*, 1999). The FTIR spectrum also showed absorption bands at 1546 and 1649 cm^{-1} (Fig. 3.4A) which were from amide I (C=O) and amide II (NH) of proteins, respectively (Belton *et al.*, 1995; Barth 2007). The spectrum indicated that the cell death-inducing elicitor consisted of polysaccharides and proteins. Furthermore, after SDS-PAGE and staining with silver nitrate, I observed many proteins. These results suggested that the cell death-inducing elicitor was a compound elicitor because it contained polysaccharide and protein (Fig. 3.6A). This point motivated us to fractionate the compound elicitor and to investigate which parts of it could cause cell death and promote *P. palmivora* infection.

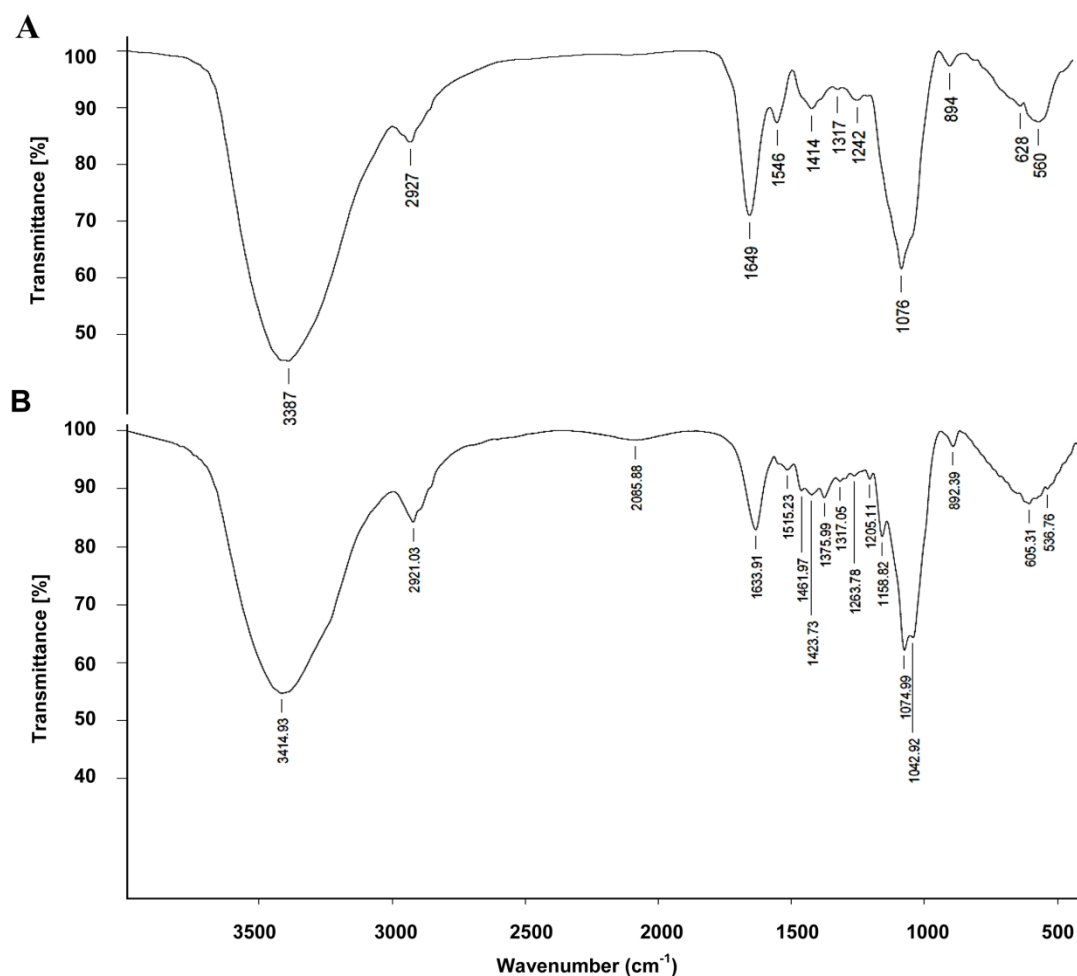


Fig. 3.4 Fourier transform infrared spectra of cell death-inducing elicitor before separation (A) and F1 fraction which was an unbound fraction from an anion exchange column chromatography (B).

3.4.3.2 By enzyme beta-1,3-glucanase and Proteinase K

The compound elicitor was digested with two enzymes, beta-1,3-glucanase for glucan degradation and Proteinase K for protein elimination. I found that Proteinase K completely neutralized cell death caused by the compound elicitor. In contrast, beta-1,3- glucanase did not inhibit cell death induction (Fig. 3.5). The results implied that the protein moiety in the compound elicitor was the causative agent of cell death.

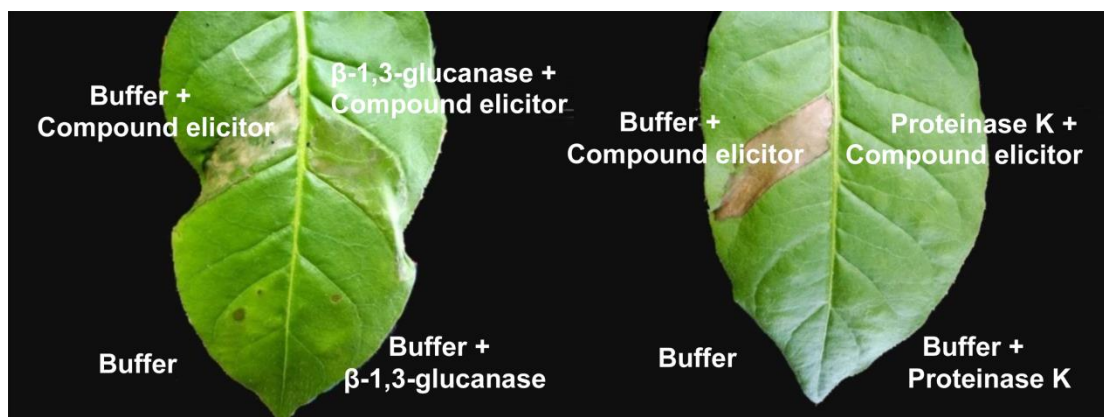


Fig. 3.5 The effect on cell death induction of beta-1,3-glucanase, at 24 hours post infiltration, and Proteinase K at 72 hours post infiltration with a cell death-inducing elicitor. The pictures are representative of three independent biological replicates and all replicates showed the same results.

3.4.4 Fractionation of the compound elicitor

I fractionated the compound elicitor by anion exchange chromatography using DEAE-Sepharose. The compound elicitor consisted of four fractions. First, I detected a polysaccharide from the unbound fraction (F1). After elution with 0.1 M NaCl, SDS-PAGE revealed that a second fraction (F2) was a high-molecular-weight protein (>97 kDa). A third fraction (F3), eluted with 0.15 M NaCl, was a broad-molecular-weight protein (66-97 kDa). The final fraction (F4), eluted with 0.3 M NaCl, consisted of a smear-band protein and 45 kDa protein (Fig. 3.6A).

3.4.4.1 Identification of F1-F4 fractions

SDS-PAGE did not indicate the presence of any protein in F1 (Fig. 3.6A). This result was supported by the FTIR analysis (Fig. 3.4B). Many of the absorption bands revealed by FTIR functional analysis (3414 , 2921 and $900-1200$ cm^{-1}) are characteristic of polysaccharides. Within and close to this range, IR bands near 1160 , 1078 , 1044 and 890 cm^{-1} are characteristic of fungal $(1\rightarrow3)(1\rightarrow6)\text{-}\beta\text{-D-glucans}$ (Gutiérrez *et al.*, 1996; Barth 2007) and absorption bands at 1155 , 1023 , 930 , 850 and 765 cm^{-1} are characteristic of fungal $(1\rightarrow4)(1\rightarrow6)\text{-}\alpha\text{-D-glucans}$ (Barth 2007). Since the FTIR spectrum of F1 showed absorption bands at 1158 , 1074 , 1042 and 892 cm^{-1} (Fig. 3.4B), I concluded that the F1 fraction was $(1\rightarrow3)(1\rightarrow6)\text{-}\beta\text{-D-glucan}$.

I stained each fraction with the periodic acid-Schiff (PAS) reagent after performing SDS-PAGE to detect glycoproteins (Zacharius *et al.*, 1969). The F2 and F3 fractions gave positive bands with the PAS reagent (Fig. 3.6B), while F4 did not. The result demonstrated that F2 and F3 were glycoproteins.

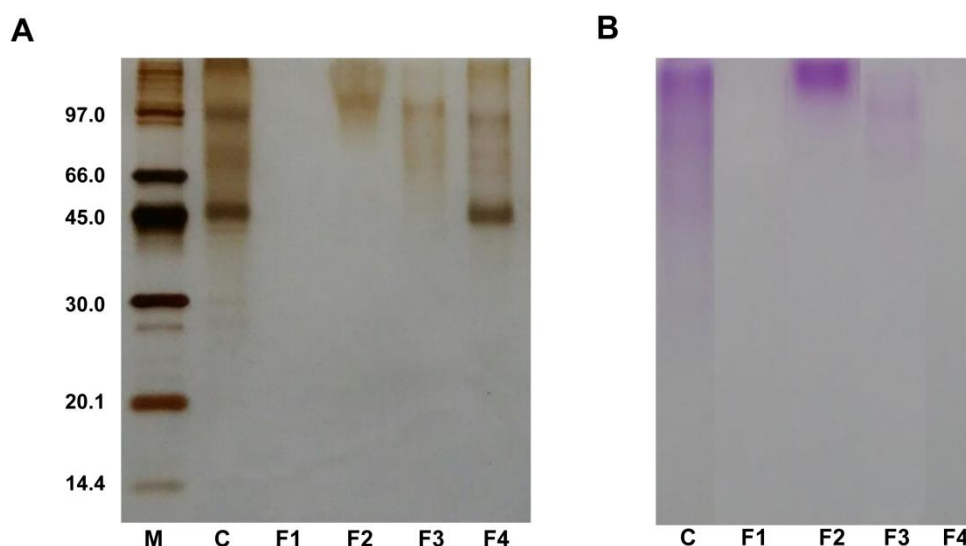


Fig. 3.6 Silver staining after SDS-PAGE (A) and periodic acid-Schiff staining (B) of protein marker (lane M), a crude elicitor (lane C), an unbound fraction (lane F1), a fraction eluted with 0.1 M NaCl (lane F2), a fraction eluted with 0.15 M NaCl (lane F3), and a fraction eluted with 0.3 M NaCl (lane F4) from anion exchange chromatography (DEAE-Sepharose).

3.4.4.2 Effects of each fraction

3.4.4.2.1 Cell death induction

At low concentration (1X) (Fig. 3.7A), only F3 caused cell death on tobacco leaves, while at high concentration (5X) (Fig. 3.7B), every fraction except F1 caused cell death on tobacco leaves. The result suggested that cell death was mainly caused by the broad-molecular-weight glycoprotein (F3) in the compound elicitor.

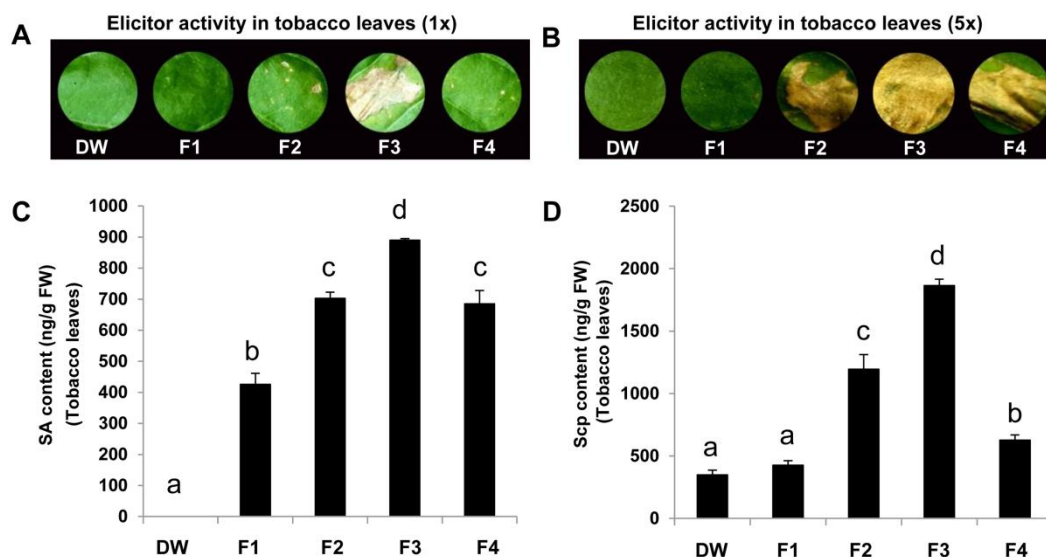


Fig. 3.7 Cell death induction on tobacco leaves by four fractions separated by anion chromatography column at low concentration (1X) (A), and at high concentration (5X) (B) of each, unbound fraction (F1), fraction eluted with 1.0 M NaCl (F2), fraction eluted with 1.5 M NaCl (F3) and fraction eluted 0.3 M NaCl (F4). Photographs were taken at 48 hours post infiltration. Accumulation of SA (C) and Scp (D) in tobacco leaves after infiltration by each fraction at 12 hours post infiltration. Data bars are the means (\pm SE) of three independent biological replicates. Significant differences, according to Duncan's multiple range test ($p \leq 0.05$) were presented by differences among treatments.

3.4.4.2.2 SA and Scp accumulation

Each fraction was infiltrated into tobacco leaves and accumulations of SA and Scp were measured by HPLC. F2, F3 and F4 fractions, which had cell death-inducing activity, caused higher levels of SA accumulation than F1 (Fig. 3.7C). Similarly, Scp was induced in tobacco leaves treated by F2, F3 and F4 fractions (Fig. 3.7D). The results suggested that the cell death induction activity was correlated with the level of SA in leaves.

3.4.4.2.3 Promoting *P. palmivora* infection

Since F2, F3 and F4 could induce cell death, each fraction was co-treated with zoospores of *P. palmivora*. I found that F2, F3, and F4 induced *P. palmivora* invasion that produced large infected areas (Fig. 3.8A and 3.8B). In contrast, rubber tree leaves

co-infected with sterile distilled water or F1 showed small infected areas (Fig. 3.8B). Thus, the fractions that induced cell death and a high level of SA could promote *P. palmivora* infection on rubber tree leaves.

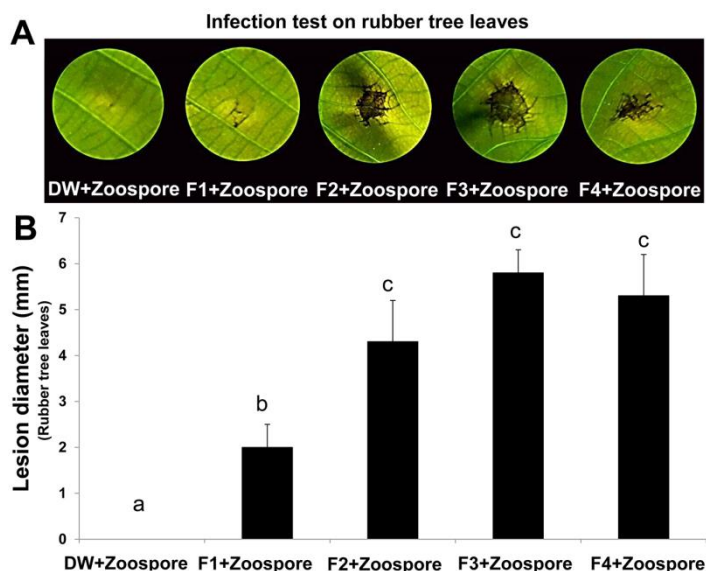


Fig. 3.8 The representative rubber tree leaves after co-treatment with each fraction and zoospores of *P. palmivora* at 5 days after treatment (A). Lesion diameter (mm) of rubber tree leaves co-treated with each fraction and zoospores of *P. palmivora* at 5 days after treatment (B). Data bars are the means (\pm SE) of four independent biological replicates. Significant differences according to Duncan's multiple range test ($p \leq 0.05$) were presented by differences among treatments.

3.4.5 Further purification of F4 fraction

Since F4 mainly consisted of 45 kDa protein (Fig. 3.6A), it was further purified by size exclusion chromatography (Sephadex-G75). Each fraction eluted from the column was infiltrated into tobacco leaves to determine cell death activity. I found that fractions 37 to 39 were able to trigger cell death on tobacco leaves (Fig. 3.9A). Surprisingly, the mobility of the causative agent was shifted to 42 kDa (Fig. 3.9B).

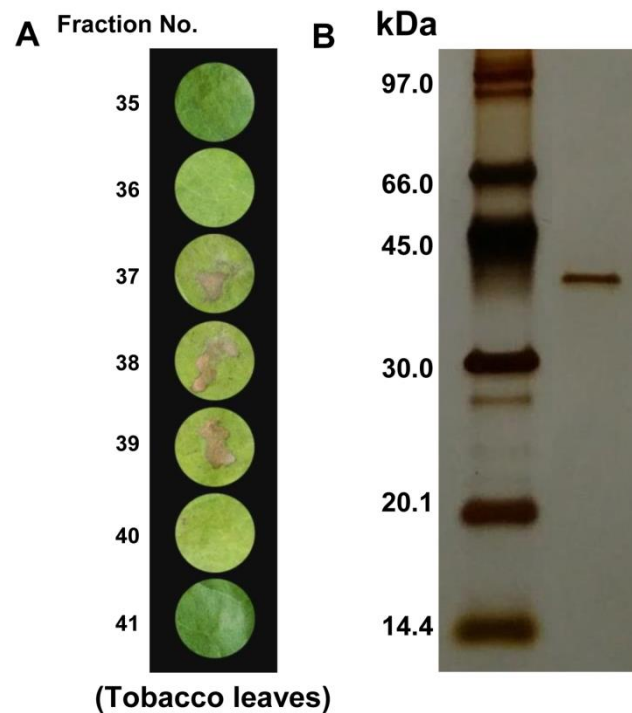


Fig. 3.9 Purification of the F4 fraction by size exclusion chromatography (Sephadex G-75): the fractions that possess cell death-inducing activity (A) and silver staining after SDS-PAGE of pooled cell death-inducing fractions (B).

3.5 Discussion

In this study, I isolated a new cell death-inducing elicitor from culture filtrate of *P. palmivora* by ethanol precipitation and deproteinization with Sevage reagent. The elicitor could induce cell death in tobacco leaves and chlorotic cell death in rubber tree leaves that had been wounded. The rubber tree leaf is covered with a thick cutin, it is not as easy to infiltrate as the tobacco leaf. Wounding could facilitate diffusion of the elicitor into rubber tree cells. Many cell death-inducing elicitors of *Phytophthora* spp. have been reported: INF1 from *P. infestans* (Kamoun *et al.*, 1997), the 32 kDa and 42 kDa glycoproteins from *P. megasperma* (Parker *et al.*, 1991; Baillieul *et al.*, 1995) and a glycoside hydrolase family 12 (GH12) protein from *P. sojae* (Ma *et al.*, 2015).

In tobacco leaves infiltrated with the elicitor, H₂O₂ and SA accumulations were detected along with cell death (Fig. 3.1C and 3.2A). Hypersensitive response (HR) cell death requires the accumulation of reactive oxygen species (ROS), O₂⁻ and H₂O₂, which lead to an increase in levels of cytosolic Ca²⁺ and activation of the protein kinase-mediated cell death process (Mehdy 1994; Levine *et al.*, 1996). Furthermore, the induction of cell death in plants is promoted by SA. Previous studies have elucidated the facilitation of cell death in plants by SA (Torres *et al.*, 2005; Lu *et al.*, 2009) and many works demonstrated that induction of H₂O₂ and SA accumulations by cell death-inducing elicitors from *Phytophthora* spp. such as the 32 kDa glycoprotein from *P. megasperma* (Baillieul *et al.*, 1995) and an oligopeptide of 13 amino acid (Pep-13) from *P. sojae* (Nürnbergger *et al.*, 1994; Hahlbrock *et al.*, 1995). In the present study, the stress hormone ABA was significantly induced at 8 hours post treatment and remained at a high level through 12 hours post treatment (Fig. 3.2C). This behavior correlated to the occurrence of cell death stained with Trypan blue dye (Fig. 3.1C, -1 and -2). Cui *et al.*, (2013) demonstrated that the spread of cell death caused by wounding is significantly induced by ABA. For our results, an increase of ABA might contribute to the expansion of cell death. Our crude elicitor also increased Scp accumulation in tobacco leaves (Fig. 3.2B). Other elicitors that caused Scp accumulation are 42 kDa glycoprotein from *P. megasperma* (Parker *et al.*, 1991) and elicitin and a new protein, 75 kDa, from *P. palmivora* (Churugchow and Rattarasarn 2000; Dutsadee and Nunta 2008). As in tobacco leaves, SA, Scp, and ABA levels were increased in rubber tree leaves (Fig. 3.3A, B and C).

Phytophthora pathogens are able to convert themselves into necrotrophs. Necrotrophic pathogens benefit from host cell death (Glazebrook 2005). As our hypothesis, elicitors which caused cell death and activated SA-signaling pathway could promote *P. palmivora* infection. I showed that the cell death-inducing elicitor promoted *P. palmivora* infection (Fig. 3.3D and F). Various low-molecular-weight phytotoxic metabolites are produced by necrotrophic pathogens (van Kan 2006) and many phytotoxic proteins induced necrosis in plants (Choquer *et al.*, 2007). *B. cinerea*, a necrotrophic pathogen, promotes its infection by producing a lytic enzyme and maintaining high levels of ROS, toxins and necrosis-inducing factors (van Kan

2006; Choquer *et al.*, 2007). The oomycete hemibiotrophic pathogen, *P. sojae*, produces a glycoside hydrolase family 12 (GH12) protein which induces cell death in *N. benthamiana* and plays as an important virulence factor during *P. sojae* infection (Ma *et al.*, 2015). When *P. palmivora* entered the necrotrophic phase in our experiment, the cell death-inducing elicitor could promote its infection (Fig. 3.3D and F).

Plants have many pathogenesis-related (PR) proteins. These proteins have been classified into 17 families according to their properties and functions (van Loon *et al.*, 2006). Many of them, such as PR2 (beta-1,3 glucanases), PR3 (chitinases) and PR7 (endoproteases), have a hydrolytic property. These enzymes are secreted into intercellular spaces where recognition and signaling activation processes occur (Dixon and Lamb 1990; van Loon *et al.*, 2006). I found that beta-1,3 glucanase did not inhibit the appearance of cell death but on the other hand, Proteinase K, a serine protease, completely neutralized the effect of the cell death-inducing elicitor (Fig. 3.5). Therefore, I concluded that the causative agent in the compound elicitor was a protein. During natural infection of rubber tree leaves by *P. palmivora*, only *HbSPA*, a subtilisin-like serine protease gene, is induced at the early stage of infection, later returning to a low level. But other subtilisin-like serine protease genes, *HbSPB* and *HbSPC*, are significantly suppressed throughout infection (Ekchaweng *et al.*, 2017). During infection by *P. palmivora*, rubber tree leaves have a low amount of cell death neutralizers, so cell death elicitors can strongly exhibit their activity. Thus, a rubber plant which could over-express protease should be more resistant than the control plants.

After fractionation, I found that the unbound fraction (F1) was beta-1,3-glucan (Fig. 3.4B). This finding is correlated with the fact that the cell wall oomycetes mainly consists of beta-1,3-glucan. Linear beta-1,3 glucan extracted from the brown alga, *Laminaria digitata* was shown as an elicitor which induced defense responses in tobacco (Klarzynski *et al.*, 2000) and a pure glucan extracted from mycelium wall of *P. megasperma* induced the synthesis of phytoalexins in soybean (Sharp *et al.*, 1984). In this study, I successfully purified exo-beta-1,3-glucan from culture filtrate of *P. palmivora*. After eluting the column with NaCl, I obtained a high-molecular-weight

glycoprotein (F2), a broad-molecular-weight glycoprotein (F3) and a fraction which mainly consisted of the 45 kDa protein (F4) (Fig. 3.6B). *Phytophthora* spp. produce many glycoproteins. The 34 kDa glycoprotein elicitor (CBEL) produced by *P. parasitica*, is localized in the cell wall (Mateos *et al.*, 1997; Gaulin *et al.*, 2006) and an oligopeptide of 13 amino acid (Pep-13) is identified within the cell wall glycoprotein (GP42) of *P. sojae* (Nürnberger *et al.*, 1994; Hahlbrock *et al.*, 1995; Brunner *et al.*, 2002).

The beta-glucan, F1 fraction, did not cause cell death on tobacco leaves neither high or low concentration (Fig. 3.7A and B). This result was similar to the result of Klarzynski *et al.*, (2000) who illustrated that laminarin, a linear beta-1,3 glucan could not induce cell death on tobacco leaves. On the other hand, fraction F2, F3 and F4 did induce cell death on tobacco leaves (Fig. 3.7A and B). The high-molecular-weight glycoprotein fraction was previously identified by Parker *et al.*, (1991), who studied the extracellular glycoprotein from *P. megasperma* without identifying its effects. I showed that the high molecular weight glycoprotein from *P. palmivora* could cause cell death on tobacco leaves (Fig. 3.7B).

Previous researches elucidated that SA facilitates cell death on plants (Torres *et al.*, 2005; Lu *et al.*, 2009). Not only cell death-inducing fractions, but beta-glucan also induced the accumulation of SA (Fig. 3.7C). Similarly, a linear beta-glucan from brown alga and beta-glucan produced by *B. cinerea* stimulate SA accumulation in plants (Klarzynski *et al.*, 2000; El Oirdi *et al.*, 2011). Interestingly, the fraction which caused larger areas of cell death induced higher levels of SA (Fig. 3.7C). Fu *et al.*, (2012) explained why high SA levels can cause cell death in plants: the level of SA affected NPR3 and NPR4, the cullin 3 (CUL3) adapters for degradation of NPR1 (a cell death suppressor). At high concentrations, SA binds to NPR3 and mediates the degradation of NPR1, which induces cell death. But at low concentrations, SA cannot bind to NPR3 and connects instead to NPR4, which blocks NPR1 degradation, resulting in cell survival.

As I expected, all cell death-inducing fractions (F2, F3 and F4) promoted *P. palmivora* infection (Fig. 3.8). Govrin and Levine 2000 suggested that the HR cell

death resists biotrophic infection by disconnecting nutrient supplies and limiting pathogen growth. However, by doing so, it may provide growth substrates for invasive necrotrophs. Hemibiotrophs kill the host cell and switch to the necrotrophic fungal phase after establishment of the biotrophic stage within the plant cell (Horbach *et al.*, 2011). PCD effectively inhibits biotrophic pathogens that are regulated by the SA-dependent pathway. On the other hand, necrotrophic pathogens benefiting from the host cell death are not restricted by the SA-dependent pathway and cell death but are controlled by the JA-signaling pathway (Glazebrook 2005). The effects of many cell death-inducing elicitors from various pathogens have been reported. An XEG1 elicitor produced by the soybean pathogen *P. sojae* plays an important virulence factor during *P. sojae* infection (Ma *et al.*, 2015). An elicitor isolated from the intercellular fluid of *A. thaliana* leaves infected with *B. cinerea* induces cell death. After infiltration with this elicitor prior to inoculation with spores of *B. cinerea*, it promotes *B. cinerea* infection by increasing lesion size (Govrin *et al.*, 2006). Dead cells caused from hypersensitive response make the plants resistant to the biotrophs, but if plants are infected by necrotrophs in the same area, the infection can spread. So, the prior activation of cell death caused by biotrophic pathogens can further promote necrotrophic pathogen infection (Kliebenstein and Rowe 2008). As *P. palmivora* is a hemibiotroph, our study showed that cell death-inducing elicitors promote its infection of rubber tree leaves. After co-infection with cell death-inducing elicitors, cell death effects did not completely inhibit *P. palmivora* infection at the early, biotrophic phase. Conversely, in the later, necrotrophic phase, they promoted *P. palmivora* infection. I propose that the activation of ROS and SA by *P. palmivora* that causes cell death also promotes its infection in the necrotrophic phase. In a cell death area, *P. palmivora* is separated from living cells, thanks to its life-cycle, it can survive and wait to spread later.

After purifying the F4 fraction with Sephadex G-75, I obtained a 42 kDa elicitor which caused cell death (Fig. 3.9B). This 42 kDa elicitor appeared as 45 kDa in the F4 fraction (Fig. 3.6A). Rath *et al.*, (2009) showed that gel shifting in SDS-PAGE is influenced by SDS binding capacity. The purification of the 42 kDa elicitor

eliminated many molecules that interfered with SDS binding, therefore providing more charge for the target protein to move in the PAGE.

3.6 Conclusion

I functionally characterized the beta-glucan (F1) and the cell death-inducing elicitors (high-molecular-weight glycoprotein (F2), broad-molecular-weight glycoprotein (F3) and 42 kDa protein (F4)) isolated from culture filtrate of *P. palmivora*. I provided evidence that cell death and SA inductions caused by elicitors promoted *P. palmivora* infection. From our finding, I suggested that the way which might make plants more resistant to *P. palmivora* was increasing the protease level in plant cell to neutralize cell death effects.

CHAPTER 4

SULPHATED POLYSACCHARIDE FROM *ACANTHOPHORA SPICIFERA* INDUCED *HEVEA BRASILIENSIS* DEFENSE RESPONSES AGAINST *PHYTOPHTHORA PALMIVORA* INFECTION

4.1 Introduction

Hevea brasiliensis (Wild.) Muell.-Arg, or the Para rubber tree, is one of the most important economic crops in Thailand. Its products are exported worldwide, producing significant revenue. *Phytophthora palmivora* infects a thousand or more plant species, including ornamental, horticultural and agricultural crops. It has been identified as a causal agent of leaf fall and black stripe that destroy the rubber plant (Dos Santos *et al.*, 1995). These diseases reduce the quality and yield of rubber latex which presents important problems to cultivators.

Plants establish a state of enhanced defensive capacity in response to appropriate stimuli. This state is called induced resistance which is highly effective against a broad range of subsequent pathogen challenges (Van Loon, 2000). Two forms of induced resistance are systemic acquired resistance (SAR) and induced systemic resistance (ISR). SAR involves accumulations of pathogenesis-related proteins and salicylic acid (SA) (Pieterse *et al.*, 1996), whereas ISR depends on jasmonic acid (JA) and ethylene (ET) pathways (Pieterse *et al.*, 1998). Many marker genes, such as pathogenesis-related genes 1 (*PR-1*), endo-1,3- β -D-glucanase (*PR-2*), and thaumatin-like protein (*PR-5*), are frequently used to illustrate an SA-mediated plant defense response. On the other hand, genes associated with the JA signaling pathway are chitinase (*PR-3*), hevein-like protein (*PR-4*), and protease inhibitor (*PR-6*) (Derksen *et al.*, 2013).

Elicitors are biofactors or chemicals from various sources that are able to induce physiological changes in targeted living organisms. Elicitors are obtained from many sources and induce morphological and physiological alterations and phytoalexin accumulation in plants. Biotic elicitors are derived from bacteria, fungi, plant cell components, viruses or herbivores, as well as chemicals which are released by plants at the attack site after infection, whereas abiotic elicitors are metal ions and organic

compounds (Zhao *et al.*, 2005). Poly- or oligosaccharides, such as chitin, xyloglucans, chitosan, β -glucan, and oligogalacturonide exhibit elicitor activity in different plant species and strongly induce phytoalexins in plants (Zhao *et al.*, 2005). Therefore, elicitors have been considered as alternative tools for disease control in crops.

Phytophthora pathogens also produce elicitors. Plants pretreated with these elicitors establish induced resistance. Elicitin (10 kDa) and a new 75 kDa elicitor from *P. palmivora* can induce peroxidase activity and accumulations of Scp and phenolic compounds both in leaves and a suspension of rubber tree cells (Dutsadee and Nunta, 2008). The OPEL from *P. parasitica* triggers callose deposition and expressions of SA-responsive genes including *PR-1* and *PR-5*. *Nicotiana benthamiana* leaves pretreated with the OPEL before being challenged with *P. parasitica* show disease resistance against the infection (Chang *et al.*, 2015). Pretreatment of tobacco leaves with a 34 kDa glycoprotein elicitor (CBEL) from *P. parasitica* causes necrosis, induces defense gene expression and disease resistance (Mateos *et al.*, 1997). However, these elicitors require many steps to purify and tend to induce cell death in plants, so they are not suitable to protect field crops.

Marine macroalgae are considered important alternative sources of polysaccharide elicitors because they do not cause cell death on plant tissues (Klarzynski *et al.*, 2000 and 2003; Ghannam *et al.*, 2013). Sourced from marine macroalgae and green, brown and red seaweed, cell wall and storage polysaccharides such as alginates, carrageenans, fucans, laminarin, and ulvans can trigger plant defense responses and enhance resistance to viral, fungal and bacterial infections (Vera *et al.*, 2011). For example, sulphated carrageenan from the red alga, *Hypnea musciformis*, induces phytoalexin accumulation, expressions of genes involved in SA and JA signaling pathways and results in resistance against tobacco mosaic virus infection (Ghannam *et al.*, 2013). Glucuronan and ulvans from the green alga, *Ulva lactuca*, induce SA and phenolic compound accumulations in tomato seedlings and also significantly induce resistance in tomatoes to *Fusarium oxysporum* infection (El Modafar *et al.*, 2012). A linear β -1,3-glucan extracted from the brown alga, *Laminaria digitata*, induces expressions of *PR-1*, *PR-2*, *PR-3* and *PR-5* genes (Klarzynski *et al.*, 2000). In addition, ulvans and oligoulvans from *U. lactuca* increase

catalase, peroxidase, and polyphenol oxidase activities and induce phenolic compounds and lignin contents in apples, which lead to resistance against *Penicillium expansum* and *Botrytis cinerea* infections (Abouraïcha *et al.*, 2015).

Acanthophora spicifera is a red seaweed of the family Rhodomelaceae (order Ceramiales). The major polysaccharides of many red macroalgae are carrageenans. The structure of carrageenan from *A. spicifera* is reported to be a λ -type-carrageenan (Parekh *et al.*, 1989). The λ -carrageenan consists of a repeating dimer of D-galactose (A unit), sulphated in C2, linked to a D-galactose (B unit) sulphated in C2 and C6. Duarte *et al.* (2004) reported that the sulphated polysaccharide from *A. spicifera* consisted of A and B units of galactose molecules. In addition, some of the B unit was 3,6-anhydro- α -L-galactose which resulted in the loss of C6-sulphate. However, an alternative purification method and applications of *A. spicifera* extract in plant protection have rarely been reported.

SPS from diverse red algae induces different defense arsenals in several plant species. Mercier *et al.* (2001) reported that the algal polysaccharide carrageenan, λ -carrageenan, causes SA production and fluorescent compound accumulation in tobacco leaves. *Arabidopsis thaliana* treated with ι - or κ -carrageenans reduces leaf damage caused by *Trichoplusia ni*, in addition, ι -carrageenan induces the expression of defense genes, including *PR-1* and *PDF1.2* (Sangha *et al.*, 2011). *Arabidopsis* pretreated with λ -carrageenan elevates expression of the JA-related genes, *AOS*, *PDF1.2*, and *PR-3* and resists *Sclerotinia sclerotiorum* infection. In contrast, the ι -carrageenan increases susceptibility to this pathogen (Sangha *et al.*, 2010). Carrageenan is not only a beneficial plant inducer that stimulated plant defense responses, but is also a compound that improves the growth of plants (Shukla *et al.*, 2016). Thus, SPS from *A. spicifera* could be an alternative source of a plant defense inducer.

Since SPS from *A. spicifera* has not yet been reported as a plant biostimulant, I investigated the effects of polysaccharide extracted from *A. spicifera* on the rubber tree plant. In this study, I utilized the CPS of this seaweed as a bioelicitor to enhance the disease resistance of *H. brasiliensis* against *P. palmivora* infection and measured inductions of SA and Scp, including expressions of *HbPR-1*, *HbGLU*, and *HbASI*.

Furthermore, I purified λ -carrageenan from the CPS. The purified λ -carrageenan was also used to test for cell death and responsive enzyme (catalase and peroxidase) induction.

4.2 Objectives

4.2.1 To isolate the sulphated polysaccharide elicitor from *A. spicifera*

4.2.2 To apply the sulphated polysaccharide extracted from *A. spicifera* as an elicitor to induce *H. brasiliensis* defense responses against *P. palmivora* infection

4.3 Materials and Methods

4.3.1 Pathogen and plants

P. palmivora isolated from *Hevea brasiliensis* was cultured on potato dextrose agar (PDA) at 25°C for 1 week. A 5-mm diameter cork-borer was used to cut agar containing *P. palmivora*. The agar plugs were maintained on a V8 agar for 1 week. For zoospore preparation, sterile distilled water was added to a V8 agar plate and further incubated at 4°C for 15 min. Zoospores of *P. palmivora* were counted with Petroff Hauser under a light microscope. The zoospore concentration at 1×10^5 zoospores/ml was used in this study.

Rubber tree seedlings (RRIM600 cultivar) at the B2C developmental stage and 8-week tobacco (*Nicotiana tabacum*) plants were maintained in a growth room with photoperiod control (12 h of light and 12 h of dark at 25°C). *A. spicifera* was kindly provided by the Phetchaburi Coastal Fisheries Research and Development Center, Phetchaburi, Thailand. Salt and sand were removed by washing with tap water. The biomass was air dried at 60°C to a constant weight then milled into fine powder.

4.3.2 Crude polysaccharide (CPS) extraction

The fine alga powder (5 g) was treated with methanol (85%, 100 ml) and stirred with a mechanical stirrer overnight to remove pigments, lipids, and low molecular-weight carbohydrates. The material was then boiled at 70°C in 500 ml of distilled water for 4 h with mechanical stirring. The CPS in the mixture was separated from the residue by centrifugation (6500xg) for 10 min. The supernatant was poured into three volumes of ethanol (95%) allowing precipitation. The CPS pellet was collected using centrifugation (6500xg) for 10 min, dissolved in distilled water,

dialyzed and lyophilized to a constant weight. Before treatment, the CPS was dissolved in sterile distilled water to a concentration of 0.5 mg/ml.

4.3.3 Induction of local resistance in rubber tree leaves

The rubber tree leaves were treated with CPS solution at 0.5 mg/ml and sterile distilled water (DW) for 24 hours using spraying. After that, the CPS- and DW-treated rubber tree leaves were infected with 1×10^5 zoospores/ml of *P. palmivora* using the same method. At five days after treatment, *P. palmivora* infection was measured by counting the disease severity on infected leaves. The disease severity index (DSI) was determined according to the modified method described by Yang *et al.* (1996). Five grades of infection symptom were used (grade 0: no symptom; grade 1: slight symptoms; grade 2: medium distortion; grade 3: rather serious distortion; grade 4: extremely serious symptoms) (Fig. 4.1A) and the DSI was calculated using the following formula.

Disease severity index (DSI)

$$= \frac{\sum(\text{disease grade} \times \text{no. of plants in each grade} \times 100)}{(\text{total no. of plants} \times \text{highest disease grade})}$$

Three replicates were performed. Each replicate consisted of 42 independent leaves from 7 independent rubber trees.

4.3.4 Salicylic acid (SA) and Scopoletin (Scp) measurements

The DW- and CPS-treated leaves were collected and extracted by the modified method according to Ederli *et al.* (2011) at designated time points. The treated leaves (0.25 g) were crushed into fine powder in liquid nitrogen in a mortar and then 750 μ l of 90% MeOH was added and mixed. The fine mashed solutions were transferred into 1.5 ml Eppendorf tubes and centrifuged at 12,000 rpm for 5 min. The supernatants were collected. Pellets were re-extracted with 500 μ l of 90% MeOH and mixed with the collected supernatants. Total supernatants were adjusted with 50% w/v trichloroacetic acid to reach the final concentration of 5% w/v of trichloroacetic acid, passed through a 0.2 μ m filter and stored in a 2 ml HPLC vial at -20°C. The samples were analyzed using an HPLC apparatus of the Agilent 1100 series equipped with a ZORBAX Eclipse XDB-C18, 4.6 x 150 mm, 5 micron column. The mobile phase

consisted of 2 solutions, 0.1% formic acid and acetonitrile. A gradient elution method was used as follows (time in min/percentage acetonitrile): 0-2/20, 2-8.50/20-40, 8.51-10/40 and 10.01-13/40-60. Fluorescence detectors, Ex 294 nm, Em 426 nm and Ex 337 nm and Em 425 nm were used to analyze the levels of SA and Scp, respectively.

4.3.5 Expression of defense-related genes

4.3.5.1 RNA extraction and cDNA synthesis

The DW- and CPS-treated rubber tree leaves were collected at designated time points and stored in liquid nitrogen. The frozen leaves were ground into fine powder with a mortar and pestle. The RNeasy Plant Mini Kit (Qiagen, Valencia, CA, USA) was used to extract RNA from samples of the ground leaves using the manufacturer's protocol. The quality and concentration of extracted RNA were determined by agarose gel electrophoresis and spectrophotometry (MaestroGen, Hsinchu, Taiwan), respectively. First-strand cDNA synthesis was performed using SuperScript III Reverse Transcriptase (Invitrogen, Carlsbad, CA, USA) and the remaining RNA was eliminated from the cDNA products with RNaseH (Invitrogen, Carlsbad, CA, USA).

4.3.5.2 Semi-quantitative polymerase chain reaction (semi-qPCR)

The expression of defense-related genes, *HbPR-1*, *HbGLU* and *HbASI*, was analyzed by semi-qPCR. The GenBank accession no. KM514666 (Khunjan *et al.*, 2016), AY325498 (Thanseem and Thulaseedharan, 2006) and KM979450 (Bunyatang *et al.*, 2016) were used in the design of the specific primers of *HbPR-1*, *HbGLU* and *HbASI* genes, respectively. A housekeeping gene, the mitosis protein YLS8 gene (*HbMito*) of *H. brasiliensis* (GenBank accession no. HQ323250) (Li *et al.*, 2011), was selected as a reference gene. The PCR reaction mixture consisted of EmeraldAmp® PCR Master Mix (Takara, Otsu, Shiga, Japan), 0.25 µM of each gene-specific primer (Table 4.1) and 4 µL of cDNA template. The reaction was performed with an initial denaturation step at 94°C for 4 min; followed by 35 cycles (for *HbPR-1* and *HbGLU*), and 40 cycles (for *HbASI*) of denaturing at 94°C for 1 min; annealing at 60°C for 30 s; extension at 72°C for 1 min, and a final elongation step at 72°C for 10 min. The PCR products were separated by electrophoresis in 2.0% agarose gel, and visualized under a UV transilluminator and photographed by a gel imager using VisionWorks LS

software (UVP BioSpectrum® MultiSpectral Imaging System™, Cambridge, UK) to measure densitometry values of the DNA bands.

Table 4.1 Specific primers used for semi-qRT-PCR.

Gene	Primer name	Sequence (5'→3')	Size (bp)
<i>HbPRI</i>	<i>HbPRI</i> -F	ATGCCCATACCAAGCACGAGCAG	364
	<i>HbPRI</i> -R	CCAGGAGGGTCGTAGTTGCATCCA	
<i>HbGLU</i>	<i>HbGLU</i> -F	GCCTTACCAATCCTTCCAATGC	449
	<i>HbGLU</i> -R	ATAACCTCGCTGACCATCCCAC	
<i>HbASI</i>	<i>HbASI</i> -F	GGGCGAAGCCCATATTCACCC	591
	<i>HbASI</i> -R	CAGAAATCAGAAGCAGACTTCTGCG	
<i>Hbmitosis protein</i>	<i>HbMito</i> -F	TGGGCTGTTGATCAGGCAATCTTGGC	577
	<i>HbMito</i> -R	TGTCAGATACATTGCTGCACACAAGG	
<i>YLS8</i>		C	

4.3.6 Carrageenan purification

Strong anion exchange chromatography with a Q sepharose fast flow column (GE Healthcare) was used to purify the SPS (λ -carrageenan) from the CPS. First, the CPS extract (0.25 mg/ml, 25 ml) was loaded into the Q sepharose fast flow column (25 ml volume of gel) at a continuous flow rate of 0.75 ml/min. After that, the column was washed with 25 ml of distilled water. Bound polysaccharides were eluted with 25 ml of 0.4 M NaCl, 30 ml of 0.8 M NaCl and 25 ml of 1.6 M NaCl, respectively. The phenol-sulfuric acid method was used to determine the eluted polysaccharides in each fraction (2.5 ml). Each fraction was pooled and further desalted by a PD-10 column (GE Healthcare). The desalted solutions were lyophilized into powder.

4.3.7 Carrageenan type identification

Each fraction was determined for functional groups using FTIR. Briefly, one gram of each fraction was ground with spectroscopic grade potassium bromide (KBr) powder, and then pressed into 1 mm pellets for FTIR measurement (wave range of 600 to 4000 cm^{-1}) using a Bruker Vertex70 spectrometer.

4.3.8 Gel permeation chromatography

The purified carrageenan was dissolved in deionized water and then separated by GPC equipment (Shimadzu/LC-10ADvp using Shodex SB 804 HQ as a column). Deionized water at 40°C was used as the mobile phase to separate carrageenan at a flow rate of 1.0 ml/min.

4.3.9 Total protein extraction

The treated and control leaves (0.5 g fresh weight) at designated time points were ground into fine powders after freezing with liquid nitrogen and homogenized using a chilled mortar and pestle with 1 mL of cold 100 mM Tris-HCl buffer at pH 7.0 containing 0.25% (v/v) Triton-X and 3% (w/v) polyvinylpyrrolidone (PVPP). The homogenates were centrifuged at 12,000 rpm for 20 min at 4°C. The supernatants were collected and stored at -20°C for further analysis of enzyme activity.

4.3.10 Antioxidant enzyme gel staining

For native polyacrylamide gel electrophoresis (PAGE), the total proteins extracted from treated leaves were separated by a 4% stacking gel and a 10% separating gel. After 3 hours of running at 100 mA, gels were stained with different solutions according to protocols for the detection of catalase and peroxidase activity.

Catalase activity staining was performed according to the method of Woodbury *et al.* (1971). Briefly, after native PAGE, the gel was immersed in 3 mM H₂O₂ for 25 min at room temperature and transferred into the staining solution containing 1% K₃Fe(CN)₆ and 1% FeCl₃ for 4 min. To stain peroxidase activity, I followed the method of Stafford and Bravinder-Bree (1972). The gel was immersed in a staining solution consisting of 50 mM sodium acetate buffer at pH 5.4, 0.05% o-dianisidine and 0.1 M H₂O₂ at room temperature for 30 min and fixed with 50% ethanol.

4.3.11 Toxicity test

λ -carrageenan at 0.5, 1 and 2 mg/ml and DW were infiltrated into tobacco leaves for cell death induction. At 5 days post infiltration, treated tobacco leaves were photographed with a digital camera.

4.3.12 Statistical analysis

The presented values are mean values \pm standard error (SE) from the results of at least three independent biological replicates. One-way analysis of variance (ANOVA) according to Duncan's multiple range tests was used to determine significance with $P \leq 0.05$ using SPSS Statistics 17.0 software. Pairwise comparisons were conducted according to Student's t test at $P \leq 0.05$.

4.4 Results

4.4.1 CPS induced resistance in rubber tree leaves.

CPS from *A. spicifera* was precipitated by ethanol for use as a plant elicitor. Leaves were treated with the CPS for 24 hours and then infected with zoospores of *P. palmivora*. The infected leaves were classified in 5 levels of infection (Fig. 4.1A). I found that the CPS reduced the numbers of *P. palmivora*-infected leaves (P -value < 0.001) (Fig. 4.1B) and infected leaves showed less severe signs of the disease (Figure 1C) (P -value = 0.003). The disease severity of the CPS-treated leaves was lower by about 2 fold than controls which were treated with sterile distilled water. The result revealed that the CPS extracted from *A. spicifera* could act as a plant defense inducer against *P. palmivora* infection on rubber tree leaves.

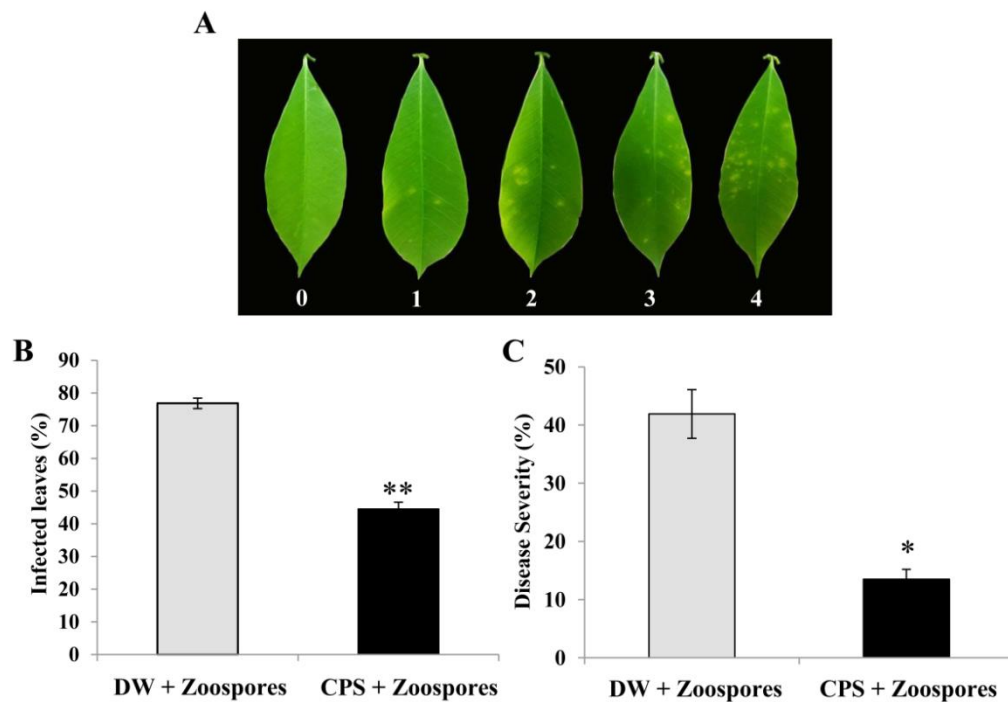


Fig. 4.1 CPS reduced infected leaves (%) and disease severity (%) in rubber tree leaves after infection by *P. palmivora*. Five grades of symptom (Grade 0: no symptom; Grade 1: slight symptoms Grade 2: medium distortion; Grade 3: rather serious distortion; Grade 4: extremely serious symptoms) were used to calculate the severity of infection (A). The percentage of infected leaves (B) and disease severity (%) (C) of rubber tree leaves after treatment with 0.5 mg/ml CPS and sterile distilled water (DW) for 24 hours and subsequent inoculation with 1×10^5 zoospores/ml of *P. palmivora*. The infected leaves and disease severity were monitored at 5 days post inoculation. Data bars were the means (\pm SE) of three replicates. Each replicate consisted of 42 independent leaves from 7 independent rubber trees. One and two asterisks (* and **) indicate statistically significant differences of CPS-treated leaves compared with DW-treated leaves (P-value < 0.01 and P-value < 0.001, respectively) using Student's t-test.

4.4.2 SA and Scp in rubber tree leaves were induced by the CPS.

Rubber tree leaves after spraying with the CPS were analyzed for levels of SA and Scp by HPLC. I found that SA was significantly induced at 48 hours post treatment (P-value = 0.037) and was slightly elevated again at 96 hours post treatment (Fig. 4.2A). Scp was highly increased at 48 hours (P-value = 0.003) and reached the

highest level at 96 hours post treatment (P-value = 0.005) (Fig. 4.2B). The results show that CPS caused accumulations of SA and Scp in rubber tree leaves.

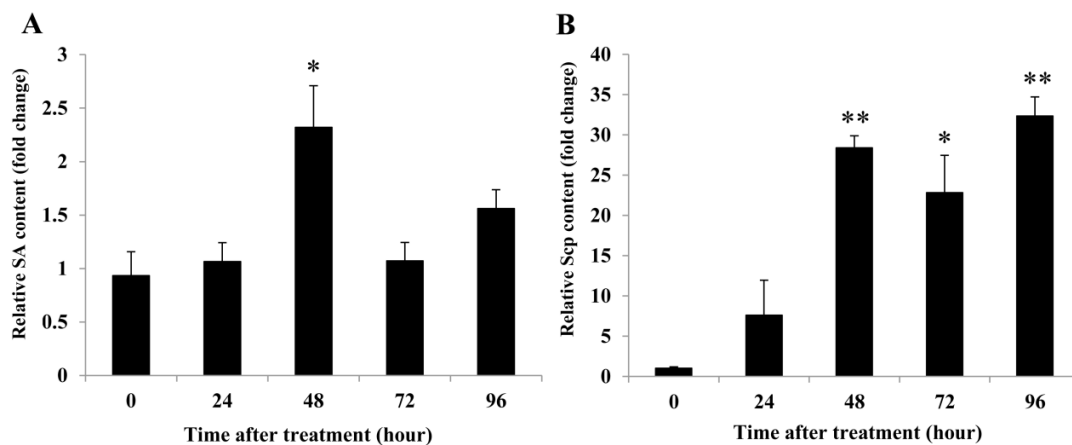


Fig. 4.2 CPS enhanced SA and Scp accumulations in rubber tree leaves. The relative SA (A) and Scp (B) contents in rubber tree leaves treated with 0.5 mg/ml CPS and sterile distilled water (DW). Data bars were the SA or Scp content (\pm SE) in CPS-treated leaves relative to DW-treated leaves at each time point. The results derived from three replicates, each replicate consisted of 4 plants. One and two asterisks (* and **) indicate statistically significant differences of relative SA or Scp content at each time point compared with relative SA or Scp content at time 0 hour (P-value < 0.05 and P-value < 0.01, respectively) using Student's t-test.

4.4.3 CPS induced expression of *HbPR-1* and *HbGLU* in rubber tree leaves but reduced the expression of *HbASI*.

As the CPS induced rubber tree defenses via inductions of SA and Scp, I further studied the expression of the pathogenesis-related protein genes, *HbPR-1*, *HbPR-2* or *HbGLU* and *HbPR-6* or *HbASI*, of this plant. To investigate whether CPS induced defenses through the SA or JA signaling pathway, half of the rubber tree leaf was used for SA and Scp analyses and the other half was used for studying expression of these genes. Compared with gene expression in control leaves, the expression of *HbPR-1* was induced about 3 fold at 24 hours post-treatment (P-value = 0.03) (Fig. 4.3A).

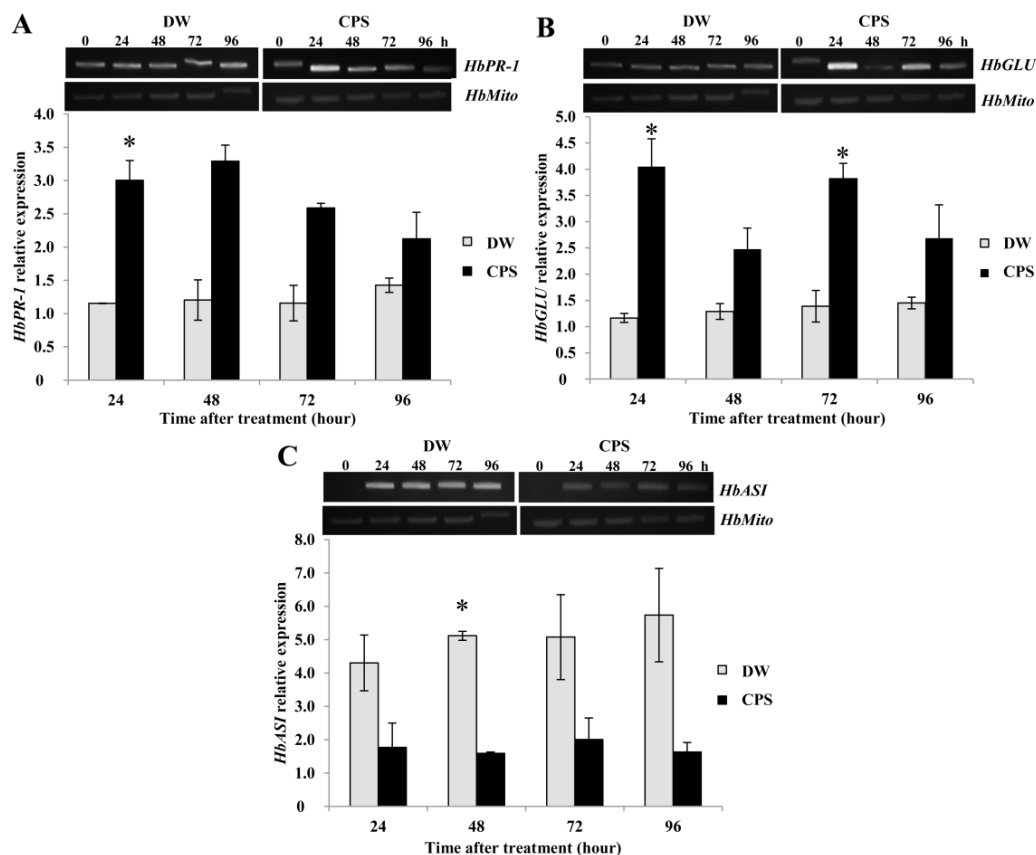


Fig. 4.3 Time course inductions of *HbPR-1* (A), *HbGLU* (B) and *HbASI* (C) expressions by semi-qRT-PCR. The expressions were analyzed on rubber tree leaves treated with 0.5 mg/ml CPS and sterile distilled water (DW). The relative gene expression was calculated in comparison with *HbMito*, a housekeeping gene, the mitosis protein YLS8 gene expression. Data bars were the means (\pm SE) of three replicates, each replicate consisted of 4 plants. One asterisk (*) indicated statistically significant differences of CPS-treated leaves compared with DW-treated leaves (P-value < 0.05) using Student's t-test.

4.4.4 The CPS consisted of three fractions and the major fraction was SPS, λ -carrageenans.

The *HbGLU* expression was significantly more induced at 24 (P-value = 0.03) and 72 (P-value = 0.02) hours post treatment by about 3 fold and 2.5 fold, respectively (Fig. 4.3B). On the other hand, rubber tree leaves treated with the CPS showed reduced expression of *HbASI*. The *HbASI* expression was down-regulated at

24 hours and significantly decreased at 48 hours post-treatment (P-value = 0.04) (Fig. 4.3C). These results revealed that the CPS induced *HbPR-1* and *HbGLU* expressions but suppressed *HbASI* expression and also suggested that CPS induced rubber tree defenses through the SA signaling pathway.

A strong anion exchanger, Q sepharose (GE Healthcare), was used to purify the CPS isolated from *A. spicifera*. I could separate the CPS into three fractions, F1, F2 and F3 which were eluted with 0.4 M, 0.8 M and 1.6 M NaCl, respectively (Fig. 4.4).

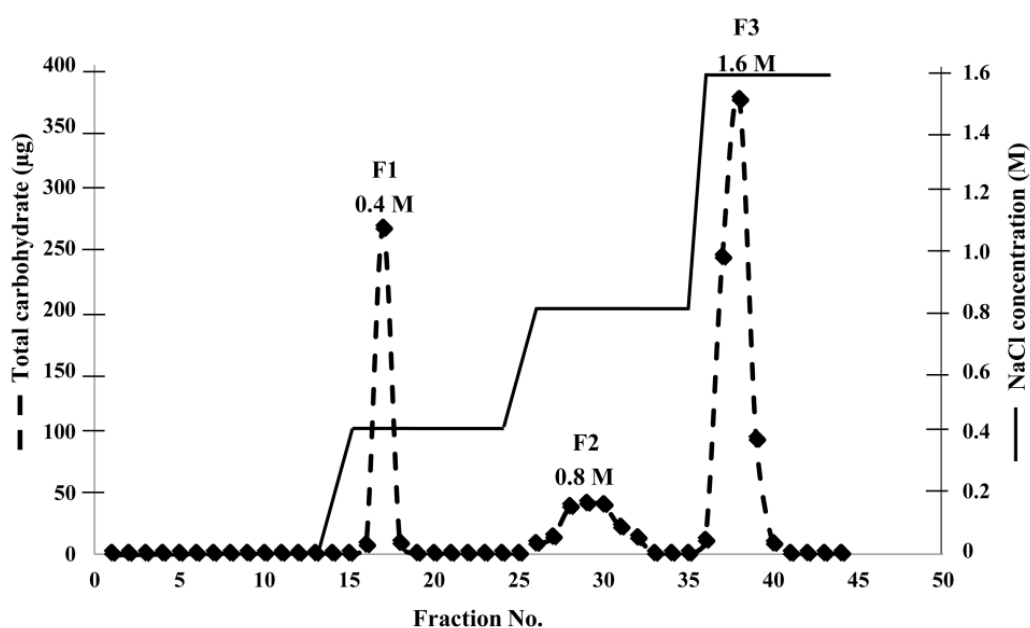


Fig. 4.4 Chromatographic elution profile of F1, F2 and F3 eluted with 0.4, 0.8 and 1.6 M NaCl, respectively, using a strong anion column, Q sepharose. 2.5 ml of the eluted solution of each fraction were collected and subsequently determined for polysaccharide content.

The chromatographic elution profiles of the three fractions demonstrated a complete separation of the fractions (Fig. 4.4). The percentages of F1, F2 and F3 were 24, 15 and 61%, respectively. The main fraction, F3, was eluted with 1.6 M NaCl (Fig. 4.4).

FTIR analysis was carried out to classify each fraction as a non-sulphated or sulphated polysaccharide and to identify the types of carrageenan present. The spectra presented a band at 2927 cm^{-1} and a broad and strong absorption band at 3387 cm^{-1} (Fig. 4.5). Šandula *et al.* (1999) suggested that the bands near 2930 and $3,405\text{ cm}^{-1}$ represented the stretching of the CH bond and OH group, respectively. The spectra also showed a broad and strong absorption band at 950 to 1200 cm^{-1} (Fig. 4.5), which is assigned to CO vibration (Šandula *et al.*, 1999). There was no absorption band of amide I (C=O) at 1546 cm^{-1} nor of amide II (NH) at 1649 cm^{-1} (Belton *et al.*, 1995; Barth, 2007). Since these bands are characteristic of proteins, the results indicated that all fractions were polysaccharides and did not contain any protein.

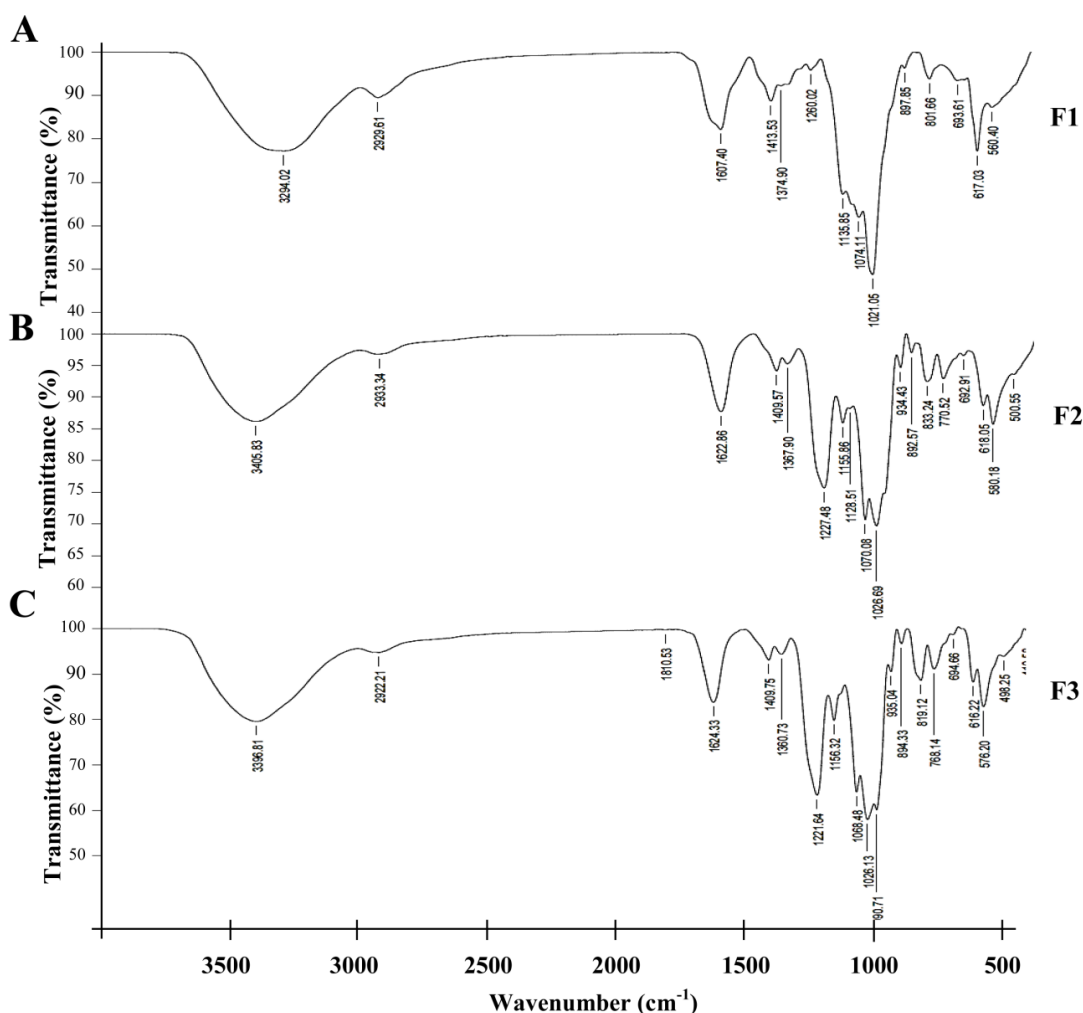


Fig. 4.5 The FTIR spectra of F1 (A), F2 (B) and F3 (C) fractions eluted with 0.4, 0.8 and 1.6 M NaCl, respectively, through a Q sepharose column.

Surprisingly, I found an absorption band near 1221 cm^{-1} in fractions F2 and F3 (Fig. 4.5B and C), but not in fraction F1 (Fig. 4.5A). The absorption band between 1210 and 1270 cm^{-1} represents the stretching vibration of the S=O bond in the sulphate group (Roberts and Quemener, 1999). This result indicated that F1 was non-sulphated while F2 and F3 were sulphated polysaccharide (SPS). Carrageenan types were identified from the characteristic peaks of κ -, ι - and λ -carrageenan. The spectra of κ - and ι - carrageenan present one important band at 845 cm^{-1} from galactose-4-sulphate (Sekkal and Legrand, 1993). Galactose-2-sulphate and galactose-6-sulphate in λ -carrageenan produced absorption bands near 830 and 820 cm^{-1} , respectively (Chopin and Whalen, 1993). I did not detect the absorption band at 845 cm^{-1} but I found absorption bands near 830 and 820 cm^{-1} in the spectra of F2 and F3 fractions (Fig. 4.5B and C).

Even though the FTIR equipment automatically labeled the absorption bands at 833.24 cm^{-1} , an absorption band near 820 cm^{-1} was also present in F2 (Fig. 4.5B). For F3, the absorption band at 819.12 cm^{-1} was automatically labeled while an absorption band near 830 cm^{-1} was also observed (Fig. 4.5C). These results suggested that F2 and F3 fractions were λ -carrageenan showing vice versa signals at 830 and 820 cm^{-1} . Thus, the CPS extracted from *A. spicifera* consisted of both non-sulphated and sulphated polysaccharide (SPS) and the SPS was λ -carrageenan.

4.4.5 The F3 fraction exhibited the highest elicitor activity in tobacco leaves and was a broad molecular weight λ -carrageenan.

The elicitor activity of each fraction was tested by infiltration into tobacco leaves which was more practical than spraying onto rubber tree leaves. I found that the F1 fraction did not induce Scp accumulation. However, in tobacco leaves infiltrated with F2 or F3 fractions, the level of Scp was higher at 48 hours post infiltration (Fig. 4.6A). In addition, only the F3 fraction was still inducing Scp at 96 hours (Fig. 4.6A). The results suggest that the SPS, λ -carrageenan in this study, possessed elicitor activity but the non-sulphated form did not and the F3 fraction exhibited the highest elicitor activity.

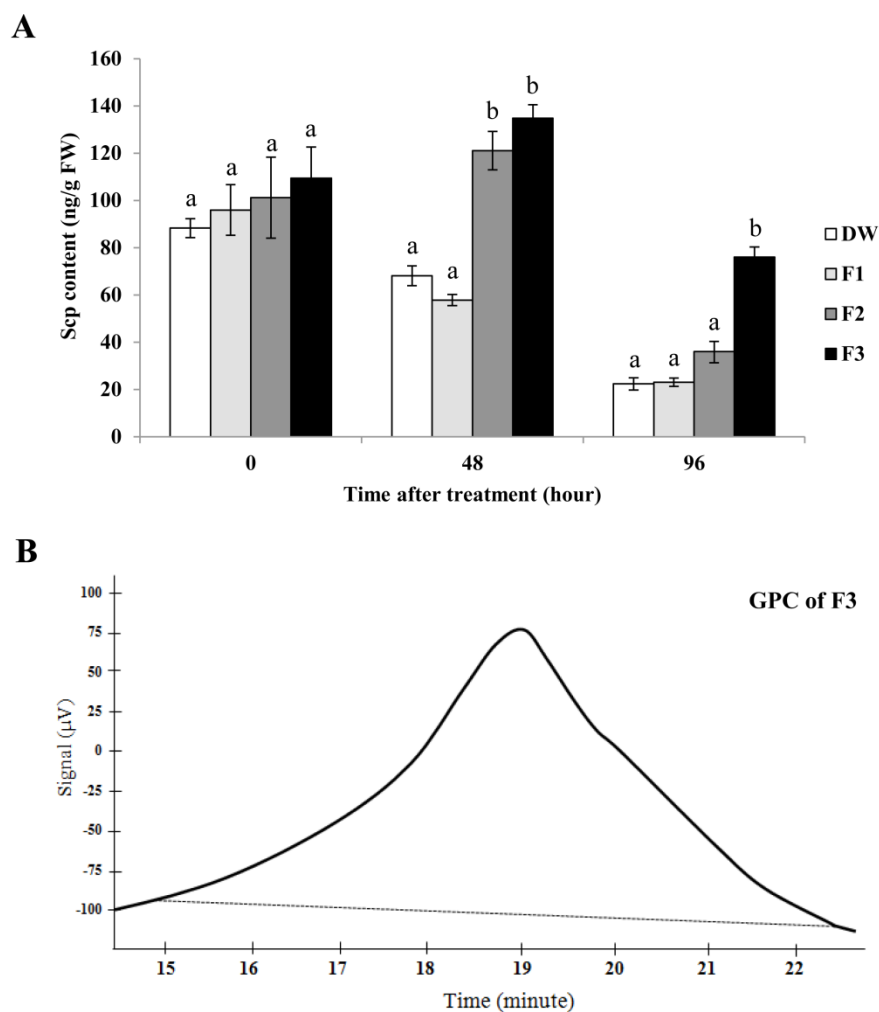


Fig. 4.6 Scp contents in tobacco leaves treated with purified F1, F2 and F3 from CPS of *A. spicifera* and sterile distilled water (DW) (A). Data bars indicate the means (\pm SE) of three replicates. Each replicate consisted of 4 independent tobacco leaves. The GPC elution curve of fraction F3 (B). Significant differences utilizing one-way analysis of variance (ANOVA), Duncan's multiple range test ($p = 0.05$) were presented by differences among treatments.

I also performed a GPC experiment to study the molecular weight distribution of F3, which exhibited the highest elicitor activity. The chromatogram revealed that this λ -carrageenan was a broad molecular weight polysaccharide (Fig. 4.6B).

4.4.6 λ -carrageenan strongly induced SA and Scp accumulations in rubber tree leaves.

Fraction F3 (λ -carrageenan) was further evaluated for SA and Scp accumulations in rubber tree leaves as earlier investigated with CPS in Figure 2. I found that the SA level started to increase at 48 hours (P-value = 0.039) and significant accumulation was present at 72 (P-value = 0.001) and 96 (P-value = 0.001) hours post treatment (Fig. 4.7A). Scp accumulation also started to increase at 48 (P-value < 0.001) and 72 (P-value < 0.001) hours and was well sustained at 96 hours (P-value < 0.001) post treatment (Fig. 4.7B). These results suggest that λ -carrageenan not only triggered Scp synthesis in the tobacco plant but also induced SA and Scp accumulation in rubber tree leaves, and that λ -carrageenan was the bioactive compound responsible for elicitor activity in the CPS.

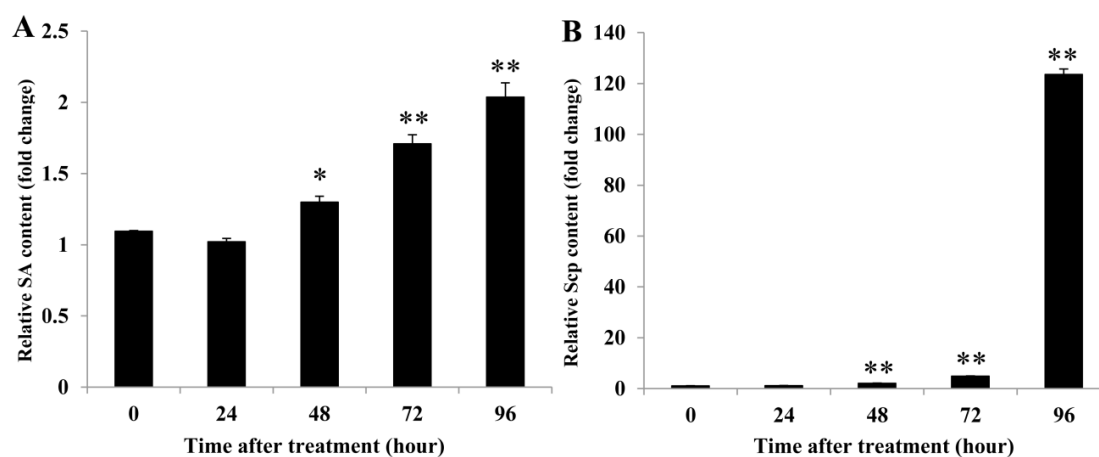


Fig. 4.7 The λ -carrageenan enhanced SA and Scp accumulations in rubber tree leaves. The relative SA (A) and Scp (B) contents in rubber tree leaves treated with 0.5 mg/ml λ -carrageenan and sterile distilled water (DW). Data bars were the SA or Scp content (\pm SE) in CPS-treated leaves relative to DW-treated leaves at each time point. The results derived from three replicates, each replicate consisted of 4 plants. One and two asterisks (* and **) indicate statistically significant differences of relative SA or Scp content at each time point compared with relative SA or Scp content at time 0 hour (P-value < 0.05 and P-value < 0.01, respectively) using Student's t-test.

4.4.7 λ -carrageenan suppressed catalase activity, but highly activated peroxidase activity.

Rubber tree leaves treated with F3, λ -carrageenan were cut in and half of each leaf was used for SA and Scp analyses while the other half was used for studying the activities of the defense-related enzymes, catalase and peroxidase. After native PAGE and staining, the results revealed that catalase activity in the λ -carrageenan-treated leaves was suppressed during 96 hours post treatment whereas catalase activity in control leaves was increased. The suppression of catalase activity was observed at 48, 72 and 96 hours post treatment (Fig. 4.8A). In contrast, peroxidase activity was strongly induced at 24 hours and was still increasing at 48 and 72 hours post treatment (Fig. 4.8B). These results suggested that catalase activity was suppressed by λ -carrageenan while peroxidase activity was increased.

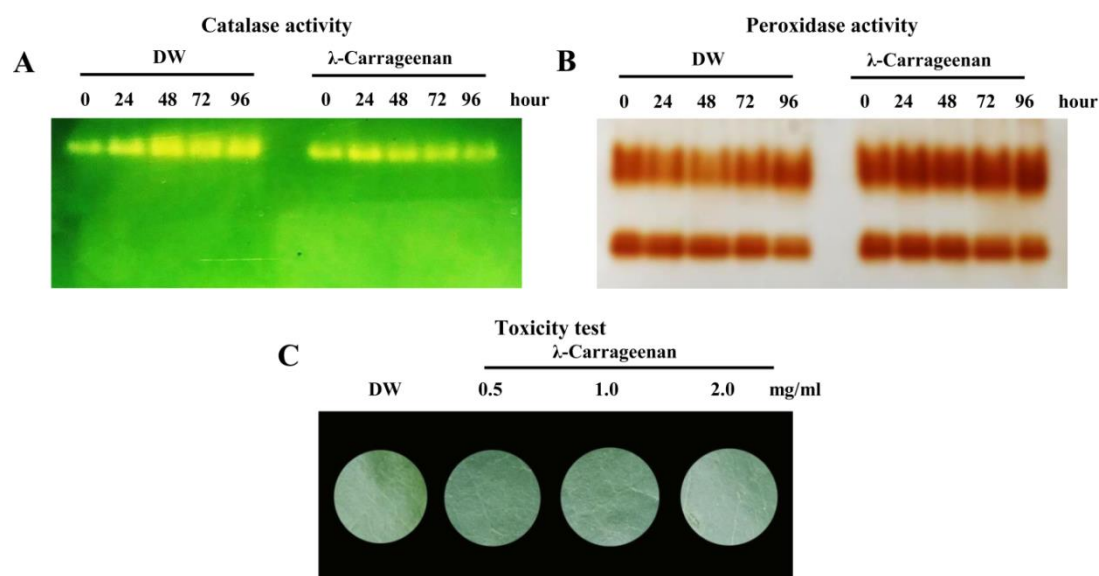


Fig. 4.8 Activity staining of catalase (A) and peroxidase (B) activity. The rubber tree leaves were treated with 0.5 mg/ml λ -carrageenan and sterile distilled water (DW). Each treatment comprised 12 leaves from different rubber trees. In the toxicity test (C), 10 tobacco leaves were infiltrated with 0.5, 1.0 and 2.0 mg/ml λ -carrageenan and sterile distilled water (DW). The symptom induction on tobacco leaves was monitored on day 5 post infiltration.

4.4.8 λ -carrageenan did not cause cell death either in tobacco or rubber tree leaves.

λ -carrageenan was sprayed on rubber tree leaves to determine its toxicity. It did not induce cell death in rubber tree leaves (data not shown). I also tested the toxicity of λ -carrageenan on tobacco leaves. λ -carrageenan was infiltrated into tobacco leaves at concentrations of 0.5, 1 and 2 mg/ml. Cell death did not occur at any of the λ -carrageenan concentrations tested (Fig. 4.8C). The result indicated that λ -carrageenan was safe to use as a plant bio-stimulant.

4.5 Discussion

Many marine-derived polysaccharides, such as alginates, carrageenans, fucans, laminarin and ulvans, trigger plant defense responses which enhance protection against viral, fungal and bacterial infections (Vera *et al.*, 2011). The results of this study revealed that CPS extracted from *A. spicifera* induced rubber tree resistance to *P. palmivora* by reducing the number of infected leaves and severity of the disease (Fig. 4.1B and 1C). Sulphated fucan oligosaccharides extracted from the marine brown alga, *Pelvetia canaliculata*, and subsequently degraded with a fucan-degrading hydrolase are able to stimulate both local and systemic resistance in tobacco leaves against the tobacco mosaic virus (Klarzynski *et al.*, 2003). The polysaccharide extracted from a red alga, *H. musciformis*, induces biological activity in tobacco leaves against the tobacco mosaic virus (Ghannam *et al.*, 2013). Ulvans extracted from a mixture of several *Ulva* species (mostly *U. armoricana*) induce protection against the fungi *Colletotrichum trifolii* in *Medicago truncatula* (Cluzet *et al.*, 2004). The diameter of the necrotic lesion caused by *Erwinia carotovora* on a tobacco plant previously injected with laminarin from the brown seaweed, *Laminaria digitata*, is reduced (Klarzynski *et al.*, 2000). Our results demonstrated that CPS from *A. spicifera* potentially contained an elicitor that induced rubber tree resistance against *P. palmivora* infection.

Interestingly, our results showed that the CPS extracted from *A. spicifera* induced SA accumulation in rubber tree leaves (Fig. 4.2A). Many seaweed extracts induce SA. The sulphated fucan oligosaccharides extracted from *P. canaliculata*

induce accumulation of SA that make tobacco plants more resistant to the tobacco mosaic virus (Klarzynski *et al.*, 2003). Sulphated laminarin (PS3) induces SA accumulation in tobacco leaves (Ménard *et al.*, 2004). CPS in the present study also increased Scp in rubber tree leaves (Fig. 4.2B). Several plants produce Scp, a coumarin phytoalexin, which is an antimicrobial substance induced by pathogen infection or elicited by abiotic agents. Klarzynski *et al.* (2003) demonstrated that Scp triggered by sulphated fucan oligosaccharides supported resistance in tobacco plants. Tobacco leaves infiltrated with sulphated polysaccharide from *H. musciformis* induce blue fluorescence metabolites which are phytoalexins (Scp and sesquiterpenoid) and derivatives from the phenylpropanoid pathways (Ghannam *et al.*, 2013). In addition, the PS3 induces Scp accumulation in tobacco leaves against the tobacco mosaic virus infection (Ménard *et al.*, 2004).

Expression of the SA-responsive genes, *HbPR-1* and *HbGLU* was induced in the CPS-treated rubber tree leaves; on the other hand, a JA-responsive gene, *HbASI* was significantly suppressed (Fig. 4.3). It has been reported that activation of the SA signaling pathway suppresses the JA signaling pathway (Pieterse *et al.*, 2012). The correlation between gene expression and accumulation of SA suggested that the CPS in this study induced rubber defense responses through the SA signaling pathway. In contrast, the sulphated polysaccharide (SPS) from *H. musciformis* enhances expression of genes involving SA and subsequently activated the JA/ET signaling pathway (Ghannam *et al.*, 2013). *P. palmivora* infection is inhibited in *N. benthamina* that expresses the PR-1 protein; furthermore, the PR-1 protein acts as an antifungal protein by inhibiting zoospore germination (Khunjan *et al.*, 2016). The cell wall of the oomycete mainly consists of β -1,3-glucan (Latijnhouwers *et al.*, 2003) which is a substrate of β -1,3-glucanase. Consequently, induction of *HbPR-1* and *HbGLU* by our elicitor could enhance rubber leaf resistance against *P. palmivora* infection.

The CPS from *A. spicifera* was purified using a Q sepharose, it was separated into three fractions (F1, F2 and F3) (Fig. 4.4). I were able to remove a non-sulphated polysaccharide fraction (F1) from sulphated polysaccharide. Both fractions (F2 and F3) displayed absorption bands near 830 and 820 cm^{-1} , but the F2 fraction displayed a strong absorption band of galactose-2-sulphate at 833.24 cm^{-1} (Fig. 4.5B), whereas

the F3 fraction showed an absorption band of galactose-6-sulphate at 819.12 cm^{-1} (Fig. 4.5C). Duarte *et al.* (2004) reported that the sulphated polysaccharide from *A. spicifera* consisted of A and B units of galactose molecules; in addition, some of the B unit was 3,6-anhydro- α -L-galactose. Consequently, the galactose-6-sulphate would not be present, resulting in a lower anion charge. Basically, the weakest ionic interaction molecule is eluted from the column first; molecules with stronger ionic interactions are eluted with a higher salt concentration. The fraction (F3) which displayed the absorption band at 819.12 cm^{-1} possibly had more galactose-6-sulphate than the F2 fraction. Therefore, F3 had a stronger negative charge than the F2 fraction.

After infiltration into tobacco leaves, the non-sulphated polysaccharide, F1 did not trigger Scp synthesis whereas the sulphated polysaccharide (F2 and F3) or λ -carrageenan did (Fig. 4.6A). The better inducer was the fraction eluted with 1.6 M NaCl (F3) because it possessed more negative charge. Similarly, the highly sulphated λ -carrageenan enhances resistance to *S. sclerotiorum*, resulting in smaller leaf lesions on *Arabidopsis*. In contrast, the ι -carrageenan which is a lower sulphated carrageenan induces susceptibility to this pathogen (Sangha *et al.*, 2010). It has been shown that after chemical sulphation, laminarin became a stronger inducer. Clearly, sulphated laminarin, but not laminarin, causes electrolyte leakage and Scp and SA accumulations. In addition, laminarin triggers expressions of ET-dependent PR proteins whereas sulphated laminarin induces expressions of ET- and SA-dependent PR proteins (Ménard *et al.*, 2004). Of two algal polysaccharides, laminarin and carrageenan, only carrageenan efficiently triggers the defense gene expression in tobacco leaves (Mercier *et al.*, 2001). Mercier *et al.* (2001) suggested that λ -carrageenan containing the highest sulphate content was the most active inducer. Furthermore, when the molecular weight distribution of the F3 fraction was analyzed, I found that it was a broad molecular weight carrageenan (Fig. 4.6B). This finding supported the report of Necas and Bartosikova (2013).

Since the F3 fraction showed the greatest effect and was the major component in the CPS, I further used the F3 fraction in purified form, which was a λ -carrageenan, to confirm the effects on rubber tree defense responses. Our results revealed that λ -

carrageenan in the F3 fraction induced SA and Scp accumulations (Fig. 4.7). Both the CPS and the purified F3 induced SA and Scp, so the active compound in the CPS that triggered rubber tree defense responses against *P. palmivora* infection was λ -carrageenan. λ -carrageenan has been reported to have different effects on plants. *Arabidopsis* leaves treated with λ -carrageenan show resistance to *S. sclerotiorum* that is correlated with increasing expression of the JA-responsive genes, *PDF1.2* and *PR-3* (Sangha *et al.*, 2010). Sangha *et al.* (2011) treated *A. thaliana* leaves with ι - or κ -carrageenan and obtained reductions of leaf damage caused by *Trichoplusia ni*. In contrast, λ -carrageenan-treated leaves show the same leaf damage as the controls. Our result was similar to the result of Mercier *et al.* (2001) who reported that λ -carrageenan (1000 $\mu\text{g/ml}$) induced the accumulation of SA in tobacco leaves.

The perception of elicitors induces phenomena such as ion flux, medium alkalization and cytoplasmic acidification, oxidative burst and reactive oxygen species production (Zhao *et al.*, 2005). In our study, I focused on the plant defensive enzymes, catalase and peroxidase. These enzymes are major H_2O_2 scavengers in plants (Willekens *et al.*, 1995). Surprisingly, our results revealed that catalase activity was highly suppressed at 48, 72 and 96 hours after treatment with λ -carrageenan (Fig. 4.8A). At these time points, the levels of SA were elevated (Fig. 4.7A). SA is able to bind SA-binding protein (SABP) (Chen *et al.*, 1993a). SABP shows catalase activity which is specifically inhibited by SA (Chen *et al.*, 1993b), therefore, at these time points, increasing SA could bind and inhibit catalase activity (Fig. 4.8A). In contrast, the activity of the other H_2O_2 scavenger, peroxidase, was increased (Fig. 4.8B). Hiraga *et al.* (2001) showed that peroxidase played important roles in various physiological processes such as lignification and defense response against pathogen infection. So, induction of peroxidase could promote rubber tree defense responses against *P. palmivora* infection.

The toxicity of λ -carrageenan was tested by infiltrating this elicitor into tobacco leaves. No cell death was detected (Fig. 4.8C), therefore, this sulphated polysaccharide from *A. spicifera* was a friendly stimulant. Similarly, another sulphated polysaccharide, extracted from the red alga *H. musciformis*, do not cause cell death in tobacco leaves (Ghannam *et al.*, 2013). Klarzynski *et al.* (2003) also

supported that sulphated oligofucans did not display signs of toxicity on tobacco leaves. Furthermore, carrageenan is not only a beneficial plant inducer to enhance plant defense responses, but has also been shown to promote plant growth (Shukla *et al.*, 2016). Consequently, the λ -carrageenan from *A. spicifera* could be an alternative elicitor used for enhancing plant defense response.

4.6 Conclusion

I successfully used the CPS from *A. spicifera* to induce rubber tree resistance against *P. palmivora* infection via activation of the SA signaling pathway. It has been reported that SA enhances rubber tree defense responses against *P. palmivora* by increasing endogenous SA and Scp contents, lignin formation, peroxidase activity and expression of *PR-1* (Deenamo *et al.*, 2018). In order to avoid the expense of commercial SA, the CPS from *A. spicifera* could be used as an alternative plant defense stimulant.

REFERENCES

- Adie, B.A.T., Perez-Perez, J., Perez-Perez, M.M., Godoy, M., Sanchez-Serrano, J.-J., Schmelz, E.A., Solano, R. 2007. ABA is an essential signal for plant resistance to pathogens affecting JA biosynthesis and the activation of defenses in *Arabidopsis*. *Plant Cell* 19, 1665–1681.
- Ahuja, I., Kissen, R., Bones, A.M., 2012. Phytoalexins in defense against pathogens. *Trends Plant Sci.* 17, 73–90.
- Ali, S.S., Shao, J., Lary, D.J., Kronmiller, B.A., Shen, D., Strem, M.D., Amoako-Attah, I., Akrofi, A.Y., Begoude, B.A.D., ten Hoopen, G.M., Coulibaly, K., Kebe, B.I., Melnick, R.L., Gultinan, M.J., Tyler, B.M., Meinhardt, L.W., Bailey, B.A., 2017. *Phytophthora megakarya* and *Phytophthora palmivora*, closely related causal agents of cacao black pod rot, underwent increases in genome sizes and gene numbers by different mechanisms. *Genome Biol. Evol.* 9, 536–557.
- Allan, A.C., Fluhr, R., 1997. Two distinct sources of elicited reactive oxygen species in tobacco epidermal cells. *Plant Cell* 9, 1559.
- Altschul, S.F., Gish, W., Miller, W., Myers, E.W., Lipman, D.J., 1990. Basic local alignment search tool. *J. Mol. Biol.* 215, 403–410.
- Ambikapathy, J., Marshall, J.S., Hocart, C.H., Hardham, A.R., 2002. The role of proline in osmoregulation in *Phytophthora nicotianae*. *Fungal Genet. Biol.* 35, 287–299.
- Apel, K., Hirt, H., 2004. Reactive oxygen species: metabolism, oxidative stress, and signal transduction. *Annu. Rev. Plant Biol.* 55, 373–99.
- Asselbergh, B., De Vleeschauwer, D., Höfte, M., 2008. Global switches and fine-tuning-ABA modulates plant pathogen defense. *Mol. Plant-Microbe Interact.* 21, 709–719.

- Ausubel, F.M., 2005. Are innate immune signaling pathways in plants and animals conserved? *Nat. Immunol.* 6, 973–979.
- Aziz, A., Poinssot, B., Daire, X., Adrian, M., Bézier, A., Lambert, B., Joubert, J.-M., Pugin, A., 2003. Laminarin elicits defense responses in grapevine and induces protection against *Botrytis cinerea* and *Plasmopara viticola*. *Mol. Plant-Microbe Interact.* 16, 1118–1128.
- Baillieux, F., Genetet, I., Kopp, M., Saindrenan, P., Fritig, B., Kauffmann, S., 1995. A new elicitor of the hypersensitive response in tobacco: a fungal glycoprotein elicits cell death, expression of defence genes, production of salicylic acid, and induction of systemic acquired resistance. *Plant J.* 8, 551–560.
- Baldauf, S.L., 2003. The deep roots of eukaryotes. *Science* 300, 1703–1706.
- Banik, R.M., Kanari, B., Upadhyay, S.N., 2000. Exopolysaccharide of the gellan family: Prospects and potential. *World J. Microbiol. Biotechnol.* 16, 407–414.
- Barth, A., 2007. Infrared spectroscopy of proteins. *Biochim. Biophys. Acta - Bioenerg.* 1767, 1073–1101.
- Beckman, K.B., Ames, B.N., 1997. Oxidative decay of DNA. *J. Biol. Chem.* 272, 19633–19636.
- Belton, P.S., Colquhoun, I.J., Grant, a, Wellner, N., Field, J.M., Shewry, P.R., Tatham, a S., 1995. FTIR and NMR studies on the hydration of a high-M(r) subunit of glutenin. *Int. J. Biol. Macromol.* 17, 74–80.
- Bent, A.F., Mackey, D., 2007. Elicitors, Effectors, and *R* Genes: The new paradigm and a lifetime supply of questions. *Annu. Rev. Phytopathol.* 45, 399–436.
- Berlett, B.S., Stadtman, E.R., 1997. Protein oxidation in aging, disease, and oxidative stress. *J. Biol. Chem.* 272, 20313–20316.

- Bouarab, K., Potin, P., Correa, J., Kloareg, B., 2007. Sulfated oligosaccharides mediate the interaction between a marine red alga and its green algal pathogenic endophyte. *Plant Cell* 11, 1635.
- Brodersen, P., Petersen, M., Nielsen, H.B., Zhu, S., Newman, M.A., Shokat, K.M., Rietz, S., Parker, J., Mundy, J., 2006. *Arabidopsis* MAP kinase 4 regulates salicylic acid- and jasmonic acid/ethylene-dependent responses via *EDS1* and *PAD4*. *Plant J.* 47, 532–546.
- Brooks, D.M., Bender, C.L., Kunkel, B.N., 2005. The *Pseudomonas syringae* phytotoxin coronatine promotes virulence by overcoming salicylic acid-dependent defences in *Arabidopsis thaliana*. *Mol. Plant Pathol.* 6, 629–639.
- Brunner, F., Rosahl, S., Lee, J., Rudd, J.J., Geiler, C., Kauppinen, S., Rasmussen, G., Scheel, D., Nürnberger, T., 2002. Pep-13, a plant defense-inducing pathogen-associated pattern from *Phytophthora* transglutaminases. *EMBO J.* 21, 6681–6688.
- Brunner, F., Wirtz, W., Rose, J.K.C., Darvill, A.G., Govers, F., Scheel, D., Nürnberger, T., 2002. A β -glucosidase/xylosidase from the phytopathogenic oomycete, *Phytophthora infestans*. *Phytochemistry* 59, 689–696.
- Bunyatang, O., Chirapongsatunkul, N., Bangrak, P., Henry, R., Churngchow, N., 2016. Molecular cloning and characterization of a novel bi-functional α -amylase/subtilisin inhibitor from *Hevea brasiliensis*. *Plant Physiol. Biochem.* 101, 76–87.
- Cao, H., Bowling, S.A., Gordon, A.S., Dong, X., 1994. Characterization of an *Arabidopsis* mutant that is nonresponsive to inducers of systemic acquired resistance. *Plant Cell* 6, 1583.
- Cardinale, F., Jonak, C., Ligterink, W., Niehaus, K., Boller, T., Hirt, H., 2000. Differential activation of four specific MAPK pathways by distinct elicitors. *J. Biol. Chem.* 275, 36734–36740.

- Carella, P., Gogleva, A., Tomaselli, M., Alfs, C., Schornack, S., 2018. *Phytophthora palmivora* establishes tissue-specific intracellular infection structures in the earliest divergent land plant lineage. *Proc. Natl. Acad. Sci.* 115, E3846–E3855.
- Chanda, B., Xia, Y., Mandal, M.K., Yu, K., Sekine, K.T., Gao, Q.M., Selote, D., Hu, Y., Stromberg, A., Navarre, D., Kachroo, A., Kachroo, P., 2011. Glycerol-3-phosphate is a critical mobile inducer of systemic immunity in plants. *Nat. Genet.* 43, 421–429.
- Chang, Y.H., Yan, H.Z., Liou, R.F., 2015. A novel elicitor protein from *Phytophthora parasitica* induces plant basal immunity and systemic acquired resistance. *Mol. Plant Pathol.* 16, 123–136.
- Chaturvedi, R., Venables, B., Petros, R.A., Nalam, V., Li, M., Wang, X., Takemoto, L.J., Shah, J., 2012. An abietane diterpenoid is a potent activator of systemic acquired resistance. *Plant J.* 71, 161–172.
- Chen, X.R., Zhang, B.Y., Xing, Y.P., Li, Q.Y., Li, Y.P., Tong, Y.H., Xu, J.Y., 2014. Transcriptomic analysis of the phytopathogenic oomycete *Phytophthora cactorum* provides insights into infection-related effectors. *BMC Genomics* 15, 980.
- Chen, Z., Silva, H., Klessig, D.F., 1993b. Active oxygen species in the induction of plant systemic acquired resistance by salicylic acid. *Science.* 262, 1883–1886.
- Chen, Z., Ricigliano, J.W., Klessig, D.F., 1993a. Purification and characterization of a soluble salicylic acid-binding protein from tobacco. *Proc. Natl. Acad. Sci.* 90, 9533–9537.
- Chisholm, S.T., Coaker, G., Day, B., Staskawicz, B.J., 2006. Host-microbe interactions: Shaping the evolution of the plant immune response. *Cell* 124, 803–814.

- Chopin, T., Whalen, E., 1993. A new and rapid method for carrageenan identification by FTIR diffuse reflectance spectroscopy directly on dried, ground algal material. *Carbohydr. Res.* 246, 51–59.
- Choquer, M., Fournier, E., Kunz, C., Levis, C., Pradier, J.M., Simon, A., Viaud, M., 2007. *Botrytis cinerea* virulence factors: New insights into a necrotrophic and polyphageous pathogen. *FEMS Microbiol. Lett.* 277, 1–10.
- Churugchow, N., Rattarasarn, M., 2000. The elicitor secreted by *Phytophthora palmivora*, a rubber tree pathogen. *Phytochemistry* 54, 33–38.
- Cluzet, S., Torregrosa, C., Jacquet, C., Lafitte, C., Fournier, J., Mercier, L., Salamagne, S., Briand, X., Esquerré-Tugayé, M.T., Dumas, B., 2004. Gene expression profiling and protection of *Medicago truncatula* against a fungal infection in response to an elicitor from green algae *Ulva* spp. *Plant, Cell Environ.* 27, 917–928.
- Cui, F., Brosché, M., Sipari, N., Tang, S., Overmyer, K., 2013. Regulation of ABA dependent wound induced spreading cell death by MYB108. *New Phytol.* 200, 634–640.
- Cui, J., Bahrami, A.K., Pringle, E.G., Hernandez-Guzman, G., Bender, C.L., Pierce, N.E., Ausubel, F.M., 2005. *Pseudomonas syringae* manipulates systemic plant defenses against pathogens and herbivores. *Proc. Natl. Acad. Sci.* 102, 1791–1796.
- Dangl, J.L., Jones, J.D.G., 2001. Plant pathogens and integrated defence responses to infection. *Nature* 411, 826–833.
- Deenamo, N., Kuyyogsuy, A., Khompatara, K., Chanwun, T., Ekchaweng, K., Churugchow, N., 2018. Salicylic acid induces resistance in rubber tree against *Phytophthora palmivora*. *Int. J. Mol. Sci.* 19, 1883.

- Delaney, T.P., Uknes, S., Vernooij, B., Friedrich, L., Weymann, K., Negrotto, D., Gaffney, T., Gut-Rella, M., Kessmann, H., Ward, E., Ryals, J., 1994. A central role of salicylic acid in plant disease resistance. *Science* 266, 1247–1250.
- Derksen, H., Rampitsch, C., Daayf, F., 2013. Signaling cross-talk in plant disease resistance. *Plant Sci.* 207, 79–87.
- Despres, C., DeLong, C., Glaze, S., Liu, E., Fobert, P.R., 2000. The *Arabidopsis* NPR1/NIM1 protein enhances the DNA binding activity of a subgroup of the TGA family of bZIP transcription factors. *Plant Cell* 12, 279–290.
- Dewdney, J., Lynne Reuber, T., Wildermuth, M.C., Devoto, A., Cui, J., Stutius, L.M., Drummond, E.P., Ausubel, F.M., 2000. Three unique mutants of *Arabidopsis* identify eds loci required for limiting growth of a biotrophic fungal pathogen. *Plant J.* 24, 205–218.
- Dixon, R.A., Lamb, C.J., 1990. Molecular communication in interactions between plants and microbial pathogens. *Annu. Rev. Plant Physiol. Plant Mol. Biol.* 41, 339–367.
- Doares, S.H., Narvaez-Vasquez, J., Conconi, A., Ryan, C.A., 1995. Salicylic acid inhibits synthesis of proteinase inhibitors in tomato leaves induced by systemin and jasmonic Acid. *Plant Physiol.* 108, 1741–1746.
- Dos Santos, A.F., Matsuoka, K., Alfenas, A., Maffia, L.A., 1995. Identification of *Phytophthora* species that infect *Hevea* sp. *Fitopatol. Bras.* 20, 151–159.
- Duarte, M.E.R., Cauduro, J.P., Nosedá, D.G., Nosedá, M.D., Gonçalves, A.G., Pujol, C.A., Damonte, E.B., Cerezo, A.S., 2004. The structure of the agaran sulfate from *Acanthophora spicifera* (Rhodomelaceae, Ceramiales) and its antiviral activity. Relation between structure and antiviral activity in agarans. *Carbohydr. Res.* 339, 335–347.

- Dutsadee, C., Nunta, C., 2008. Induction of peroxidase, scopoletin, phenolic compounds and resistance in *Hevea brasiliensis* by elicitor and a novel protein elicitor purified from *Phytophthora palmivora*. *Physiol. Mol. Plant Pathol.* 72, 179–187.
- Ederli, L., Madeo, L., Calderini, O., Gehring, C., Moretti, C., Buonauro, R., Paolucci, F., Pasqualini, S., 2011. The *Arabidopsis thaliana* cysteine-rich receptor-like kinase CRK20 modulates host responses to *Pseudomonas syringae* pv. tomato DC3000 infection. *J. Plant Physiol.* 168, 1784–1794.
- Ekchaweng, K., Evangelisti, E., Schornack, S., Tian, M., Churngchow, N., 2017. The plant defense and pathogen counterdefense mediated by *Hevea brasiliensis* serine protease *HbSPA* and *Phytophthora palmivora* extracellular protease inhibitor *PpEPI10*. *PLoS One* 12, e0175795.
- Ekchaweng, K., Khunjan, U., Churngchow, N., 2017. Molecular cloning and characterization of three novel subtilisin-like serine protease genes from *Hevea brasiliensis*. *Physiol. Mol. Plant Pathol.* 97, 79–95.
- El Modafar, C., Elgadda, M., El Boutachfai, R., Abouraicha, E., Zehhar, N., Petit, E., El Alaoui-Talibi, Z., Courtois, B., Courtois, J., 2012. Induction of natural defence accompanied by salicylic acid-dependant systemic acquired resistance in tomato seedlings in response to bioelicitors isolated from green algae. *Sci. Hortic. (Amsterdam)*. 138, 55–63.
- El Oirdi, M., El Rahman, T.A., Rigano, L., El Hadrami, A., Rodriguez, M.C., Daayf, F., Vojnov, A., Bouarab, K., 2011. *Botrytis cinerea* manipulates the antagonistic effects between immune pathways to promote disease development in tomato. *Plant Cell* 23, 2405–21.
- Erwin, D.C., Ribeiro, O.K., 1996. *Phytophthora Diseases Worldwide*. St Paul, MN, USA.

- Evangelisti, E., Gogleva, A., Hainaux, T., Doumane, M., Tulin, F., Quan, C., Yunusov, T., Floch, K., Schornack, S., 2017. Time-resolved dual transcriptomics reveal early induced *Nicotiana benthamiana* root genes and conserved infection-promoting *Phytophthora palmivora* effectors. *BMC Biol.* 15, 39.
- Fan, W., Dong, X., 2002. In vivo interaction between NPR1 and transcription factor TGA2 leads to salicylic acid-mediated gene activation in *Arabidopsis*. *Plant Cell* 14, 1377–1389.
- Fang, Y., Cui, L., Gu, B., Arredondo, F., Tyler, B.M., 2017. Efficient genome editing in the oomycete *Phytophthora sojae* using CRISPR/Cas9. *Curr. Protoc. Microbiol.* 44, 21A.1.1–21A.1.26.
- Fang, Y., Tyler, B.M., 2016. Efficient disruption and replacement of an effector gene in the oomycete *Phytophthora sojae* using CRISPR/Cas9. *Mol. Plant Pathol.* 17, 127–139.
- Fawke, S., Doumane, M., Schornack, S., 2015. Oomycete interactions with plants: Infection strategies and resistance principles. *Microbiol. Mol. Biol. Rev.* 79, 263–280.
- Felix, G., Grosskopf, D.G., Regenass, M., Basse, C.W., Boller, T., 1991. Elicitor-induced ethylene biosynthesis in tomato cells: characterization and use as a bioassay for elicitor action. *PLANT Physiol.* 97, 19–25.
- Ferna, P., Gimenez-ibanez, S., Geerinck, J., Eeckhout, D., Schweizer, F., Godoy, M., Franco-zorrilla, M., Pauwels, L., Witters, E., Puga, I., Paz-ares, J., Gene, D., 2011. The *Arabidopsis* bHLH transcription factors MYC3 and MYC4 are targets of JAZ repressors and act additively with MYC2 in the activation of jasmonate responses. *Plant Cell* 23, 701–715.
- Fonseca, S., Chini, A., Hamberg, M., Adie, B., Porzel, A., Kramell, R., Miersch, O., Wasternack, C., Solano, R., 2009. (+)-7-iso-Jasmonoyl-L-isoleucine is the endogenous bioactive jasmonate. *Nat. Chem. Biol.* 5, 344–350.

- Fu, Z.Q., Yan, S., Saleh, A., Wang, W., Ruble, J., Oka, N., Mohan, R., Spoel, S.H., Tada, Y., Zheng, N., Dong, X., 2012. NPR3 and NPR4 are receptors for the immune signal salicylic acid in plants. *Nature* 486, 228–232.
- Gaulin, E., Dramé, N., Lafitte, C., Torto-Alalibo, T., Martinez, Y., Ameline-Torregrosa, C., Khatib, M., Mazarguil, H., Villalba-Mateos, F., Kamoun, S., Mazars, C., Dumas, B., Bottin, A., Esquerré-Tugayé, M.-T., Rickauer, M., 2006. Cellulose binding domains of a *Phytophthora* cell wall protein are novel pathogen-associated molecular patterns. *Plant Cell* 18, 1766–1777.
- Gfeller, A., Dubugnon, L., Liechti, R., Farmer, E.E., 2010. Jasmonate biochemical pathway. *Sci. Signal.* 3, cm3.
- Ghannam, A., Abbas, A., Alek, H., Al-Waari, Z., Al-Ktaifani, M., 2013. Enhancement of local plant immunity against tobacco mosaic virus infection after treatment with sulphated-carrageenan from red alga (*Hypnea musciformis*). *Physiol. Mol. Plant Pathol.* 84, 19–27.
- Glazebrook, J., 2005. Contrasting mechanisms of defense against biotrophic and necrotrophic pathogens. *Annu. Rev. Phytopathol.* 43, 205–227.
- Govrin, E.M., Levine, A., 2000. The hypersensitive response facilitates plant infection by the necrotrophic pathogen *Botrytis cinerea*. *Curr. Biol.* 10, 751–757.
- Govrin, E.M., Rachmilevitch, S., Tiwari, B.S., Solomon, M., Levine, A., 2006. An elicitor from *Botrytis cinerea* induces the hypersensitive response in *Arabidopsis thaliana* and other plants and promotes the gray mold disease. *Phytopathology* 96, 299–307.
- Gumtow, R., Wu, D., Uchida, J., Tian, M., 2018. A *Phytophthora palmivora* extracellular cystatin-like protease inhibitor targets papain to contribute to virulence on papaya. *Mol. Plant-Microbe Interact.* 31, 363–373.

- Gupta, R., Jung, E., Brunak, S., 2002. Prediction of *N*-glycosylation sites in human proteins. *Pacific Symp. Biocomput.* 7, 310–322.
- Gupta, R., Jung, E., Gooley, A.A., Williams, K.L., Brunak, S., Hansen, J., 1999. Scanning the available *Dictyostelium discoideum* proteome for O-linked GlcNAc glycosylation sites using neural networks. *Glycobiology* 9, 1009–1022.
- Gutiérrez, A., Prieto, A., Martínez, A.T., 1996. Structural characterization of extracellular polysaccharides produced by fungi from the genus *Pleurotus*. *Carbohydr. Res.* 281, 143–154.
- Hahlbrock, K., Scheel, D., Logemann, E., Nurnberger, T., Parniske, M., Reinold, S., Sacks, W.R., Schmelzer, E., 1995. Oligopeptide elicitor-mediated defense gene activation in cultured parsley cells. *Proc. Natl. Acad. Sci.* 92, 4150–4157.
- Halim, V.A., Eschen-Lippold, L., Altmann, S., Birschwilks, M., Scheel, D., Rosahl, S., 2007. Salicylic acid is important for basal defense of *Solanum tuberosum* against *Phytophthora infestans*. *Mol. Plant-Microbe Interact.* 20, 1346–1352.
- Hardham, A.R., Shan, W., 2009. Cellular and molecular biology of *Phytophthora*–Plant Interactions, in: *The Mycota*. pp. 4–27.
- Hein, I., Gilroy, E.M., Armstrong, M.R., Birch, P.R.J., 2009. The zig-zag-zig in oomycete-plant interactions. *Mol. Plant Pathol.* 10, 547–562.
- Henniger, H., 1963. Zur Kultur von *Phytophthora infestans* auf vollsynthetischen Nährsubstraten. *Z. Allg. Mikrobiol.* 3, 126–135.
- Hiraga, S., Katsutomo, S., Ito, H., Yuko, O., Hirokazu, M., 2001. A large family of class III plant peroxidases. *Plant Cell Physiol.* 42, 462–468.
- Ho, W., Ko, W., 1997. A simple method for obtaining single-spore isolates of fungi. *Bot. Bull. Acad. Sin.* 38, 41–44.

- Hogenhout, S.A., Van der Hoorn, R.A.L., Terauchi, R., Kamoun, S., 2009. Emerging concepts in effector biology of plant-associated organisms. *Mol. Plant-Microbe Interact.* 22, 115–122.
- Huisman, R., Bouwmeester, K., Brattinga, M., Govers, F., Bisseling, T., Limpens, E., 2015. Haustorium formation in *Medicago truncatula* roots infected by *Phytophthora palmivora* does not involve the common endosymbiotic program shared by arbuscular mycorrhizal fungi and rhizobia. *Mol. Plant-Microbe Interact.* 28, 1271–1280.
- Jones, J.D.G., Dangl, J.L., 2006. The plant immune system. *Nature.* 444, 323–329.
- Jones, P., Binns, D., Chang, H.Y., Fraser, M., Li, W., McAnulla, C., McWilliam, H., Maslen, J., Mitchell, A., Nuka, G., Pesseat, S., Quinn, A.F., Sangrador-Vegas, A., Scheremetjew, M., Yong, S.Y., Lopez, R., Hunter, S., 2014. InterProScan 5: Genome-scale protein function classification. *Bioinformatics* 30, 1236–1240.
- Judelson, H.S., 1997. The genetics and biology of *Phytophthora infestans*: Modern approaches to a historical challenge. *Fungal Genet. Biol.* 22, 65–76.
- Judelson, H.S., Blanco, F.A., 2005. The spores of *Phytophthora*: Weapons of the plant destroyer. *Nat. Rev. Microbiol.* 3, 47–58.
- Kamoun, S., van der Lee, T., van den Berg-Velthuis, G., de Groot, K.E., Govers, F., 1998a. Loss of production of the elicitor protein INF1 in the clonal lineage US-1 of *Phytophthora infestans*. *Phytopathology* 88, 1315–23.
- Kamoun, S., 2003. Molecular genetics of pathogenic oomycetes. *Eukaryot. Cell* 2, 191–199.
- Kamoun, S., 2006. A catalogue of the effector secretome of plant pathogenic oomycetes. *Annu. Rev. Phytopathol.* 44, 41–60.
- Kamoun, S., Furzer, O., Jones, J.D.G., Judelson, H.S., Ali, G.S., Dalio, R.J.D., Roy, S.G., Schena, L., Zambounis, A., Panabières, F., Cahill, D., Ruocco, M.,

- Figueiredo, A., Chen, X.R., Hulvey, J., Stam, R., Lamour, K., Gijzen, M., Tyler, B.M., Grünwald, N.J., Mukhtar, M.S., Tomé, D.F.A., Tör, M., Van Den Ackerveken, G., Mcdowell, J., Daayf, F., Fry, W.E., Lindqvist-Kreuze, H., Meijer, H.J.G., Petre, B., Ristaino, J., Yoshida, K., Birch, P.R.J., Govers, F., 2015. The Top 10 oomycete pathogens in molecular plant pathology. *Mol. Plant Pathol.* 16, 413–434.
- Kamoun, S., van West, P., Vleeshouwers, V.G.A.A., de Groot, K.E., Govers, F., 1998b. Resistance of *Nicotiana benthamiana* to *Phytophthora infestans* is mediated by the recognition of the elicitor protein INF1. *Plant Cell* 10, 1413–1426.
- Kamoun, S., West, P. Van, Jong, A.J. De, Groot, K.E. De, Vleeshouwers, V.G.A.A., Govers, F., 1997. A gene encoding a protein elicitor of *Phytophthora infestans* is down-regulated during infection of potato. *Mol. Plant-Microbe Interact.* 10, 13–20.
- Kamoun, S., Young, M., Glascock, C.B., Tyler, B.M., 1993. Extracellular protein elicitors from *Phytophthora*: Host-specificity and induction of resistance to bacterial and fungal phytopathogens. *Mol. Plant-Microbe Interact.* 6, 15–25.
- Kariduraganavar, M.Y., Kittur, A.A., Kamble, R.R., 2014. Polymer synthesis and processing in Natural and Synthetic Biomedical Polymers. pp. 1–31.
- Khunjan, U., Ekchaweng, K., Panrat, T., Tian, M., Churngchow, N., 2016. Molecular cloning of *HbPR-1* gene from rubber tree, expression of *HbPR-1* gene in *Nicotiana benthamiana* and its inhibition of *Phytophthora palmivora*. *PLoS One* 11, e0157591.
- Klarzynski, O., Descamps, V., Plesse, B., Yvin, J.-C., Kloareg, B., Fritig, B., 2003. Sulfated fucan oligosaccharides elicit defense responses in tobacco and local and systemic resistance against tobacco mosaic virus. *Mol. Plant-Microbe Interact.* 16, 115–122.

- Klarzynski, O., Plesse, B., Joubert, J.-M., Yvin, J.-C., Kopp, M., Kloareg, B., Fritig, B., 2000. Linear β -1,3 glucans are elicitors of defense responses in tobacco. *Plant Physiol.* 124, 1027–1038.
- Kliebenstein, D.J., Rowe, H.C., 2008. Ecological costs of biotrophic versus necrotrophic pathogen resistance, the hypersensitive response and signal transduction. *Plant Sci.* 174, 551–556.
- Koncz, C., Schell, J., 1986. The promoter of TL-DNA gene 5 controls the tissue-specific expression of chimaeric genes carried by a novel type of *Agrobacterium* binary vector. *MGG Mol. Gen. Genet.* 204, 383–396.
- Koornneef, A., Leon-Reyes, A., Ritsema, T., Verhage, A., Den Otter, F.C., Van Loon, L.C., Pieterse, C.M.J., 2008. Kinetics of salicylate-mediated suppression of jasmonate signaling reveal a role for redox modulation. *Plant Physiol.* 147, 1358–1368.
- Kuc, J., 1987. Translocated signals for plant immunization. *Ann. N. Y. Acad. Sci.* 494, 221–223.
- Latijnhouwers, M., De Wit, P.J.G.M., Govers, F., 2003. Oomycetes and fungi: Similar weaponry to attack plants. *Trends Microbiol.* 11, 462–469.
- Le Fevre, R., O’Boyle, B., Moscou, M.J., Schornack, S., 2016. Colonization of barley by the broad-host hemibiotrophic pathogen *Phytophthora palmivora* uncovers a leaf development–dependent involvement of Mlo. *Mol. Plant-Microbe Interact.* 29, 385–395.
- Lee, S.J., Rose, J.K.C., 2010. Mediation of the transition from biotrophy to necrotrophy in hemibiotrophic plant pathogens by secreted effector proteins. *Plant Signal. Behav.* 5, 769–772.

- Leite, M., Quinta-Costa, M., Leite, P.S., Guimarães, J.E., 1999. Critical evaluation of techniques to detect and measure cell death-study in a model of UV radiation of the leukaemic cell line HL60. *Anal. Cell. Pathol.* 19, 139–51.
- Levine, A., Pennell, R.I., Alvarez, M.E., Palmer, R., Lamb, C., 1996. Calcium-mediated apoptosis in a plant hypersensitive disease resistance response. *Curr. Biol.* 6, 427–437.
- Li, H., Qin, Y., Xiao, X., Tang, C., 2011. Screening of valid reference genes for real-time RT-PCR data normalization in *Hevea brasiliensis* and expression validation of a sucrose transporter gene *HbSUT3*. *Plant Sci.* 181, 132–139.
- Li, J., Brader, G., Palva, E.T., 2004. The WRKY70 Transcription Factor: A node of convergence for jasmonate-mediated and salicylate-mediated signals in plant defense. *Plant Cell* 16, 319–331.
- Lieberei, R., 2007. South American leaf blight of the rubber tree (*Hevea* spp.): New steps in plant domestication using physiological features and molecular markers. *Ann. Bot.* 100, 1125–1142.
- Lindbo, J.A., 2007. TRBO: A high-efficiency tobacco mosaic virus RNA-based overexpression vector. *Plant Physiol.* 145, 1232–1240.
- Linthorst, H.J.M., Van Loon, L.C., 1991. Pathogenesis-related proteins of plants. *CRC. Crit. Rev. Plant Sci.* 10, 123–150.
- Liu, M., Khan, N.U., Wang, N., Yang, X., Qiu, D., 2016. The protein elicitor PevD1 enhances resistance to pathogens and promotes growth in *Arabidopsis*. *Int. J. Biol. Sci.* 12, 931–943.
- Lu, H., Salimian, S., Gamelin, E., Wang, G., Fedorowski, J., Lacourse, W., Greenberg, J.T., 2009. Genetic analysis of *acd6-1* reveals complex defense networks and leads to identification of novel defense genes in *Arabidopsis*. *Plant J.* 58, 401–412.

- Ma, Z., Song, T., Zhu, L., Ye, W., Wang, Y., Shao, Y., Dong, S., Zhang, Z., Dou, D., Zheng, X., Tyler, B.M., Wang, Y., 2015. A *Phytophthora sojae* glycoside hydrolase 12 protein is a major virulence factor during soybean infection and is recognized as a PAMP. *Plant Cell* 27, 2057–2072.
- Marchler-Bauer, A., Bo, Y., Han, L., He, J., Lanczycki, C.J., Lu, S., Chitsaz, F., Derbyshire, M.K., Geer, R.C., Gonzales, N.R., Gwadz, M., Hurwitz, D.I., Lu, F., Marchler, G.H., Song, J.S., Thanki, N., Wang, Z., Yamashita, R.A., Zhang, D., Zheng, C., Geer, L.Y., Bryant, S.H., 2017. CDD/SPARCLE: Functional classification of proteins via subfamily domain architectures. *Nucleic Acids Res.* 45, D200–D203.
- Mateos, F.V., Rickauer, M., Esquerré-Tugayé, M.-T., 1997. Cloning and characterization of a cDNA encoding an elicitor of *Phytophthora parasitica* var. *nicotianae* that shows cellulose-binding and lectin-like activities. *Mol. Plant-Microbe Interact.* 10, 1045–1053.
- Mauch, F., Mauch-Mani, B., Gaille, C., Kull, B., Haas, D., Reimann, C., 2001. Manipulation of salicylate content in *Arabidopsis thaliana* by the expression of an engineered bacterial salicylate. *Plant J.* 25, 67–77.
- McGarvey, P.B., Hammond, J., Dienelt, M.M., Hooper, D.C., Fang Fu, Z., Dietzschold, B., Koprowski, H., Michaels, F.H., 1995. Expression of the rabies virus glycoprotein in transgenic tomatoes. *Bio/Technology* 13, 1484–1487.
- Mehdy, M., 1994. Active oxygen species in plant defense against pathogens. *Plant Physiol.* 105, 468–472.
- Memelink, J., 2009. Regulation of gene expression by jasmonate hormones. *Phytochemistry* 70, 1560–1570.
- Ménard, R., Alban, S., de Ruffray, P., Jamois, F., Franz, G., Fritig, B., Yvin, J.-C., Kauffmann, S., 2004. Beta-1,3 glucan sulfate, but not beta-1,3 glucan, induces

- the salicylic acid signaling pathway in tobacco and *Arabidopsis*. *Plant Cell* 16, 3020–32.
- Mendgen, K., Hahn, M., 2002. Plant infection and the establishment of fungal biotrophy. *Trends Plant Sci.* 7, 352–356.
- Mercier, L., Lafitte, C., Borderies, G., Briand, X., Esquerré-Tugayé, M.T., Fournier, J., 2001. The algal polysaccharide carrageenans can act as an elicitor of plant defence. *New Phytol.* 149, 43–51.
- Miao, J., Chi, Y., Lin, D., Tyler, B.M., Liu, X., 2018. Mutations in ORP1 conferring oxathiapiprolin resistance confirmed by genome editing using CRISPR/Cas9 in *Phytophthora capsici* and *P. sojae*. *Phytopathology* 108, 1412–1419.
- Moeder, W., Barry, C.S., Tauriainen, A.A., 2002. Ethylene synthesis regulated by biphasic induction of 1-aminocyclopropane-1-carboxylic acid synthase and 1-aminocyclopropane-1-carboxylic acid oxidase genes is required for hydrogen peroxide accumulation and cell death in ozone-exposed tomato. *Plant Physiol.* 130, 1918–1926.
- Montillet, J.-L., Chamnongpol, S., Rusterucci, C., Dat, J., Van de Cotte, B., Agnel, J.-P., Battesti, C., Inze, D., Van Breusegem, F., Triantaphylides, C., 2005. Fatty acid hydroperoxides and H₂O₂ in the execution of hypersensitive cell death in tobacco leaves. *Plant Physiol.* 138, 1516–1526.
- Nagorskaia, V.P., Reunov, A.V., Lapshina, L.A., Ermak, I.M., Barabanova, A.O., 2008. Influence of kappa/beta-carrageenan from red alga *Tichocarpus crinitus* on development of local infection induced by tobacco mosaic virus in Xanthi-nc tobacco leaves. *Izv Akad Nauk Ser Biol* 3, 360–364.
- Necas, J., Bartosikova, L., 2013. Carrageenan: a review. *Vet. Med. (Praha)*. 58, 187–205.

- Nei, M., Saitou, N., 1987. The neighbor-joining method: a new method for reconstructing phylogenetic trees. *Mol Biol Evol* 4, 406–425.
- Newman, M.-A., Sundelin, T., Nielsen, J.T., Erbs, G., 2013. MAMP (microbe-associated molecular pattern) triggered immunity in plants. *Front. Plant Sci.* 4, 139.
- Nürnbergger, T., Nennstiel, D., Jabs, T., Sacks, W.R., Hahlbrock, K., Scheel, D., 1994. High affinity binding of a fungal oligopeptide elicitor to parsley plasma membranes triggers multiple defense responses. *Cell* 78, 449–460.
- Orwa, C., Mutua, A., Kindt, R., Jamnadass, R., Anthony, S., 2009. Agroforestry Database: a tree reference and selection guide version 4.0, World Agroforestry Centre, Kenya.
- Parekh, R., Doshi, Y., Chauhan, V., 1989. Polysaccharides from marine red algae *Acanthophora spicifera*, *Grateloupia indica* and *Halymenia porphyroides*. *Indian J. Mar. Sci.* 18, 139–140.
- Parker, J.E., Schulte, W., Hahlbrock, K., Scheel, D., 1991. An extracellular glycoprotein from *Phytophthora megasperma* f. sp. *glycinea* elicits phytoalexin synthesis in cultured parsley cells and protoplasts. *Mol. Plant-Microbe Interact.* 4, 19–27.
- Pauwels, L., Barbero, G.F., Geerinck, J., Tilleman, S., Grunewald, W., Pérez, A.C., Chico, J.M., Bossche, R. Vanden, Sewell, J., Gil, E., García-Casado, G., Witters, E., Inzé, D., Long, J.A., De Jaeger, G., Solano, R., Goossens, A., 2010. NINJA connects the co-repressor TOPLESS to jasmonate signalling. *Nature* 464, 788–791.
- Pauwels, L., Goossens, A., 2011. The JAZ proteins: a crucial interface in the jasmonate signaling cascade. *Plant Cell* 23, 3089–3100.

- Pennell, R.I., and Lamb, C., 1997. Programmed cell death (PCD) in plants. *Plant Cell* 9, 1157–1168.
- Penninckx, I.A., Eggermont, K., Terras, F.R., Thomma, B.P., De Samblanx, G.W., Buchala, A., Métraux, J.P., Manners, J.M., Broekaert, W.F., 1996. Pathogen-induced systemic activation of a plant defensin gene in *Arabidopsis* follows a salicylic acid-independent pathway. *Plant Cell* 8, 2309–23.
- Petersen, M., Brodersen, P., Naested, H., Andreasson, E., Lindhart, U., Johansen, B., Nielsen, H.B., Lacy, M., Austin, M.J., Parker, J.E., Sharma, S.B., Klessig, D.F., Martienssen, R., Mattsson, O., Jensen, A.B., Mundy, J., 2000. *Arabidopsis* MAP kinase 4 negatively regulates systemic acquired resistance. *Cell* 103, 1111–1120.
- Petersen, T.N., Brunak, S., von Heijne, G., Nielsen, H., 2011. SignalP 4.0: discriminating signal peptides from transmembrane regions. *Nat. Methods* 8, 785–786.
- Pieterse, C.M., van Wees, S.C., van Pelt, J. a, Knoester, M., Laan, R., Gerrits, H., Weisbeek, P.J., van Loon, L.C., 1998. A novel signaling pathway controlling induced systemic resistance in *Arabidopsis*. *Plant Cell* 10, 1571–1580.
- Pieterse, C.M.J., van Wees, S.C.M., Hoffland, E., van Pelt, J.A., van Loon, L.C., 1996. Systemic resistance in *Arabidopsis* induced by biocontrol bacteria is independent of salicylic acid accumulation and pathogenesis-related gene expression. *Plant Cell* 8, 1225.
- Pieterse, C.M.J., Van der Does, D., Zamioudis, C., Leon-Reyes, A., Van Wees, S.C.M., 2012. Hormonal modulation of plant immunity. *Annu. Rev. Cell Dev. Biol.* 28, 489–521.
- Pryce-Jones, E., Carver, T., Gurr, S.J., 1999. The roles of cellulase enzymes and mechanical force in host penetration by *Erysiphe graminis* f.sp. *hordei*. *Physiol. Mol. Plant Pathol.* 55, 175–182.

- Rath, A., Glibowicka, M., Nadeau, V.G., Chen, G., Deber, C.M., 2009. Detergent binding explains anomalous SDS-PAGE migration of membrane proteins. *Proc. Natl. Acad. Sci.* 106, 1760–1765.
- Reed, C.F., 1976. Information summaries on 1000 economic plants, Typescripts submitted to the USDA.
- Rey, T., Chatterjee, A., Buttay, M., Toulotte, J., Schornack, S., 2015. *Medicago truncatula* symbiosis mutants affected in the interaction with a biotrophic root pathogen. *New Phytol.* 206, 497–500.
- Roberts, M.A., Quemener, B., 1999. Measurement of carrageenans in food: Challenges, progress, and trends in analysis. *Trends Food Sci. Technol.* 10, 169–181.
- Ross, A.F., 1961. Systemic acquired resistance induced by localized virus infections in plants. *Virology* 14, 340–358.
- Sacks, W.R., Hahlbrock, K., Scheel, D., 1993. Characterization of a glycoprotein elicitor from *Phytophthora megasperma*. L.M. Fritig B., ed. Springer, Dordrecht., pp. 144–147.
- Sambrook J, Fritsch EF, M.T., 1989. *Molecular cloning: a laboratory manual*, 2nd Ed., Cold Spring Harbor Laboratory, Cold Spring Harbor, NY., in: New York. pp. 931–957.
- Šandula, J., Kogan, G., Kačuráková, M., MacHová, E., 1999. Microbial (1→3)-β-D-glucans, their preparation, physico-chemical characterization and immunomodulatory activity. *Carbohydr. Polym.* 38, 247–253.
- Sangha, J.S., Khan, W., Ji, X., Zhang, J., Mills, A.A.S., Critchley, A.T., Prithiviraj, B., 2011. Carrageenans, sulphated polysaccharides of red seaweeds, differentially affect *Arabidopsis thaliana* resistance to *Trichoplusia ni* (Cabbage Looper). *PLoS One* 6, e26834.

- Sangha, J.S., Ravichandran, S., Prithiviraj, K., Critchley, A.T., Prithiviraj, B., 2010. Sulfated macroalgal polysaccharides λ -carrageenan and ι -carrageenan differentially alter *Arabidopsis thaliana* resistance to *Sclerotinia sclerotiorum*. *Physiol. Mol. Plant Pathol.* 75, 38–45.
- Sansome, E., 1997. Polyploidy and induced gametangial formation in british isolates of *Phytophthora infestans*. *J. Gen. Microbiol.* 99, 311–316.
- Schmittgen, T.D., Livak, K.J., 2008. Analyzing real-time PCR data by the comparative CT method. *Nat. Protoc.* 3, 1101–1108.
- Sejalon-Delmas, N., Mateos, F. V, Bottin, A., Rickauer, M., Dargent, R., Esquerré-Tugayé, M.T., 1997. Purification, elicitor activity, and cell wall localization of a glycoprotein from *Phytophthora parasitica* var. *nicotianae*, a fungal pathogen of tobacco. *Phytopathology* 87, 899–909.
- Sekkal, M., Legrand, P., 1993. A spectroscopic investigation of the carrageenans and agar in the 1500-100 cm^{-1} spectral range. *Spectrochim. Acta Part A Mol. Spectrosc.* 49, 209–221.
- Seo, H.S., Song, J.T., Cheong, J.-J., Lee, Y.-H., Lee, Y.-W., Hwang, I., Lee, J.S., Choi, Y.D., 2001. Jasmonic acid carboxyl methyltransferase: A key enzyme for jasmonate-regulated plant responses. *Proc. Natl. Acad. Sci.* 98, 4788–4793.
- Serino, L., Reimmann, C., Baur, H., Beyeler, M., Visca, P., Haas, D., 1995. Structural genes for salicylate biosynthesis from chorismate in *Pseudomonas aeruginosa*. *Mgg Mol. Gen. Genet.* 249, 217–228.
- Seviour, R.J., Stasinopoulos, S.J., Auer, D.P.F., Gibbs, P.A., 1992. Production of pullulan and other exopolysaccharides by filamentous fungi. *Crit. Rev. Biotechnol.* 12, 279–298.
- Shah, J., 2003. The salicylic acid loop in plant defense. *Curr. Opin. Plant Biol.* 6, 365–371.

- Shah, J., Tsui, F., Klessig, D.F., 1997. Characterization of a salicylic acid insensitive mutant (*sai1*) of *Arabidopsis thaliana*, identified in a selective screen utilizing the SA-inducible expression of the *tms2* Gene. *Mol. Plant-Microbe Interact.* 10, 69–78.
- Sharp, J.K., Valent, B., Albersheim, P., 1984. Purification and partial characterization of a beta-glucan fragment that elicits phytoalexin accumulation in soybean. *J. Biol. Chem.* 259, 11312–11320.
- Sheard, L.B., Tan, X., Mao, H., Withers, J., Ben-Nissan, G., Hinds, T.R., Kobayashi, Y., Hsu, F.F., Sharon, M., Browse, J., He, S.Y., Rizo, J., Howe, G.A., Zheng, N., 2010. Jasmonate perception by inositol-phosphate-potentiated COI1-JAZ co-receptor. *Nature* 468, 400–407.
- Shukla, P.S., Borza, T., Critchley, A.T., Prithiviraj, B., 2016. Carrageenans from red seaweeds as promoters of growth and elicitors of defense response in Plants. *Front. Mar. Sci.* 3, 81.
- Shulaev, V., Silverman, P., Raskin, I., 1997. Airborne signalling by methyl salicylate in plant pathogen resistance. *Nature* 385, 718–721.
- Spoel, S.H., Johnson, J.S., Dong, X., 2007. Regulation of tradeoffs between plant defenses against pathogens with different lifestyles. *Proc. Natl. Acad. Sci.* 104, 18842–18847.
- Spoel, S.H., Koornneef, A., Claessens, S.M., Korzelius, J.P., Van Pelt, J.A., Mueller, M.J., Buchala, A., Métraux, J.P., Brown, R., Kazan, K., Van Loon, L.C., Dong, X., Pieterse, C.M., 2003. NPR1 modulates cross-talk between salicylate- and jasmonate-dependent defense pathways through a novel function in the cytosol. *Plant Cell* 15, 760–770.
- Stafford, H. a, Bravinder-Bree, S., 1972. Peroxidase isozymes of first internodes of sorghum: tissue and intracellular localization and multiple peaks of activity isolated by gel filtration chromatography. *Plant Physiol.* 49, 950–6.

- Stajich, J.E., Harris, T., Brunk, B.P., Brestelli, J., Fischer, S., Harb, O.S., Kissinger, J.C., Li, W., Nayak, V., Pinney, D.F., Stoeckert, C.J., Roos, D.S., 2012. FungiDB: An integrated functional genomics database for fungi. *Nucleic Acids Res.* 40, D675–D681.
- Stassen, J.H.M., Van den Ackerveken, G., 2011. How do oomycete effectors interfere with plant life? *Curr. Opin. Plant Biol.* 14, 407–414.
- Staswick, P.E., Tiryaki, I., 2004. The oxylipin signal jasmonic acid is activated by an enzyme that conjugates it to isoleucine in *Arabidopsis*. *Plant Cell* 16, 2117–2127.
- Sutherland, I.W., 1994. Structure-function relationships in microbial exopolysaccharides. *Biotechnol. Adv.* 12, 393–448.
- Tada, Y., Spoel, S.H., Pajerowska-Mukhtar, K., Mou, Z., Song, J., Wang, C., Zuo, J., Dong, X., 2008. Plant immunity requires conformational changes of NPR1 via S-nitrosylation and thioredoxins. *Science* 321, 952–956.
- Taguchi, G., Yazawa, T., Hayashida, N., Okazaki, M., 2001. Molecular cloning and heterologous expression of novel glucosyltransferases from tobacco cultured cells that have broad substrate specificity and are induced by salicylic acid and auxin. *Eur. J. Biochem.* 268, 4086–4094.
- Tamura, K., Stecher, G., Peterson, D., Filipowski, A., Kumar, S., 2013. MEGA6: Molecular evolutionary genetics analysis version 6.0. *Mol. Biol. Evol.* 30, 2725–2729.
- Thanseem, I., Thulaseedharan, A., 2006. Optimization of RQRT-PCR protocols to measure beta-1,3-glucanase mRNA levels in infected tissues of rubber tree (*Hevea brasiliensis*). *Indian J. Exp. Biol.* 44, 492–498.
- Thordal-Christensen, H., Zhang, Z., Wei, Y., Collinge, D.B., 1997. Subcellular localization of H₂O₂ in plants. H₂O₂ accumulation in papillae and hypersensitive response during the barley-powdery mildew interaction. *Plant J.* 11, 1187–1194.

- Ton, J., Mauch-Mani, B., 2004. β -amino-butyric acid-induced resistance against necrotrophic pathogens is based on ABA-dependent priming for callose. *Plant J.* 38, 119–130.
- Torres, M.A., Jones, J.D.G., Dangl, J.L., 2005. Pathogen-induced, NADPH oxidase-derived reactive oxygen intermediates suppress spread of cell death in *Arabidopsis thaliana*. *Nat. Genet.* 37, 1130–1134.
- Valepyn, E., Cabrera, J.C., Richel, A., Paquot, M., 2014. Water soluble exopolysaccharide from *Syncephalastrum racemosum*, a strong inducer of plant defence reactions. *Carbohydr. Polym.* 101, 941–946.
- Van Breusegem, F., Dat, J.F., 2006. Reactive oxygen species in plant cell death. *Plant Physiol.* 141, 384–390.
- van Kan, J.A.L., 2006. Licensed to kill: the lifestyle of a necrotrophic plant pathogen. *Trends Plant Sci.* 11, 247–253.
- Van Loon, L.C., 2000. Systemic induced resistance in: *Mechanisms of Resistance to Plant Diseases*. pp. 521–574.
- van Loon, L.C., Bakker, P.A.H.M., Pieterse, C.M.J., 1998. Systemic resistance induced by rhizosphere bacteria. *Annu. Rev. Phytopathol.* 36, 453–483.
- van Loon, L.C., Rep, M., Pieterse, C.M.J., 2006. Significance of inducible defense-related proteins in infected plants. *Annu. Rev. Phytopathol.* 44, 135–162.
- Vera, J., Castro, J., Gonzalez, A., Moenne, A., 2011. Seaweed polysaccharides and derived oligosaccharides stimulate defense responses and protection against pathogens in plants. *Mar. Drugs.* 9, 2514–2525.
- Verberne, M.C., Verpoorte, R., Bol, J.F., Mercado-Blanco, J., Linthorst, H.J.M., 2000. Overproduction of salicylic acid in plants by bacterial transgenes enhances pathogen resistance. *Nat. Biotechnol.* 18, 779–783.

- Wawra, S., Belmonte, R., Löbach, L., Saraiva, M., Willems, A., van West, P., 2012. Secretion, delivery and function of oomycete effector proteins. *Curr. Opin. Microbiol.* 15, 685–691.
- Werner, S., Steiner, U., Becher, R., Kortekamp, A., Zyprian, E., Deising, H.B., 2002. Chitin synthesis during in planta growth and asexual propagation of the cellulosic oomycete and obligate biotrophic grapevine pathogen *Plasmopara viticola*. *FEMS Microbiol. Lett.* 208, 169–173.
- Willekens, H., Inzé, D., Van Montagu, M., van Camp, W., 1995. Catalases in plants. *Mol. Breed. New Strateg. Plant Improv.* 1, 207–228.
- Woodbury, W., Spencer, A.K., Stahmann, M.A., 1971. An improved procedure using ferricyanide for detecting catalase isozymes. *Anal. Biochem.* 44, 301–305.
- Woodward, J.R., Keane, P.J., Stone, B.A., 1980. Structures and properties of wilt-inducing polysaccharides from *Phytophthora* species. *Physiol. Plant Pathol.* 16, 439–454.
- Wu, D., Navet, N., Liu, Y., Uchida, J., Tian, M., 2016. Establishment of a simple and efficient *Agrobacterium*-mediated transformation system for *Phytophthora palmivora*. *BMC Microbiol.* 16, 204.
- Wu, Y., Zhang, D., Chu, J.Y., Boyle, P., Wang, Y., Brindle, I.D., De Luca, V., Després, C., 2012. The *Arabidopsis* NPR1 protein is a receptor for the plant defense hormone salicylic acid. *Cell Rep.* 1, 639–647.
- Yang, H., He, G., 2008. Influence of nutritional conditions on exopolysaccharide production by submerged cultivation of the medicinal fungus *Shiraia bambusicola*. *World J. Microbiol. Biotechnol.* 24, 2903–2907.
- Yang, X., Kang, L., Tien, P., 1996. Resistance of tomato infected with cucumber mosaic virus satellite RNA to potato spindle tuber viroid. *Ann. Appl. Biol.* 129, 543–551.

Yu, K., Soares, J.M., Mandal, M.K., Wang, C., Chanda, B., Gifford, A.N., Fowler, J.S., Navarre, D., Kachroo, A., Kachroo, P., 2013. A feedback regulatory loop between G3P and lipid transfer proteins DIR1 and AZI1 mediates azelaic-acid-induced systemic immunity. *Cell Rep.* 3, 1266–1278.

Zacharius, R.M., Zell, T.E., Morrison, J.H., Woodlock, J.J., 1969. Glycoprotein staining following electrophoresis on acrylamide gels. *Anal. Biochem.* 30, 148–152.

Zhao, J., Davis, L.C., Verpoorte, R., 2005. Elicitor signal transduction leading to production of plant secondary metabolites. *Biotechnol. Adv.* 23, 283–333.

Zipfel, C., Felix, G., 2005. Plants and animals: A different taste for microbes? *Curr. Opin. Plant Biol.* 8, 353–360.

http://en.wikipedia.org/wiki/Hevea_brasiliensis

<http://ippc.acfs.go.th/pest/G001/T008/FUNGI105>

http://pnpandbest.com/rubber/pnp_problems/pnp_problems07.html

http://www.algaebase.org/search/species/detail/?species_id=3309

<https://siamrath.co.th/n/70707>

www.itis.gov/servlet/SingleRpt/SingleRpt?search_topic=TSN&search_value=506431

www.cpkelco.com

VITAE

Name Mr. Sittiporn Pettongkhao

Student ID 5610230018

Educational Attainment

Degree	Name of Institution	Year of Graduation
Bachelor of Science (Public Health)	Mahidol University	2012

Scholarship Awards during Enrolment

1. The Excellent Scholarships in Biochemistry, Department of Biochemistry, Faculty of Science, Prince of Songkla University, Thailand
2. The Graduate School of Prince of Songkla University, Thailand
3. The Royal Golden Jubilee Graduated Program (RGJ-PHD) through the Thailand Research Fund (TRF) to Mr. Sittiporn Pettongkhao (PHD/0067/2556)

List of Publication and Proceeding

Pettongkhao, S. and Churngchow, N. 2016. *Hevea brasiliensis* defense responses induced by seaweed extract elicitor containing sulphated polysaccharide from *Acanthophora spicifera*. The 5th International Biochemistry and Molecular biology Conference. B.P. Samila Beach hotel, Songkhla, Thailand, May 26-27, 2016.

Pettongkhao, S. and Churngchow, N. 2016. A novel carbohydrate elicitor produced by *Phytophthora palmivora* and its effects on plant defense responses. RGJ Seminar Series 115th. Prince of Songkla University, Thailand, July 28-29, 2016.

Pettongkhao, S., Khompatara, K., and Churngchow, N. 2017. The effects of novel compound elicitor produced by *Phytophthora palmivora* on plant defense response. RGJ-Ph.D. Congress 18. Richmond Stylish Convention Hotel, Nonthaburi Thailand, June 8-10, 2017.

Pettongkhao, S., Bilanglod, A., Khompatara, K., Churngchow, N., 2019. Sulphated polysaccharide from *Acanthophora spicifera* induced *Hevea brasiliensis* defense responses against *Phytophthora palmivora* infection. *Plants* 8, 73.

Pettongkhao, S., Churngchow, N., 2019. Novel cell death-inducing elicitors from *Phytophthora palmivora* promote infection on *Hevea brasiliensis* (Accepted for publication in *Phytopathology*, June 24, 2019).